Technische Universität München

TUM School of Medicine and Health

Analysis of alpha-synuclein fibril spreading in mouse brain

Shuyu Zhang

Vollständiger Abdruck der von der TUM School of Medicine and Health der Technischen Universität München zur Erlangung einer

Doktorin der Medizin (Dr. med.)

genehmigten Dissertation.

Vorsitz: Prof. Dr. Florian Eyer

Prüfende der Dissertation:

1. Prof. Dr. Paul Lingor
2. Priv.-Doz. Dr. Friederike Liesche-Starnecker
3. Prof. Dr. Thomas Misgeld

Die Dissertation wurde am 12.12.2023 bei der Technischen Universität München eingereicht und durch die TUM School of Medicine and Health am 07.08.2024 angenommen.

Parts of this thesis have previously been published:

Zhang S, Dauer K, Strohäker T, Tatenhorst L, Caldi Gomes L, Mayer S, Jung BC, Kim WS, Lee SJ, Becker S, Liesche-Starnecker F, Zweckstetter M, Lingor P. Alpha-synuclein fibrils amplified from multiple system atrophy and Parkinson's disease patient brain spread after intracerebral injection into mouse brain. Brain Pathol. 2023 Jul 24. doi: 10.1111/bpa.13196. PMID: 37485772.

Table of Content

List of figures

List of tables

List of abbreviations

123I-MIBG	[123I]metaiodobenzylguanidine scintigraphy
ANOVA	analysis of variance
ANS	autonomous nervous system
APS	atypical Parkinsonian syndrome
BSA	bovine serum albumin
CBD	corticobasal degeneration
CNPase	2',3'-cyclic nucleotide-3'-phosphodiesterase
CNS	central nervous system
COMT	catechol-o-methyl-transferase
CSF	cerebrospinal fluid
DAPI	4‘,6-diamidino-2-phenylindole
DJ-1	Daisuke-Junko-1
DLB	dementia with Lewy bodies
DMV	dorsal motor nucleus of the vagal nerve
DNER	delta and notch-like epidermal growth factor-related receptor
dpi	days post injection
GBA1	beta-glucocerebrosidase
GCI	glial cytoplasmatic inclusion
GFAP	glial fibrillary acid protein
HEPES	4-(2-hydroxyethyl)-1-piperazineethanesulfonic acid
IBD	inflammatory bowel disease
IRBD	isolated rapid-eye-movement sleep behavior disorder
LB	Lewy body
LBD	Lewy body disorder
LCO	luminescent conjugated oligothiophenes
LPS	lipopolysaccharide
LRRK2	Leucine-rich repeat kinase 2
MAO-B	monoamine oxidase-B
MHC	major histocompatibility complex

MRI	magnetic resonance imaging
MSA	multiple system atrophy
NFL	neurofilament light chain
NGS	normal goat serum
NLRP-3	nucleotide-binding oligomerization domain-like receptor pyrin domain-containing-3
NMR	nuclear magnetic resonance
OB	olfactory bulb
PAF	pure autonomic failure
PBS	phosphate buffered saline
PD	Parkinson's disease
PET	positron emission tomography
PFA	paraformaldehyde
PFFs	pre-formed fibrils
PIGD	postural instability and gait dominated
PINK1	PTEN-induced putative kinase 1
PMCA	protein misfolding cyclic amplification
PNS	peripheral nervous system
PRKN	Parkin RBR E3 ubiquitin-protein ligase
PSP	progressive supranuclear palsy
PTM	post-translational modification
REM	rapid eye movement
ROI	region of interest
RT-QuIC	real-time quaking-induced conversion
SAA	seed amplification assay
SN	substantia nigra
SNARE	soluble N-ethylmaleimide-sensitive-factor attachment receptor
SNP	single-nucleotide polymorphism
SNpc	substantia nigra pars compacta
SOC	alpha-synuclein origin site and connectome
TH	tyrosine hydroxylase

TLR	toll-like receptor
α-syn	alpha-synuclein
β-NGF	beta nerve growth factor

1 Introduction

1.1 Alpha-synucleinopathies

1.1.1 Parkinson's disease

For the last decades, the prevalence of neurodegenerative diseases has been rising globally due to the increasingly aging society. Parkinson's disease (PD) is the second most common neurodegenerative disease, and around one percent of the population aged 60 years or older and three percent of those aged 80 years or older are suffering from PD (Lee and Gilbert, 2016; Tysnes and Storstein, 2017). As the fastest-growing neurological disease in the world, some authors even speak of a "Parkinson pandemic" with an estimated 12 million or more patients suffering from PD by 2040 (Dorsey et al., 2018). Therefore, understanding disease mechanisms and developing disease-modifying therapies becomes essential to alleviate the individual and socioeconomic burden caused by PD.

1.1.1.1 Etiology and pathophysiology

The pathological hallmark in PD patients' brains is the loss of dopaminergic neurons in the substantia nigra pars compacta (SNpc) and the presence of Lewy bodies (LBs) (Spillantini et al., 1997). These intracytoplasmatic LBs are composed of fibrillar aggregates, most of which are phosphorylated alpha-synuclein (α-syn) aggregates (Fujiwara et al., 2002; Wakabayashi et al., 2013). α-syn is a small, soluble, lipid-binding protein that has multiple functions, including the regulation of synaptic vesicle release (Bendor et al., 2013; Kubo et al., 2005). When mutated, duplicated, or triplicated, α-syn can cause forms of familial PD (Krüger et al., 1998; Zarranz et al., 2004). Most PD cases are sporadic, whereas 5-15 % are linked to familial forms (Balestrino and Schapira, 2020). Genes including SNCA, Leucine-rich repeat kinase 2 (LRRK2), VPS35, EIF4G1, DNAJC13, and CHCHD2 are associated with autosomal dominant forms of PD, while Parkin RBR E3 ubiquitin-protein ligase (PRKN), PTEN-induced putative kinase 1 (PINK1), and Daisuke-Junko-1 (DJ-1) cause autosomal recessive forms of PD (Kalia and Lang, 2015). Additionally, gene loci such as single-nucleotide polymorphisms (SNPs) in α-syn or mutations

in β-glucocerebrosidase (GBA1) increase the risk for sporadic PD (Kalia and Lang, 2015; Nalls et al., 2014).

The aforementioned genes encode proteins in molecular pathways that are also disrupted in sporadic disease (Dexter and Jenner, 2013). Common mechanisms, for example, include neuroinflammation, oxidative stress, impaired autophagy, and mitochondrial dysfunction (Dexter and Jenner, 2013; Johnson et al., 2019). The molecular mechanisms triggering the initial disease stage may differ from later phases and can be divided into triggers, facilitators, and aggravators (Johnson et al., 2019). These processes are hypothesized to result in neuronal death of dopaminergic neurons, but multiple other regions of the nervous system can also be affected – resulting in a plethora of motor and non-motor symptoms. The loss of nigral dopaminergic neurons leads to an imbalance between excitatory and inhibitory circuits, causing bradykinesia, one of the cardinal symptoms in PD patients (Bloem et al., 2021).

While genetic influences on the etiology of PD play an important role (Gasser, 1998; Wright Willis et al., 2010), environmental impacts and toxins such as pesticides and rural living should not be neglected as risk factors (Breckenridge et al., 2016; Pan-Montojo and Reichmann, 2014). The rise in the incidence of PD is linked to an aging population and increased life expectancy. Interestingly, it also correlates with the growth of gross national income, suggesting that economic growth is followed by industrialization and environmental pollution with pesticides, solvents, and metals, thus becoming risk factors for developing PD (Dorsey et al., 2018). In China, for example, rapid industrial growth gave rise to an increase in the age-adjusted prevalence of PD by more than 100 % between 1990 and 2016 (Global, regional, and national burden of Parkinson's disease, 1990-2016: a systematic analysis for the Global Burden of Disease Study 2016, 2018). Occupational exposure to metals, including mercury, lead, manganese, copper, iron, aluminum, bismuth, thallium, and zinc, is further associated with a higher risk of PD (Bjorklund et al., 2018). Conversely, smoking, caffeine consumption, non-steroidal anti-inflammatory (e.g., ibuprofen) drug uptake, and physical activity were associated with a reduced risk of PD (Ascherio and Schwarzschild, 2016). For most PD cases, no single cause can be identified. Therefore, a multifactorial etiology with an interplay of genetics, lifestyle, and environmental factors is most likely to cause the disease.

1.1.1.2 Symptomatology

PD has been known since ancient times with descriptions appearing in early Indian and Egyptian texts (García Ruiz, 2004). Clinically, PD was first described by James Parkinson as "Shaking Palsy" in 1817 (Parkinson, 2002). The primary symptoms of PD include resting tremor, rigidity, brady-/hypo-/akinesia, and postural instability. Therefore, PD is considered a movement disorder, but most patients also experience additional non-motor symptoms such as hyposmia, constipation, urinary dysfunction, orthostatic hypotension, and cognitive impairment (Balestrino and Schapira, 2020). They also suffer from sleep disturbances, including insomnia, circadian rhythm disruption, and rapid eye movement (REM) sleep behavior disorder (Videnovic, 2017). While motor symptoms are associated with nigral degeneration and dopamine depletion in the striatum, non-motor symptoms are linked to neurodegeneration of structures in the peripheral autonomic nervous system and the central nervous system (CNS), including olfactory, enteric, and brainstem neurons (Gelpi et al., 2014; Goldman and Postuma, 2014). The prodromal phase can extend more than 20 years before the first motor symptoms occur (Savica et al., 2010). With disease progression, non-motor symptoms increase the disease burden, reduce the quality of life (Barone et al., 2017), and drive up the overall cost of care (Tolosa et al., 2021).

1.1.1.3 Diagnosis

PD is diagnosed clinically with a particular degree of certainty but can only be confirmed in a post-mortem autopsy. According to the Movement Disorder Society (MDS), the essential diagnostic criterion for PD is bradykinesia in combination with tremor and/or rigidity. Supportive criteria for PD include response to dopaminergic therapy, levodopa-induced dyskinesia, and rest tremor of a limb (Postuma et al., 2015). Red flags such as early falls or a wide-based gait in combination with the inability to take ten consecutive steps along a narrow line may indicate a form of atypical parkinsonism (Abdo et al., 2006). In these cases, ancillary testing using magnetic resonance imaging (MRI), dopaminergic neuroimaging, or cardiac [^{123}I]metaiodobenzylguanidine scintigraphy (123I-MIBG) helps physicians establish the correct diagnosis (Bloem et al., 2021).

1.1.1.4 Treatment options

No disease-modifying medications are available as of today, and PD patients can only be treated symptomatically to alleviate motor and non-motor symptoms. Currently, established treatment options for PD include medication such as carbidopa-levodopa, monoamine oxidase-B (MAO-B) inhibitors, catechol-o-methyl-transferase (COMT) inhibitors, and dopamine agonists complemented by rehabilitation and exercise. Patients experiencing complications can benefit from advanced and surgical treatments such as deep brain stimulation or infusion therapies, including carbidopa-levodopa enteral suspension or continuous subcutaneous apomorphine infusion (Armstrong and Okun, 2020; van Laar et al., 2023).

1.1.2 Atypical Parkinsonian syndromes – MSA

Atypical Parkinsonian syndromes (APS) represent a group of neurodegenerative disorders that share symptoms similar to Parkinson's disease but have distinct features and underlying causes. These conditions include multiple system atrophy (MSA), progressive supranuclear palsy (PSP), corticobasal degeneration (CBD), and dementia with Lewy bodies (DLB). MSA is a disorder that affects both the autonomic nervous system and the motor system leading to autonomic failure, parkinsonism, and cerebellar dysfunction. It is further divided into two subtypes depending on the symptoms at diagnosis: MSA with predominant parkinsonism (MSA-P) and MSA with predominant cerebellar ataxia (MSA-C) (Gilman et al., 2008).

APS are typically more aggressive in their progression than PD and may involve dysautonomia, early cognitive decline, or early postural instability (Levin et al., 2016). APS also tend to be less responsive to typical PD medications, making management more challenging. Treatment options for APS are, similar to PD, focused on symptom management, and involve a multidisciplinary approach, including physical therapy, occupational therapy, speech therapy, and medications to address specific symptoms.

Histologically, MSA is characterized by the presence of α-syn inclusions in neurons and glial cells, so-called glial cytoplasmatic inclusions (GCIs) or Papp-Lantos bodies (Cykowski et al., 2015; Papp and Lantos, 1994; Spillantini et al., 1998). GCIs are typically found in MSA patients, but they can also be present in PD patients (Wakabayashi et al., 2000). While widespread α-

syn pathology is present in the form of GCIs, variable neuronal cytoplasmatic inclusions can be observed in the putamen, pontine nuclei, and inferior olivary nuclei, which are not susceptible to LBs (Koga et al., 2021). Similar to PD, neuronal cytoplasmic inclusions can also be detected in the substantia nigra, cingulate cortex, amygdala, hippocampus, entorhinal cortex, hypothalamus, and neocortex (Cykowski et al., 2015). Next to α-syn positive GCIs, neurodegenerative changes in striatonigral and olivopontocerebellar structures are also found in MSA patients' brains (Trojanowski and Revesz, 2007). A positive correlation between the density of GCIs and the severity of neuronal cell loss suggests an association between GCIs, demyelination, and neurodegeneration (Ozawa et al., 2004; Poewe et al., 2022).

1.2 Alpha-synuclein (α-syn)

α-syn is a 14-kDa protein that misfolds in α-synucleinopathies, such as PD and MSA, and is found in LBs and GCIs (Spillantini et al., 1998; Spillantini et al., 1997). Physiologically, α-syn exists in an unfolded soluble state but can also assemble into α-helix rich tetramers (Dettmer et al., 2015). It is predominantly located in neuronal presynaptic terminals and modulates the soluble N-ethylmaleimide-sensitive-factor attachment receptor (SNARE) complex and the synaptic vesicle cycle. As a player in vesicle trafficking, α-syn can remodel and sense membrane curvature (Sulzer and Edwards, 2019) and can convert large vesicles into highly curved membrane tubules and vesicles (Varkey et al., 2010). At higher levels, it may also target mitochondrial membranes being a possible reason for its toxicity in PD patients (Bendor et al., 2013).

Under pathological conditions, α-syn misfolds into different β-sheet rich oligomers or protofibrils, ultimately forming insoluble fibrils that aggregate into LBs and GCIs (Lashuel et al., 2013). Although the precise triggers of α-syn misfolding remain elusive, factors such as α-syn mutations, cellular stress, mitochondrial dysfunction, and increased levels of endogenous α-syn have been proposed to contribute to misfolding (Mehra et al., 2019). Posttranslational modifications (PTMs) such as phosphorylation, ubiquitination, nitration, and truncation enhance the aggregation-prone propensities of α-syn (Beyer and Ariza, 2013), and 90 % of pathological α-syn in LBs was shown to be phosphorylated at serine 129 (Fujiwara et al., 2002).

In addition to phosphorylated α-syn, LBs contain a mixture of more than 90 other proteins, including ubiquitin (Kuzuhara et al., 1988; Lowe et al., 1988), mitochondria-related proteins, and proteins involved in autophagy and aggresome formation (Wakabayashi et al., 2013). While the process of LB formation is thought to be one of the significant drivers of neurodegeneration (Mahul-Mellier et al., 2020), neurologically healthy patients with incidental Lewy body disease can also exhibit Lewy pathology, indicating that additional factors are required to cause neurodegeneration (Frigerio et al., 2011). In post-mortem studies, LBs do not always correlate with disease severity in PD patients (Colosimo et al., 2003; Parkkinen et al., 2008). So far, the role of pathological α-syn and LBs is not fully understood. Some hypothesize that LBs are formed to protect the cell from the toxic α-syn aggregates, while others suggest a direct effect of LBs on cell death (Dexter and Jenner, 2013; Lu et al., 2005;

Olanow et al., 2004). Cell- or region-dependent factors may also render selective neurons more vulnerable than others to Lewy pathology (Surmeier et al., 2017).

The following chapter dives further into the spreading of α-syn and Lewy pathology following specific patterns.

1.2.1 α-syn spreading

1.2.1.1 Prion-like spreading

Potential mechanisms of PD and MSA disease progression include prion-like cell-to-cell transmission of pathological α-syn where misfolded α-syn acts as a template for monomeric α-syn to generate more α-syn aggregates. It has been shown that α-syn spreads from neuron to neuron and recruits endogenous α-syn to form insoluble inclusions (Brundin and Melki, 2017; Desplats et al., 2009; Volpicelli-Daley et al., 2011). These α-syn seeds can propagate throughout the brain leading to a prion-like spreading of α-syn pathology (Goedert et al., 2017; Volpicelli-Daley and Brundin, 2018). Studies have shown that α-syn pathology propagates from mouse brain to grafted dopaminergic neurons and that it seeds aggregation in cultured human cells, as intercellularly transferred α-syn interacts with cytoplasmic α-syn (Hansen et al., 2011). Ten to 24 years after the transplantation of fetal dopaminergic neurons into PD patients' brains, LBs were found in the grafted cells indicating a host to graft transmission (Brundin and Kordower, 2012; Kordower et al., 2008; Li et al., 2016; Li et al., 2008). Interestingly, LBs were not found in patients who died 2-5 years after the surgery, suggesting that transplanted neurons require time to develop Lewy pathology (Kordower et al., 1995; Mendez et al., 2005; Olanow et al., 2003). Prusiner and colleagues confirmed the prion-like properties of α-syn, as α-syn from MSA patient brains seeded pathology in both cell and animal models (Prusiner et al., 2015).

1.2.1.2 Braak's hypothesis

Pathological α-syn is suggested to spread following specific patterns. According to Braak and colleagues, α-syn aggregates spread throughout the brain in six stages in PD. The pathology

starts in the dorsal motor nucleus of the glossopharyngeal and vagal nerves and in the anterior olfactory nucleus. Then, it ascends through the brain stem, and reaches the basal ganglia and other midbrain nuclei, in particular the SNpc, before finally affecting the neocortex (Braak et al., 2003). With more widespread Lewy pathology and neurodegeneration, motor symptoms worsen, and cognitive functions decline (Braak et al., 2006; Irwin et al., 2017).

Others, however, discovered that the spreading of LBs is less predictable than proposed in the Braak's staging system, not following a strictly caudal-rostral progression pattern (Jellinger, 2009; Kalaitzakis et al., 2008). Upon post-mortem analyses of 417 PD patients, Braak's staging system was applicable to only around half the patients analyzed (Beach et al., 2009). Thus, other models, including the gut-brain axis and the α-syn origin site and connectome (SOC) model, were proposed, which will be explained here.

1.2.1.3 Gut-brain axis in PD

Next to spreading within the CNS, α-syn pathology can propagate from the CNS to the peripheral nervous system (PNS) and vice versa (Breen et al., 2019; Ulusoy et al., 2017). Lewy pathology could originate in the vagal dorsal motor nucleus and progress to the spinal cord and the gut in an anterograde fashion. Alternatively, it could start in the gut and advance retrogradely to the brain via the vagal nerve. Supporting the existence of a gut-brain axis in PD, Lewy pathology was found in the gastrointestinal tract of patients up to 20 years prior to their PD diagnosis (Stokholm et al., 2016). Animal models support the hypothesis of a gut-brain axis as duodenum-injected α-syn leads to the spreading of α-syn pathology along the whole axis and in the brainstem (Kim et al., 2019; van den Berge et al., 2019). In some animal and human studies, vagotomy reduced the risk of PD, indicating that a connection between the gut and brain is relevant in the pathogenesis of PD (Liu et al., 2017; Pan-Montojo et al., 2012; Svensson et al., 2015; Tysnes et al., 2015). In another animal model, intrastriatal or enteric injection of LB extracts from PD patients induced nigrostriatal lesions and enteric nervous system pathology, demonstrating a two-way spreading of α-syn. In contrast to the hypothesis of vagal α-syn spreading, no α-syn pathology was found in the vagal nerve (Arotcarena et al., 2020). Next to the possible involvement of the vagus nerve, inflammatory reactions in the gut may also play a role in the development of α-syn pathology. In vivo, intestinal inflammation

increased cerebral α-syn accumulation in mice models (Kishimoto et al., 2019). Patients suffering from inflammatory bowel disease (IBD) are more likely to develop PD than those not affected by IBD, suggesting once more that inflammation in the gut may promote α-syn aggregation (Peter et al., 2018; Villumsen et al., 2019). Interestingly, α-syn pathology is not only limited to the brain and the gut, but the sympathetic cardiac nerve, heart tissue, and skin may be affected as well (Donadio et al., 2016; Orimo et al., 2008).

1.2.1.4 α-syn origin site and connectome (SOC) model

Recently, a new model has been proposed to explain different disease courses in PD patients. According to the α-syn origin site and connectome (SOC) model, the spreading of α-syn depends on the anatomical location of the initial α-syn aggregates and the ipsilateral connectivity of the brain (Borghammer, 2021). When α-syn pathology first appears in the CNS, in the case of the so-called brain-first subtype of PD, it is usually unilateral and often present in the amygdala. Due to the connectivity, pathology spreads in the ipsilateral hemisphere, especially to the substantia nigra. This leads to the asymmetric formation of α-syn aggregates and asymmetric degeneration of dopaminergic neurons resulting in asymmetric motor symptoms. In the case of the body-first subtype, however, α-syn pathology begins in the PNS and ascends via the gut-brain axis through the vagal nerve to the right and left dorsal motor nuclei of the vagal nerve (DMV). Therefore, α-syn aggregates spread more symmetrically, inducing symmetric dopaminergic degeneration. Clinical imaging data also confirms symmetric versus asymmetric dopaminergic cell loss for body-first vs. brain-first subtypes (Knudsen et al., 2021). The SOC model is further supported by imaging data in early PD and isolated rapid-eye-movement sleep behavior disorder (IRBD) patients (Horsager et al., 2020).

Braak's staging system suggesting initial α-syn pathology in the olfactory bulb (OB) with subsequent spreading to other regions was successfully modeled in vivo (Braak et al., 2003; Rey et al., 2018). However, this could also represent a form of body-first PD, as isolated OB pathology does not exclude the possible existence of pathological α-syn in the gut before the DMV is affected (van den Berge and Ulusoy, 2022). In rare cases of multiple disease onsets, Lewy pathology may spread multifocally, driving disease progression in an accelerated manner (Borghammer et al., 2021). Future investigations using animal models simulating the brain-first

or body-first subtype may deepen our understanding of α-syn spreading mechanisms. However, it is worth noting that anatomic differences between humans and rodents could affect spreading patterns.

1.2.2 Animal models with α-syn-fibrils

Several animal models were developed to reproduce the pathophysiology of α-synucleinopathies. For instance, these models are based on overexpression of wild-type α-syn, expression of PD-linked α-syn mutations, viral vectors inducing α-syn overexpression, or injection of in vitro-generated α-syn oligomers or fibrils into transgenic mice (Wong and Krainc, 2017). A promising animal model to study α-synucleinopathies is the intracerebral injection of pre-formed fibrils (PFFs) generated from recombinant α-syn proteins. Luk et al. were one of the first to apply this in a mouse model (Luk et al., 2012a), followed by others who injected the α-syn PFFs into other rodents and primates (Paumier et al., 2015; Shimozawa et al., 2017). Recasens et al. inoculated PD-derived LB extracts in mice and monkeys by intranigral or intrastriatal injection resulting in progressive nigrostriatal neurodegeneration (Recasens et al., 2014). Host neurons quickly internalized human α-syn and triggered aggregation of endogenous α-syn (Recasens et al., 2014). Shimozawa et al. obtained similar results after intracerebral injection of recombinant α-syn into marmoset brains (Shimozawa et al., 2017).

Injection of α-syn PFFs induces the formation of phosphorylated α-syn aggregates, which are proteinase-K-resistant and thioflavin-S-positive, and colocalize with ubiquitin and p62 similar to human LBs (Dauer Née Joppe et al., 2021; Paumier et al., 2015). After propagation in a mouse model, recombinant and brain-derived α-syn strains present variable clinical and pathological manifestations (Lau et al., 2020). Factors influencing α-syn pathology include disease incubation periods, regional and cellular vulnerability to α-syn aggregates, and structural conformation of these aggregates. Table 1 provides an overview of different mouse models with intracerebral injection of human or mouse α-syn fibrils and the main findings of each model.

Source	Material injected	Dose	Injection site	Animal model	Duration	Finding
Luk et al., 2012a	recombinant mouse α-syn PFF	5 µg	striatum	C57BL6 /C3H	30, 90, 180 dpi	pS129-α-syn pathology at 30+ dpi, TH+ cell loss in the SNpc at 90+ dpi
Masuda-Suzukake et al., 2014	recombinant mouse α-syn fibrils	10 µg	SN, striatum, or entorhinal cortex	C57BL/ 6J	1 month p.i.	propagation of phosphorylated α-syn pathology depending on the injection site, phosphorylated tau and TDP-43 pathologies
Duffy et al., 2018a	chimeric human or mouse α-syn PFF	5 µg	striatum	C57BL6 /C3H	14, 30, 90, 180 dpi	pS129-α-syn pathology at 14+ dpi for mouse PFFs and 30+ for human PFFs, TH+ cell loss in the SNpc at 180 dpi for mouse PFFs and none for human PFFs
Fares et al., 2016	recombinant human or mouse α-syn PFF	5 µg	striatum	C57BL6 /C3H	30 dpi	pS129-α-syn pathology at 30 dpi, more pathology induced by mouse than by human PFFs
Sorrentino et al., 2017	recombinant human or mouse α-syn PFF	4 µg (bilateral)	striatum	M20 WT Hu aSyn	120 dpi	pS129-α-syn pathology and TH+ cell loss in the SNpc at 120 dpi, microglia activation and astrogliosis
Milanese et al., 2018	human α-syn PFF generated from monomeric α-syn	5 µg	striatum	C57BL/ 6	4 months p.i.	pS129-α-syn pathology and TH+ cell loss in the SNpc at 120 dpi, DNA damage
Peng et al., 2018	sarkosyl-insoluble α-syn from MSA and PD brains or mouse α-syn PFF	50 ng sarkosyl-insoluble α-syn or 6.25 µg mouse PFF in C57BL6/C3H, 18.75 ng α-syn in KOM2	striatum or thalamus	C57BL6 /C3H or KOM2	1, 3 and 6 months p.i.	more neuronal pathology induced by α-syn from MSA brains than from PD brains, strain-dependent spreading pattern, distinct α-syn strains are generated by different intracellular milieus

Rey et al., 2018	recombinant human or mouse α-syn PFF	4 µg	olfactory bulb	C57BL/6J	270, 540, 690 dpi	pS129-α-syn pathology at 270 dpi for mouse PFFs with decrease after 18 months, pS129-α-syn pathology at 270+ for human PFFs
Mavroeidi et al., 2019	human α-syn PFF generated from monomeric α-syn	4 µg	striatum	C57BL6/C3H	30 dpi	LB-509 haSyn+ and Syn303+ aggregates in MBP+ oligodendrocytes at 30 dpi
Earls et al., 2020	recombinant human α-syn PFF	5 µg	striatum	M83 A53T Hu aSyn	70 dpi	pS129-α-syn pathology at 70 dpi, no TH+ cell loss in the SNpc, microglia activation and NK cell infiltration, exacerbated α-syn pathology upon NK cell depletion
Lau et al., 2020	recombinant human A53T α-syn fibrils, M83+/+ extract or MSA extract	1 µg	hippo-campus or thalamus	hemizy-gous TgM83 mice	sacrificed at end-stage disease	strain-specific differences for neurological illness, disease onset, morphology of α-syn aggregates and conformational properties
Marotta et al., 2021	LB-derived α-syn from diseased brains or recombinant human α-syn PFFs	500 ng of amplified LBs or 5 µg of PFFs	striatum	C57BL6/C3H	6 months p.i.	more pronounced pS129-α-syn pathology for brains injected with amplified LBs than with PFFs

Table 1: Overview of mouse models with intracerebral injection of human or mouse α-syn fibrils. Sources were selected corresponding to the review of Polinski (Polinski, 2021) and by Pubmed search on the 9/10/2023 for *alpha-synuclein spreading, alpha-synuclein fibril, alpha-synuclein preformed fibril, alpha-synuclein PFF injection, alpha-synuclein striatum, and alpha-synuclein strains*, with focus on mouse models with intracerebral injection of human PFFs. dpi, days post injection. TH, tyrosine hydroxylase.

1.2.3 Different conformations and strains of α-syn

α-syn can adopt different conformations, including monomers, tetramers, oligomers, and fibrils (Wong and Krainc, 2017). The exact mechanism of how α-syn monomers are formed into α-syn fibrils is unclear. However, the formation of α-syn oligomers is thought to be required in this process (Chen et al., 2015; Iljina et al., 2016). Researchers have suggested that oligomers are the more toxic form, as α-syn mutants that promote oligomer formation induced more dopaminergic cell loss than those favoring fibril formation (Winner et al., 2011). PD-linked α-syn mutations (A53T and A30P) accelerated oligomerization but not fibrilization (Conway et al., 2000). In contrast, others demonstrated that fibrils are the most toxic form (Pieri et al., 2012). Injection of different α-syn aggregates into the SN of rats showed that α-syn fibrils induced more motor symptoms, dopaminergic cell loss, and synaptic impairment than α-syn ribbons or oligomers (Peelaerts et al., 2015).

Animal models do not only differ in the conformation of misfolded α-syn injected into the animals but also in the strains of α-syn applied. Different α-syn strains were indicated to have distinct levels of toxicity, seeding, and propagation properties explaining disease-specific variability (Bousset et al., 2013). Distinct α-syn strains also varied in their efficiency to cross-seed tau aggregation (Guo et al., 2013). For instance, α-syn forming Lewy pathology was less potent in seeding aggregates than α-syn associated with GCIs (Peelaerts et al., 2015; Peng et al., 2018). Previously, MSA brain extracts were injected into heterozygous mice transgenic for A53T α-synuclein, which expresses the human mutant protein predominantly in neurons (Prusiner et al., 2015). These injections led to the formation of α-syn inclusions and their spreading. MSA extracts also induced α-syn inclusions in cultured human embryonic kidney cells expressing mutant human α-syn (Woerman et al., 2015). PD extracts, in contrast, did not cause α-syn pathology in these cell cultures (Prusiner et al., 2015; Woerman et al., 2015).

1.3 Aims of this thesis

This doctoral thesis aims to investigate the propagation of α-syn in the mouse brain after injection of α-syn fibrils amplified from brain homogenates of two MSA and two PD patients. Different α-syn strains with distinct properties have previously been described. However, interindividual strain variability and their effects on α-syn seeding and aggregation are yet to be elucidated. Thus, the two main questions are whether α-syn pathology and spreading differ between the MSA- and PD-fibril injected groups and whether individual differences within the same disease entity can be found to explain variable disease phenotypes. Immunohistochemical staining against pS129-α-syn was employed to detect pathological α-syn aggregation. To reveal further effects induced by the injection of the patient material-amplified fibrils, microglia, astrocytes, and dopaminergic neurons in the SNpc were quantified, as well as the colocalization between pS129-α-syn and the oligodendrocytic marker 2',3'-cyclic nucleotide-3'-phosphodiesterase (CNPase).

2 Material and Methods

2.1 Material

2.1.1 Reagents

Reagent	Supplier
Bovine serum albumin (BSA)	Sigma Aldrich (Taufkirchen, Germany)
Citric acid monohydrate	Merck Millipore (Darmstadt, Germany)
4‘,6-Diamidino-2-Phenylindole (DAPI)	Thermo Fisher Scientific (Waltham, USA)
EcoMount	Biocare Medical (Pacheco, USA)
Enthellan	Merck Millipore (Darmstadt, Germany)
Ethanol absolute for molecular biology	Applichem (Darmstadt, Germany)
Gibco DPBS 1x	Thermo Fisher Scientific (Waltham, USA)
Glycine	AppliChem (Darmstadt, Germany)
Isopropanol	AppliChem (Darmstadt, Germany)
Methanol	Merck Millipore (Darmstadt, Germany)
Normal goat serum (NGS)	Cedarlane (Burlington, Canada)
Hydrogen peroxide 33% (H_2O_2)	AppliChem (Darmstadt, Germany)
Sodium citrate	Sigma Aldrich (Taufkirchen, Germany)
TritonX 100	AppliChem (Darmstadt, Germany)
Xylene	Sigma Aldrich (Taufkirchen, Germany)

2.1.2 Solutions

Solution	Composition
Blocking solution for immunofluorescence staining	5 % NGS, 5 % BSA, 0.3 % TritonX, 25 mM Glycine in PBS
Blocking solution for anti-TH staining	5 % NGS, 0.05 % TritonX in PBS
Citrate buffer (10 mM)	Mix 41.5 mL of 0.1 M Sodium citrate and 9.5 mL of 0.1 M Citric acid for 50 mL of 100 mM

	Citrate buffer, dilute 1:10 for 10 mM Citrate buffer
DAPI solution	1 µg/mL DAPI in PBS

2.1.3 Primary antibodies

Antibody	Origin	Clonality	Supplier
Anti-pS129-α-syn (EP1536Y)	Rabbit	Monoclonal	Abcam (Cambridge, UK)
Anti-CD68 (FA-11, ab53444)	Rat	Monoclonal	Abcam (Cambridge, UK)
Anti-CNPase (ab6319)	Mouse	Monoclonal	Abcam (Cambridge, UK)
Anti-GFAP (13-0300)	Rat	Monoclonal	Invitrogen (Waltham, USA)
Anti-Iba1 (019-19741)	Rabbit	Polyclonal	Fujifilm Wako (Osaka, Japan)
Anti-Iba1 (011-27991)	Goat	Polyclonal	Fujifilm Wako (Osaka, Japan)
Anti-tyrosine hydroxylase (620-0336)	Rabbit	Polyclonal	Zytomed (Berlin, Germany)

2.1.4 Secondary antibodies

Origin	Target	Labelling	Supplier
Goat	Anti-rabbit	Cy3 (111-165-003)	Jackson ImmunoResearch (West Grove, USA)
Donkey	Anti-goat	Alexa Fluor 647 (A32849)	Invitrogen (Waltham, USA)
Goat	Anti-rat	Alexa Fluor 488 (A-11006)	Invitrogen (Waltham, USA)
Goat	Anti-mouse	Alexa Fluor 488 (A32723)	Invitrogen (Waltham, USA)
Goat	Anti-rabbit	Biotinylated (111-065-003)	Jackson ImmunoResearch (West Grove, USA)

2.1.5 Kits

Kit	Supplier
Vectastain ABC PK-4004 Peroxidase Kit	Vector Laboratories (Burlingame, USA)
DAB SK 4100 Substrate Kit, Peroxidase	Vector Laboratories (Burlingame, USA)

2.1.6 Equipment

Equipment	Supplier
Axio Observer Z1 microscope	Zeiss (Oberkochen, Germany)
Tissue-Tek® O.C.T.™ Compound	Sakura Finetek (Alphen aan den Rijn, Netherlands)
Cryostat CM 3050S	Leica Microsystems (Wetzlar, Germany)
ImmEdge pen	Vector Laboratories (Burlingame, USA)
Microscope Cover Glasses	VWR International (Radnor, USA)
SuperFrost Plus Microscope Slides	Thermo Fisher Scientific (Waltham, USA)

2.1.7 Software

Software	Supplier
AxioVision (Rel. 4.8)	Zeiss (Oberkochen, Germany)
Ilastik (version 1.3.3post3)	Open source
ImageJ (version 1.53c)	Open source
RStudio (version 1.4.1106)	Open source
Inkscape (version 1.1)	Open source

2.2 Methods

The workflow and exemplary images for immunohistochemical stainings are shown in Figures 1 and 2. In summary, adult C57Bl6/J mice were injected with α-syn fibrils amplified from brain homogenates of two MSA patients and two PD patients, or α-syn monomers as a control. At 12 weeks post-injection, mice were sacrificed, and their brains were cryosectioned. Immunohistochemical stainings were performed, and the brain sections were imaged by fluorescence microscopy and analyzed using ImageJ, ilastik, and RStudio.

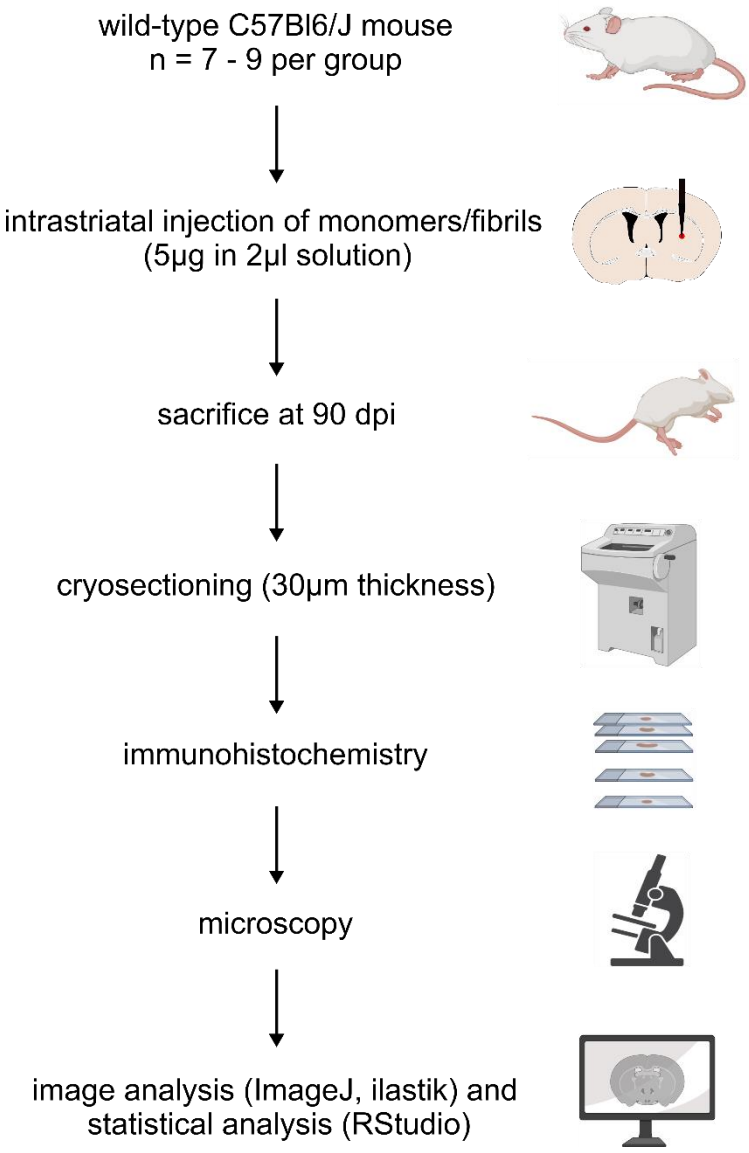

Figure 1: Workflow of the study. Fibril injection in wildtype mice, cryosectioning, immunohistochemical staining, microscopy, image analysis and statistical analysis. dpi, days post injection. Adapted from (Zhang et al., 2023).

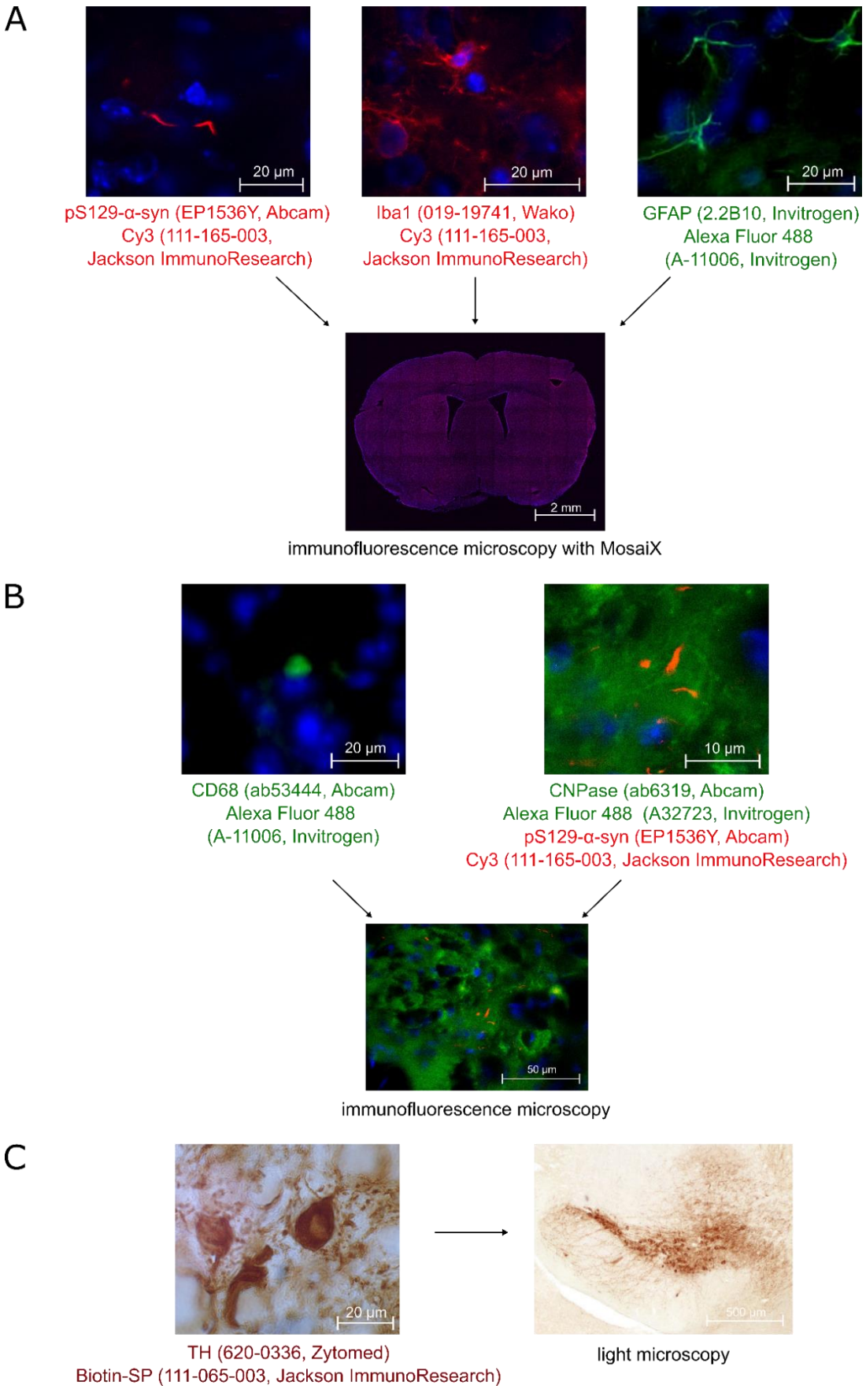

Figure 2: Immunohistochemistry. Antibodies used for immunohistochemical analyses are indicated below representative images. CNPase, 2',3'-cyclic nucleotide-3'-phosphodiesterase. GFAP, glial fibrillary acid protein. TH, tyrosine hydroxylase. Adapted from (Zhang et al., 2023).

2.2.1 Generation of α-syn fibrils and α-syn monomers

The α-syn fibrils used in this study were kindly provided by the lab of Prof. Dr. Markus Zweckstetter, Göttingen, and the α-syn monomers by the lab of Dr. Stefan Becker, Göttingen. Methods for the generation of α-syn fibrils and α-syn monomers as performed in the labs of Zweckstetter and Becker are summarized in brief:

For the generation of α-syn fibrils, α-syn aggregates were amplified from brain extracts of patients pathologically confirmed with PD and MSA using protein misfolding cyclic amplification (PMCA) (Strohäker et al., 2019). These PMCA-amplified amyloid fibrils were used to seed recombinant α-syn to gather larger quantities for further analysis (Strohäker et al., 2019). Table 2 shows the demographic information on the brain samples used for α-syn fibril amplification and the number of animals for each treatment group.

Group	Patient/Source	Disease duration (years)	Age at death	Sex	Cause of death	Number of mice injected
PD	PD1	7	79	M	Acute myocardial infarction	8
	PD2	8	82	F	Pneumonia	7
MSA	MSA1	7	82	M	Cardiorespiratory failure	7
	MSA2	6	71	F	Hypostatic pneumonia	8
α-syn monomer	recombinantly expressed from Escherichia coli	n. a.				8

Table 2: Information of patient material and monomer used in this study. The number of mice injected with each fibril/monomer preparation is given additionally. Adapted from (Zhang et al., 2023).

N-terminally acetylated α-syn was produced by co-transfecting Escherichia coli BL21 (DE3) cells with pT7-7 plasmid encoding for human α-syn, which were kindly provided by the Lansbury Laboratory, Harvard Medical School, Cambridge, MA, and Schizosaccharomyces pombe NatB acetylase complex (Johnson et al., 2010) using pNatB plasmid (pACYCduet-naa20-naa25,

Addgene, #53613, kindly provided by Dan Mulvihill). Proteins were expressed and purified as previously described (Hoyer et al., 2002).

α-syn fibrils were produced at 37 °C from monomeric, N-terminally acetylated α-syn taken from the supernatant of freshly thawed α-syn on ice after ultracentrifugation with the Beckman Coulter Optima MAX-XP using a TLA 100.3 rotor at a rotor speed of 55,000 rpm. 0.5% (w/w) PMCA product was added to 250 µM αSyn stock solution (50 mM HEPES, 100 mM NaCl, pH 7.4, 0.02% NaN3). This mixture was water bath sonicated for 10 minutes and then aggregated under quiescent conditions in 1.5 mL Eppendorf cups in a ThermoScientific Heratherm incubator.

2.2.2 Animal experiments

Karina Dauer kindly performed the animal experiments in Göttingen. Wild-type C57BI6/J male mice (RRID: IMSR_JAX:000664) were used in our animal experiments. The animals were acquired from Charles River (Wilmington, USA). They were treated according to the regulations of the local animal research council and the EU Directive 2010/63/EU for animal experiments. According to the legislation of the State of Lower Saxony, Germany (ethics approval number: 33.9-42502-04-15/1982), the exploratory study has received approval from the institutional ethics committee.

Mice were accommodated in the Central Animal Care Unit of the University Medical Center Göttingen, Germany, and were housed in individually ventilated cages (IVC, Tecniplast). They received standard ad libitum food, water, and had a 12-hour dark/light cycle. No exclusion criteria were pre-determined, and no randomization was performed to allocate subjects to the study. This study was not pre-registered. In total, 42 male mice were used in this study. The average body weight of all mice was 25.4 g.

Mice were injected according to the protocol from Dauer et al. 2021 at the age of 12 weeks (Dauer Née Joppe et al., 2021). α-syn monomers or fibrils were diluted in 50 mM HEPES buffer, and 5 µg of monomer or fibril in 2 µL of volume were injected into the right striatum (anteroposterior axis + 0.4 mm; mediolateral axis −1.8 mm; dorsoventral axis −3.5 mm relative

to Bregma). α-syn fibrils were sonicated before the injection for 30 sec in one cycle at 10 % power (Bandelin Sono Plus, Bandelin, Berlin, Germany).

There were four treatment groups (PD1 n=8, PD2 n=7, MSA1 n=7, MSA2 n=8) and one control group (monomeric α-syn n=9). Three mice died due to complications of the surgery.

Metamizole (1.5 mg/mL) was given to the animals two days before and two days after the injection as an analgesic treatment. For the surgery, mice received anesthesia by intraperitoneal injection of ketamine (150 mg/kg body weight) and xylazine (10 mg/kg body weight) and were fixed in a stereotactic frame. Eyes were protected with an eye ointment and incision and trepanation were performed. α-syn monomers or fibrils in the aforementioned solution were injected at an injection rate of 500 nL/min using a glass capillary of 100 µm diameter and a microinjector (Micro 4, World Precision Instruments, Friedberg, Germany). The injection capillary was left in place for 4 min before it was slowly removed to prevent reflux. Finally, the incision was closed with tissue glue (DermaBond, Ethicon, Raritan, USA). Animals were placed on a warming pad until they woke up and were eventually returned to their home cage.

Ninety days post-injection, the animals were sacrificed by a lethal intraperitoneal injection of ketamine (300 mg/kg body weight) and xylazine (15 mg/kg body weight) solution. Mice were transcardially perfused with 50 mL ice-cold PBS within 5 min under deep anesthesia. After another perfusion with 50 mL of 4 % paraformaldehyde (PFA, Applichem, Darmstadt, Germany) at pH 7.4 within 5 min, the mouse brains were removed. Brains were fixed in 4 % PFA/PBS for 24 h at 4 °C, transferred into 30 % sucrose in PBS for cryopreservation, and frozen at -80 °C.

2.2.3 Cryosectioning

Using a Leica CM3050S Cryostat (Leica, Wetzlar, Germany), complete coronal sections of all 39 brains were prepared at a thickness of 30 µm at -20 °C. Eleven regions were selected based on critical anatomical hallmarks for immunohistochemical staining and defined by their distance to Bregma according to the Paxinos Brain Atlas (Paxinos and Franklin, 2019): + 1.54 mm, + 1.18 mm, + 0.38 mm, + 0.26 mm, + 0.02 mm, - 0.34 mm, - 1.34 mm, - 1.58 mm, - 3.08 mm, - 3.16 mm, - 3.28 mm. All these sections were stained for pS129-α-syn and Iba1.

2.2.4 Immunohistochemistry

Immunohistochemical stainings were performed as previously described (Dauer Née Joppe et al., 2021).

At first, sections were taken out of the freezer and dried at 21 °C for 45 min. Then, they were rehydrated in PBS for 15 min before being steamed at 80°C in 10 mM citrate buffer (pH = 6.0) for 30 min. Sections were washed in PBS two times for 5 min and incubated in 25 mM glycine in PBS for 20 min. After another two times of washing for 5 min in PBS, sections were incubated in blocking solution (5 % NGS, 5 % BSA, 0.3 % TritonX, 25 mM Glycine in PBS) for 60 min and washed for 5 min in PBS. The primary and secondary antibodies were diluted in a blocking solution, according to Table 3. Sections were incubated overnight with the primary antibodies in a moist chamber at 4 °C. The following day, sections were washed three times for 10 min in PBS and incubated with the secondary antibody in a dark chamber for 60 min at 21°C. Sections were rewashed three more times for 10 min in PBS and incubated in 1 µg/mL DAPI in PBS for 5 min. Following another washing step in PBS with two times for 10 min, sections were dried at 37 °C in an incubator for 10 min. Finally, they were mounted with EcoMount and stored in a 4 °C fridge before microscopy.

To visualize the dopaminergic neurons in the SN, we also stained three sections at around Bregma + 3.00 mm, + 3.15 mm, and + 3.30 mm for tyrosine hydroxylase (TH). Sections were dried for 45 min at 21 °C before rehydrating in PBS for 10 min. Then, they were incubated in PBS with 40 % methanol and 1 % H_2O_2 followed by washing with PBS three times for 5 min. Sections were blocked for 60 min using a solution consisting of 5 % normal goat serum and 0.05 % Triton X-100 in PBS. Following an incubation period of 24 h with the primary anti-TH antibody (diluted 1:1000 in 2.5 % NGS and 0.025 % TritonX in PBS) at 4 °C, sections were washed three times for 5 min. Afterwards, they were incubated for 2 h with the biotinylated secondary antibody (diluted 1:200 in 2 % NGS in PBS). The tissue was washed another three times for 5 min and incubated in the Vectastain ABC Peroxidase Kit for 2 h to enhance the signal before it was rewashed. To visualize the TH-staining with 3,3'-Diaminobenzidine, sections were then incubated for 8 min in the Vector DAB substrate kit (2 drops DAB Reagent 1, 4 drops DAB reagent 2, 2 drops DAB Reagent 3). The reaction was stopped in distilled water for 5 min, and the slides were washed in PBS twice for 5 min. Finally, slides were mounted with Entellan and dried at 21 °C.

Primary antibody with dilution	Secondary antibody with dilution	Regions related to Bregma (in mm)	ROIs for microscopy imaging	Imaging magnification	Number of sections analyzed
anti-pS129-α-syn (EP1536Y) 1:500	Cy3 (111-165-003) 1:250	+ 1.54, + 1.18, + 0.38, + 0.26, + 0.02, - 0.34, - 1.34, - 1.58, - 3.08, - 3.16, - 3.28	Right and left hemisphere	10x	392 (MSA1 = 70, MSA2 = 86, PD1 = 87, PD2 = 71, Monomer = 78) (392 MosaiX images)
anti-Iba1 (019-19741) 1:300	Cy3 (111-165-003) 1:250	+ 1.54, + 0.38, + 0.02, - 1.58, - 3.08, - 3.28	3 circular ROIs per hemisphere	10x	221 (MSA1 = 41, MSA2 = 47, PD1 = 47, PD2 = 41, Monomer = 45) (221 MosaiX images)
anti-Iba1 (011-27991) 1:250	Alexa Fluor 647 (A32849) 1:250	+ 1.18, + 0.26, - 0.34, - 1.34, - 3.16	3 circular ROIs per hemisphere	10x	85 (MSA1 = 14, MSA2 = 18, PD1 = 19, PD2 = 16, Monomer = 18) (85 MosaiX images)
anti-CD68 (FA-11, ab53444) 1:500	Alexa Fluor 488 (A-11006) 1:250	+ 1.18, + 0.26	1 circular ROI per hemisphere	10x	40 (MSA1 = 6, MSA2 = 11, PD1 = 10, PD2 = 5, Monomer = 8) (40 MosaiX images)
anti-CNPase (ab6319) 1:150	Alexa Fluor 488 (A32723) 1:150	+ 0.20	Systematic meandering through section, image taken when α-syn positive signal was detected	63x	30 (MSA1 = 7, MSA2 = 8, PD1 = 8, PD2 = 7) (264 images)
anti-GFAP (13-0300) 1:250	Alexa Fluor 488 (A-11006) 1:250	+ 1.18, + 0.26, - 0.34, - 1.34, - 3.16	3 circular ROIs per hemisphere	10x	166 (MSA1 = 28, MSA2 = 38, PD1 = 39, PD2 = 30, Monomer = 31) (166 MosaiX images)
anti-TH (620-0336) 1:1000	biotinylated (111-065-003) 1:200	+ 3.00, + 3.15, + 3.30	Right and left SNpc	5x	114 (MSA1 = 21, MSA2 = 24, PD1 = 21, PD2 = 24, Monomer = 24) (114 MosaiX images)

Table 3: Overview of immunohistochemical stainings. Primary and secondary antibody with dilutions, regions stained related to Bregma, regions of interest (ROIs), imaging magnification, and number of sections analyzed. Adapted from (Zhang et al., 2023).

2.2.5 Microscopy and image analysis

The mouse brain tissue was imaged using the Axio Observer Z1 (Zeiss, Oberkochen). To generate whole-brain sections, we used the MosaiX function in the AxioVision software with 10x magnification for immunofluorescence imaging. The anti-CNPase anti-α-syn co-staining was imaged with 63x magnification by meandering through the entire section. For the anti-TH staining, the SN was imaged separately with 5x magnification for each hemisphere.

Images of whole-brain sections were analyzed in ImageJ/Fiji (version 1.53c). For the pS129-α-syn staining, regions of interest (ROIs) were defined manually by outlining each hemisphere. The areas of the ROIs were quantified, and the channels were split. The background was subtracted in the red channel depicting the pS129-α-syn-positive signal, and a manual threshold was defined. A Kruskal-Wallis rank sum test to exclude bias due to manual thresholding indicated no significant difference between the thresholds of the five groups (Kruskal-Wallis chi-squared = 1.3457, df = 4, p-value = 0.8536) (Figure 3). The area of pS129-α-syn-positive aggregates was calculated for each hemisphere with the analyze particles function. This area was divided by the total area of the corresponding hemisphere.

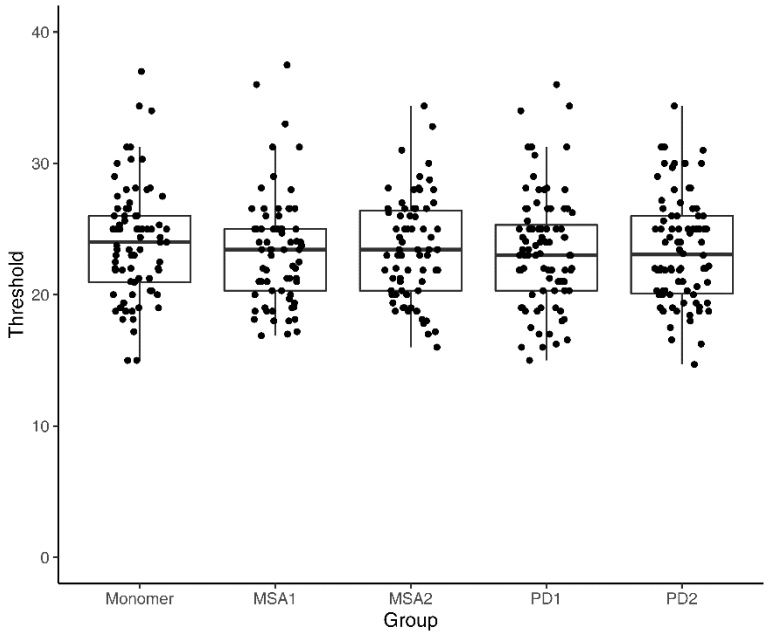

Figure 3: Manual threshold values for the pS129-α-syn analysis. Variance in threshold values due to weakening of microscopy lamp over the course of imaging for hundreds of hours.

The anti-Iba1-staining and the anti-GFAP-staining were analyzed by applying six circular ROIs defined for each brain section. After subtracting the background, an automatic threshold was set. The Iba1-/GFAP-positive area covering the total area of each ROI was quantified with the analyze particles function. For the anti-CD68-staining, a similar approach was used with only one circular ROI in the striatum. Sections at + 0.20 mm from Bregma were stained for the anti-CNPase/anti-α-syn double immunofluorescence staining. The images were analyzed using the JACoP plugin in ImageJ/Fiji (Bolte and Cordelières, 2006). Pearson's and Manders' coefficient were calculated for the original and the thresholded images.

For the analysis of the anti-TH DAB staining, ROIs were defined manually in ImageJ/Fiji by outlining the SNpc (Schindelin et al., 2012). The pixel classification function of the software ilastik (version 1.3.3post3) was used to create a mask for TH-positive cells (Berg et al., 2019). Finally, these were quantified in ImageJ/Fiji.

2.2.6 Statistical analysis

For statistical analysis, RStudio version 1.4.1106 was used. A Shapiro-Wilks test was applied to test for the normality of the data. An analysis of variance (ANOVA) was performed on normally distributed data, as in the anti-TH staining, to compare the different groups, and a paired t-test was used to compare both hemispheres. For not normally distributed data, such as on the anti-α-syn-staining, the anti-Iba1-staining, the anti-GFAP-staining, and the anti-CNPase-staining, a Kruskal-Wallis rank sum test with a post hoc Dunn's test was executed.

3 Results

3.1 α-syn spreading depends on the type of injected fibrils

Mice were injected with α-syn fibrils from patient PD1, PD2, MSA1, MSA2, or with monomeric α-syn as a control to assess α-syn pathology induced by different fibrils. After quantification of the pS129-α-syn-positive area for each hemisphere, we found significant differences in the amount of α-syn-positive signal between the five groups (Figure 4, Figure 5).

Brains from the MSA2 group showed the highest abundance of pS129-α-syn-positive aggregates in the injected (right) hemisphere and the non-injected (left) hemisphere, followed by PD2 and MSA1 (Table 4). A Kruskal-Wallis rank sum test was performed on the not normally distributed data of the injected hemisphere (Kruskal-Wallis chi-squared = 18.8, df = 4, p-value = 0.0009 for all regions of the injected hemisphere). The pairwise comparison in the post-hoc Dunn's test with Benjamini-Hochberg p-value correction implied significant differences between PD1 and MSA2 (p = 0.0058), MSA1 and MSA2 (p = 0.0222) and MSA2 and control (p = 0.0004) (Figure 4A). For the non-injected (left) hemisphere, the Kruskal-Wallis rank sum test also indicated significant differences between the five groups (Kruskal-Wallis Chi-squared = 20.4, df = 4, p-value = 0.0004 for all the regions of the non-injected hemisphere). A Dunn's test with Benjamini-Hochberg p-value correction revealed significant differences between brains injected with α-syn fibrils from PD1 and MSA2 (p = 0.0166), PD2 and MSA2 (p = 0.0402), MSA1 and control (p = 0.0402) as well as MSA2 and control (p = 0.0001) (Figure 4B).

The injected hemisphere showed generally more α-syn pathology than the non-injected hemisphere (Figure 5). Little to no signal was found in the brains of the control group injected with α-syn monomers. Brains injected with the MSA2-derived fibrils were the most abundant in α-syn for both hemispheres, and brains injected with PD1-derived fibrils showed the lowest abundance among the fibril-injected groups (Figure 4, Table 4). Moreover, pS129-α-syn aggregates in the two MSA groups were larger and more variable in their morphology (Figure 6).

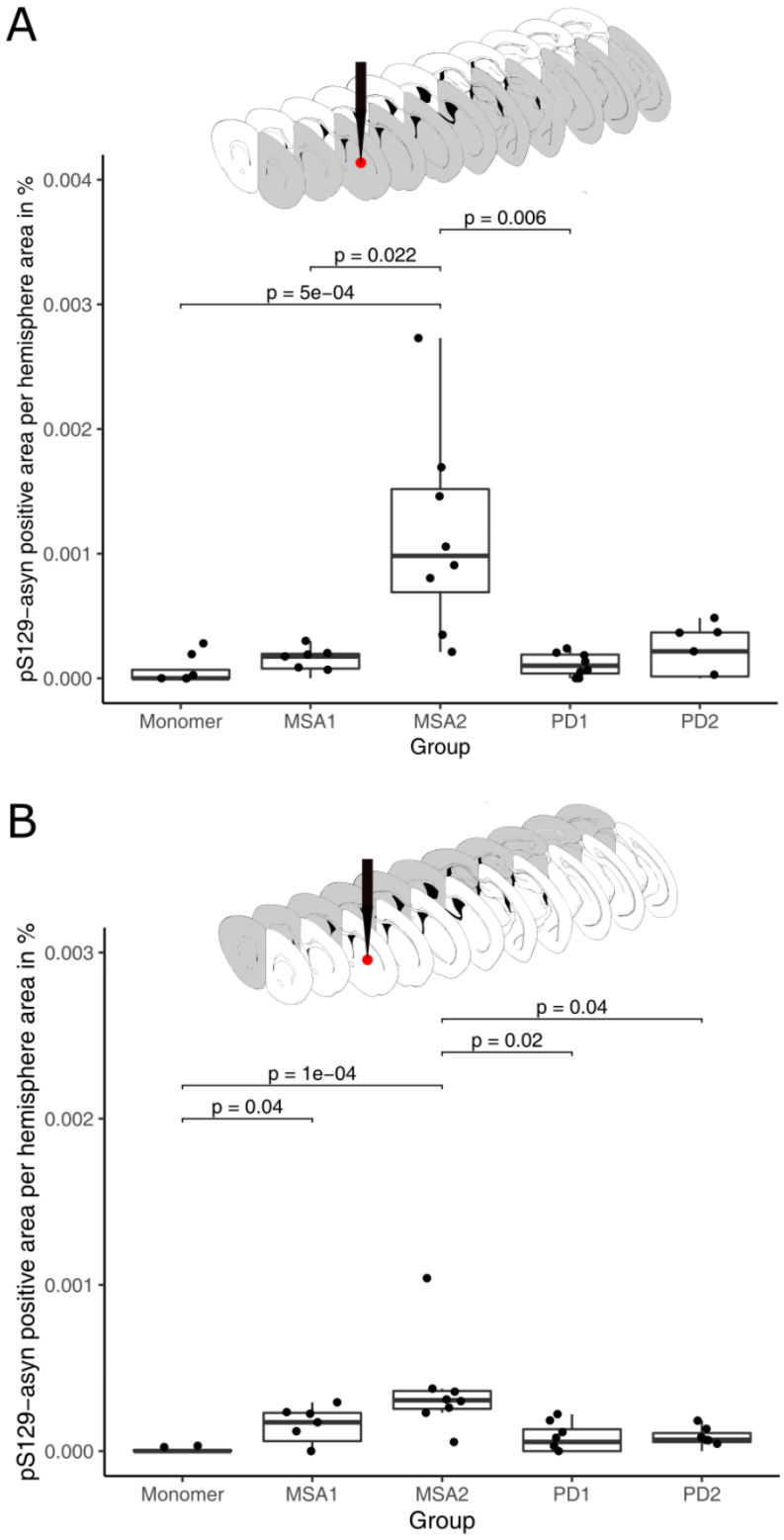

Figure 4: pS129-α-syn-positive signal in mouse brains injected with α-syn fibrils or monomers for all analyzed brain regions combined. Signal positive area per hemisphere area in the injected (A) and non-injected hemispheres (B), respectively. A p-value < 0.05 was considered significant according to the Kruskal-Wallis test and the Dunn's test. Adapted from (Zhang et al., 2023).

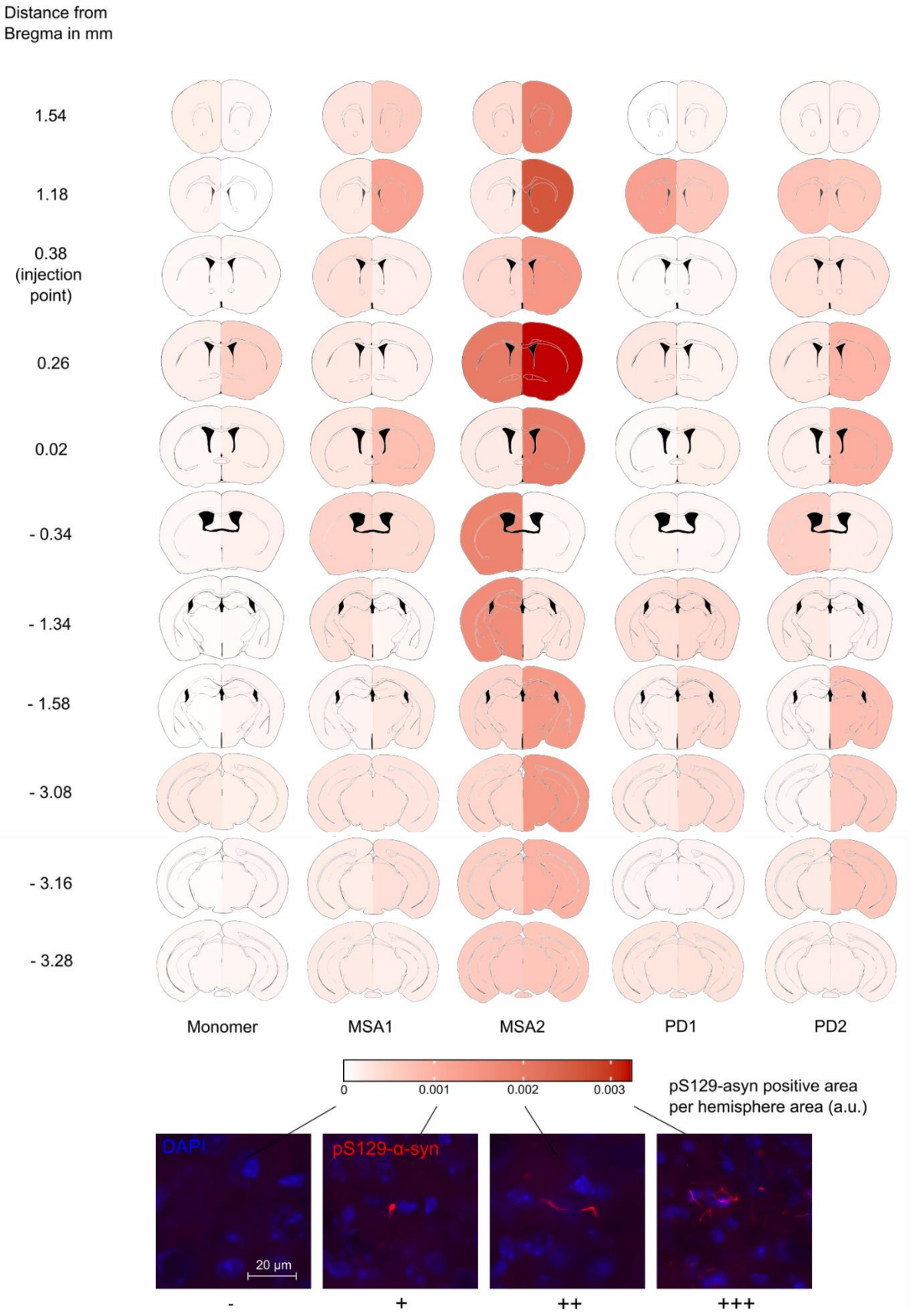

Figure 5: Heatmap of pS129-α-syn-positive aggregates. Data shown for the five treatment groups (MSA2, MSA1, PD2, PD1, α-syn monomer as control) and eleven regions throughout the brain with each hemisphere depicted separately. Injection point at 0.38 mm relative to Bregma. Pathology was graded from no aggregates (-) to high abundance of aggregates (+++). Adapted from (Zhang et al., 2023).

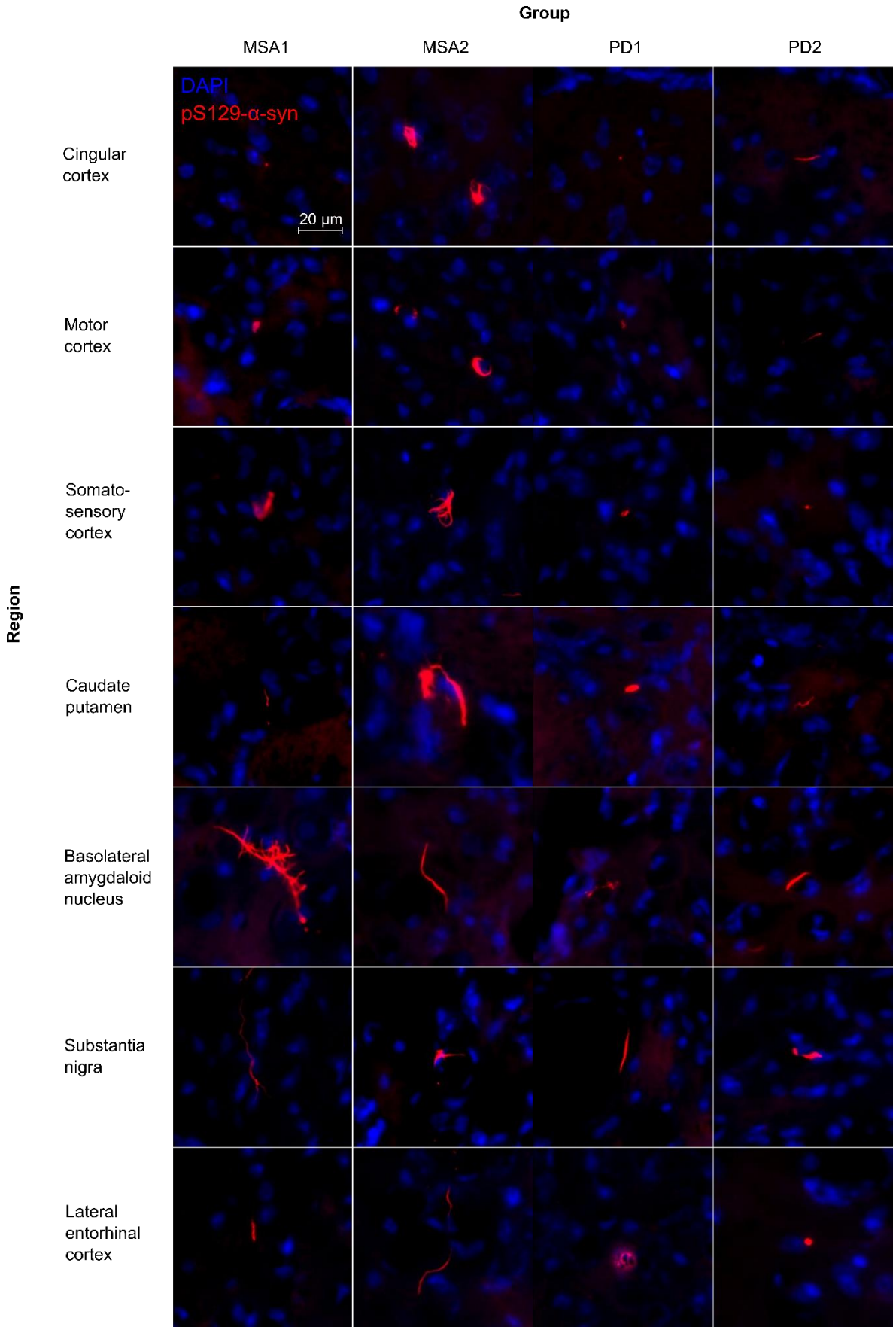

Figure 6: Morphology of α-syn aggregates in different brain regions for all four fibril-injected groups. Adapted from (Zhang et al., 2023).

3.2 Microglia infiltration depends on the type of injected fibrils

To assess microglial response to α-syn pathology, we quantified the signal of Iba1-positive microglia in eleven regions. Overall, significantly more Iba1-positive signal was detected in the injected hemispheres of MSA2- and PD2-fibril-treated mice compared to controls (p=0.06, respectively, according to Dunn's test with Benjamini-Hochberg p-value correction) (Figure 7A, Table 4). In the non-injected hemispheres, the Iba1-positive signal was not significantly different between the groups (Figure 7B). Iba1-positive microglia were found throughout the entire brain, though different levels of microglia activation were visible (Figure 8).

	pS129-α-syn right		**pS129-α-syn left**		**Iba1 right**		**Iba1 left**	
Group	Mean	SD	Mean	SD	Mean	SD	Mean	SD
Monomer	6.25E-05	1.10E-04	6.98E-06	1.30E-05	0.84	0.14	0.81	0.21
MSA1	1.46E-04	1.00E-04	1.49E-04	1.15E-04	1.17	0.36	0.85	0.15
MSA2	1.15E-03	8.10E-04	3.67E-04	2.90E-04	1.24	0.29	0.92	0.18
PD1	1.10E-04	9.38E-05	7.88E-05	8.78E-05	1.08	0.32	0.78	0.28
PD2	2.09E-04	2.02E-04	8.25E-05	5.99E-05	1.22	0.15	1.04	0.21

Table 4: Quantification of immunofluorescence for the anti-pS129-α-syn and the anti-Iba1-staining. Data represents signal-positive area/total ROI area and is given as mean and standard deviation [SD] for the right and left hemisphere, respectively. Adapted from (Zhang et al., 2023).

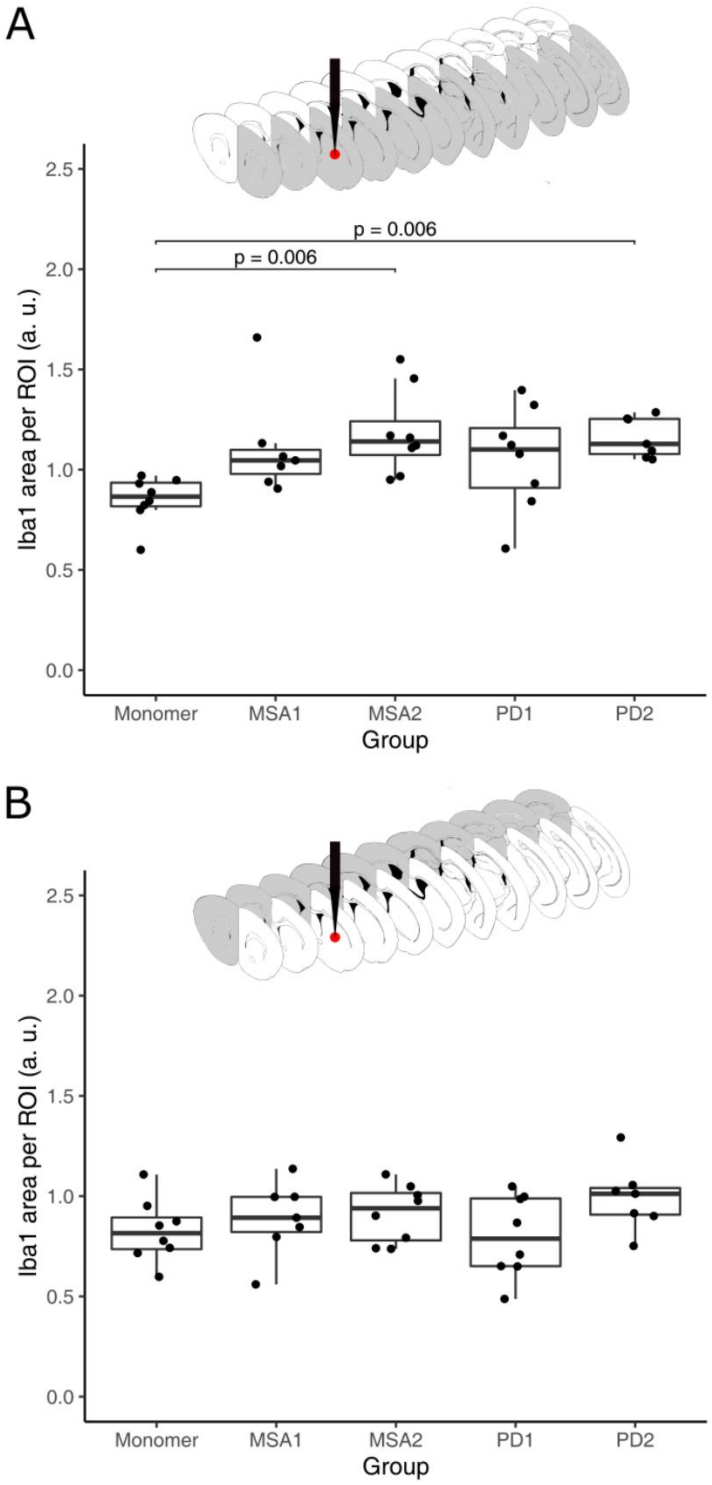

Figure 7: Iba1-positive signal per region of interest (ROI) in mouse brains injected with α-syn fibrils or monomers for all analyzed brain regions combined. Quantification by area of activated Iba1-positive microglia divided by the total area of ROI. Data shown for the injected (A) and the non-injected (B) hemisphere. A p-value < 0.05 was considered significant according to the Kruskal-Wallis test and Dunn's test. ROI, region of interest. Adapted from (Zhang et al., 2023).

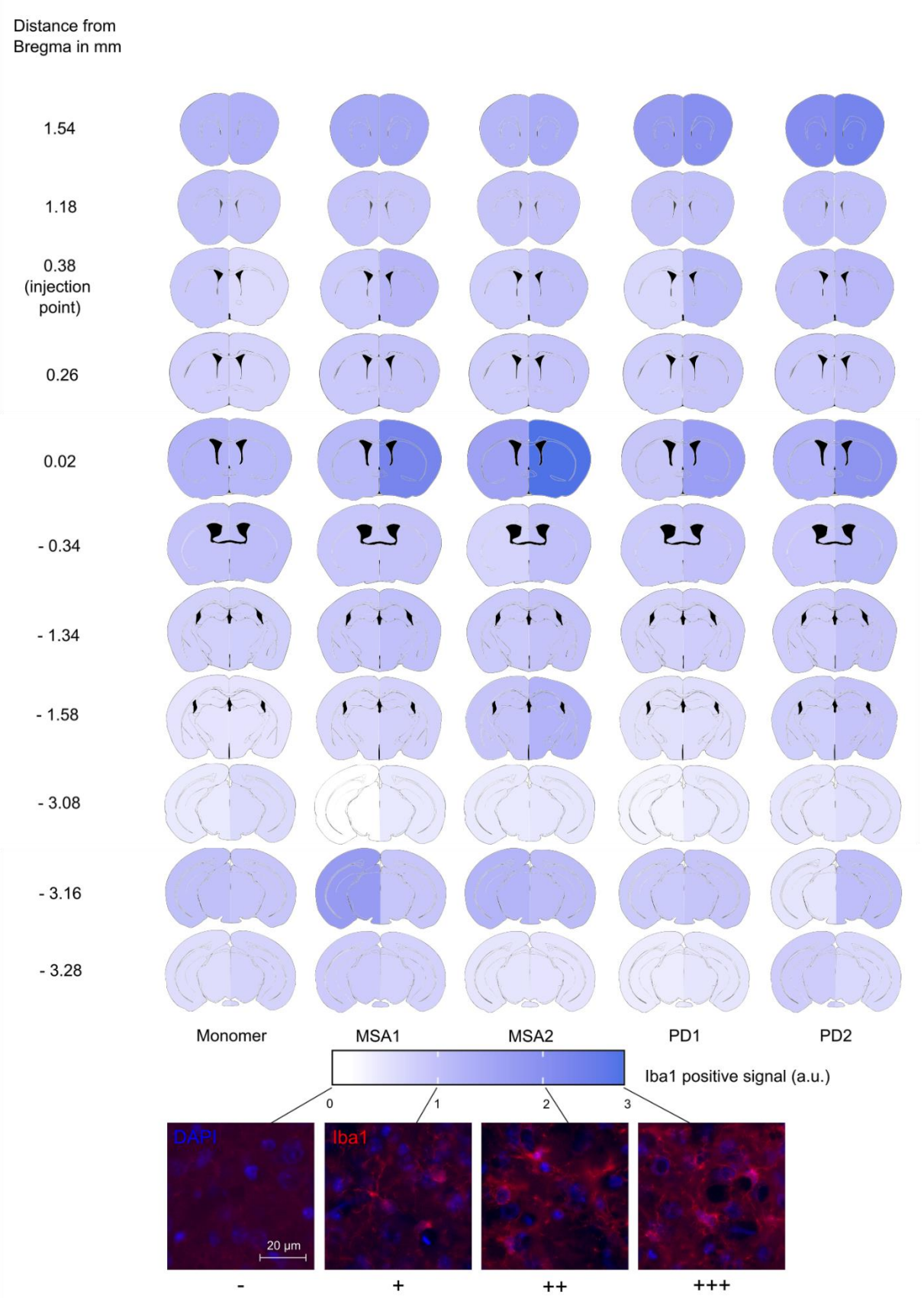

Figure 8: Heatmap of Iba1-positive signal. Data shown for all five treatment groups (MSA2, MSA1, PD2, PD1, α-syn monomer as control) and eleven regions throughout the brain. Injection point at 0.38 mm relative to Bregma. Iba1-positive signal ranging from no signal (-) to strongest signal (+++). Adapted from (Zhang et al., 2023).

To further analyze microglia activation, two regions (1.18 and 0.26 mm related to Bregma) were stained for CD68, a marker for macrophage lineage cells and highly expressed in activated microglia. These sections were specifically analyzed in striatal regions where more Iba1-activation was found than in other regions. The treatment groups did not differ significantly in CD68-positive signal (injected hemisphere: Kruskal-Wallis chi-squared = 3.8933, df = 4, p-value = 0.4206; non-injected hemisphere: Kruskal-Wallis chi-squared = 2.4669, df = 4, p-value = 0.6506). However, in the injected hemispheres, the groups of MSA2 and PD2 showed a trend for more CD68-positive signals compared to the monomer group (Figure 9).

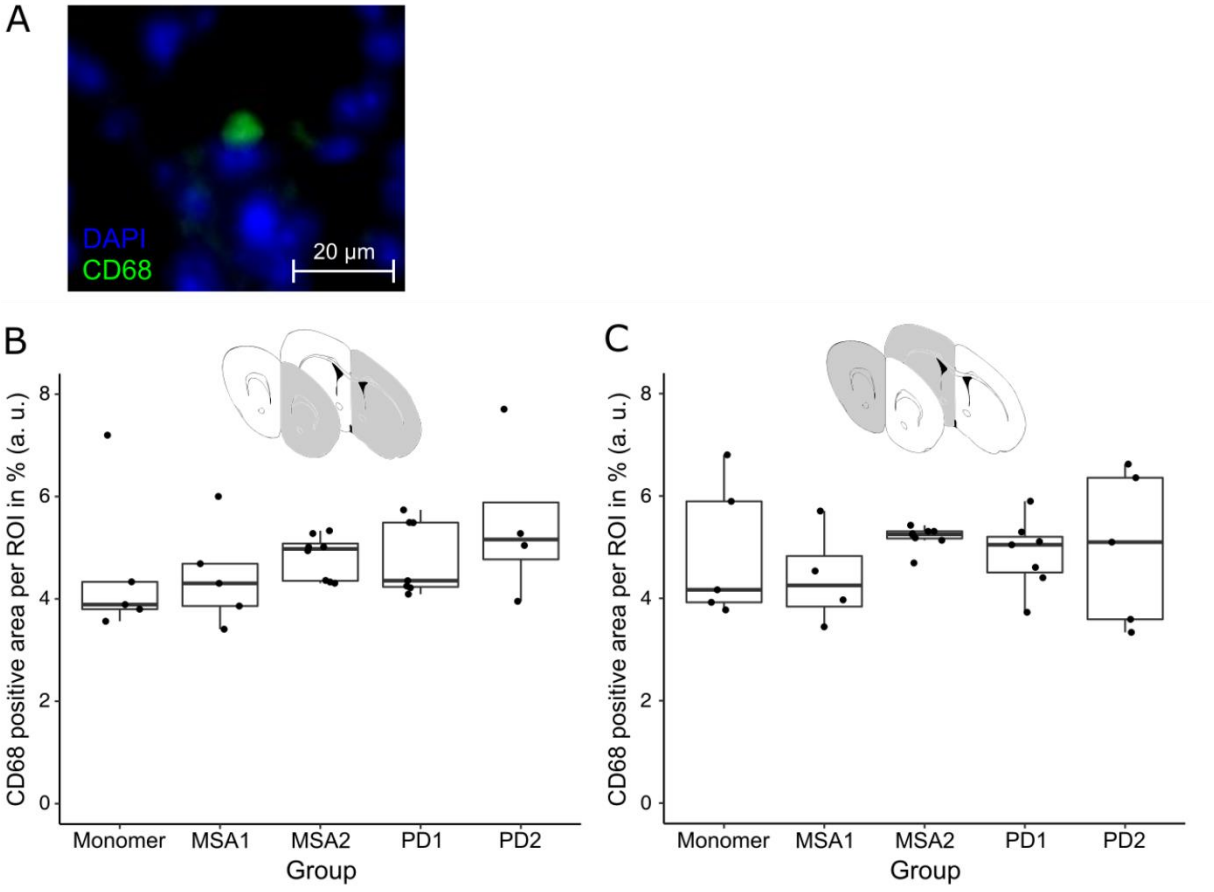

Figure 9: CD68-positive signal per region of interest (ROI). Exemplary image (A). Data shown for the injected (B) and the non-injected (C) hemisphere. Quantification by area of CD68-positive microglia divided by the total area of ROI. Adapted from (Zhang et al., 2023).

3.3 Positive correlation between pS129-α-syn-positive area and Iba1-positive area

After observing similar heatmaps for pS129-α-syn pathology (Figure 5) and Iba1-activation (Figure 8), the two variables were correlated using Spearman correlation. This analysis revealed a weak but significant positive correlation between the two variables for the injected hemispheres (rho = 0.44, p = 0.0055) (Figure 10A). In the non-injected hemispheres, no significant correlation between pS129-α-syn pathology and Iba1-positive signal was detected (rho = -0.027, p = 0.87) (Figure 10B).

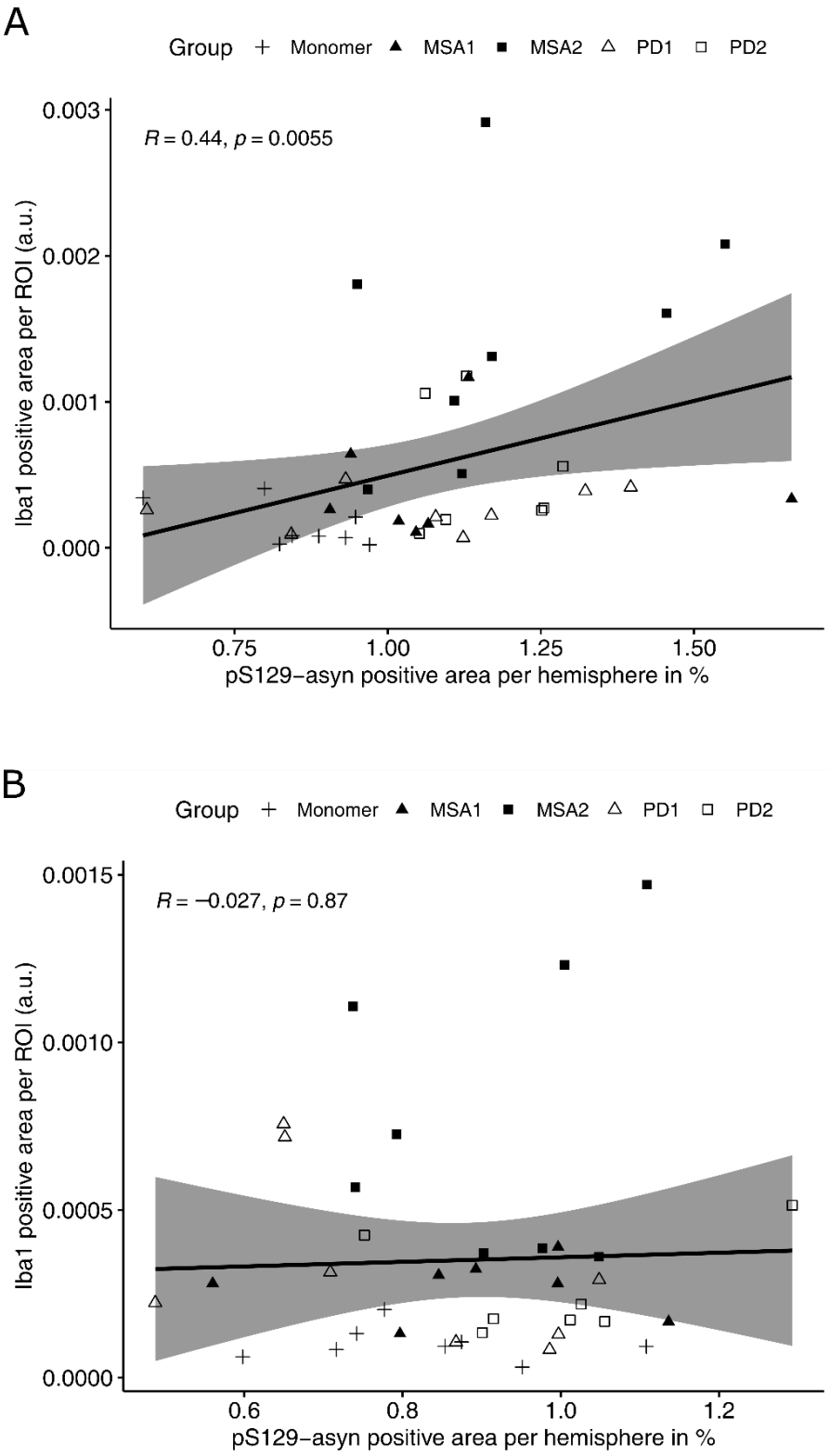

Figure 10: Correlation between pS129-α-syn-positive area per hemisphere in % and Iba1-positive area per ROI. Data shown for the injected (A) and non-injected (B) hemisphere. Shapes indicate the treatment group. ROI, region of interest. Adapted from (Zhang et al., 2023).

3.4 No significant differences in the M1 coefficient for the fibril-injected groups

Usually, α-syn pathology is localized in oligodendrocytes as glial cytoplasmatic inclusions (GCI) in MSA patients' brains (Papp and Lantos, 1994). Therefore, sections were stained for pS129-α-syn and CNPase to examine possible differential colocalization of pS129-α-syn pathology and oligodendrocytes in MSA- and PD-fibril injected brains. The fraction of the pixels in the α-syn channel overlapping with those in the CNPase channel was represented by the thresholded Manders' coefficient M1. The M1 coefficient did not differ significantly between MSA-fibril or PD-fibril injected brains in general (Wilcoxon rank-sum test, W = 8992.5, p-value = 0.6464), nor between the four treatment groups (Kruskal-Wallis chi-squared = 2.101, df = 3, p-value = 0.5517) (Figure 11).

A

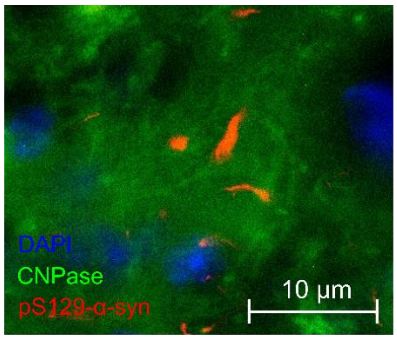

B

$$M_1 = \frac{\sum R_{i,\text{coloc}}}{\sum R_1}$$

C

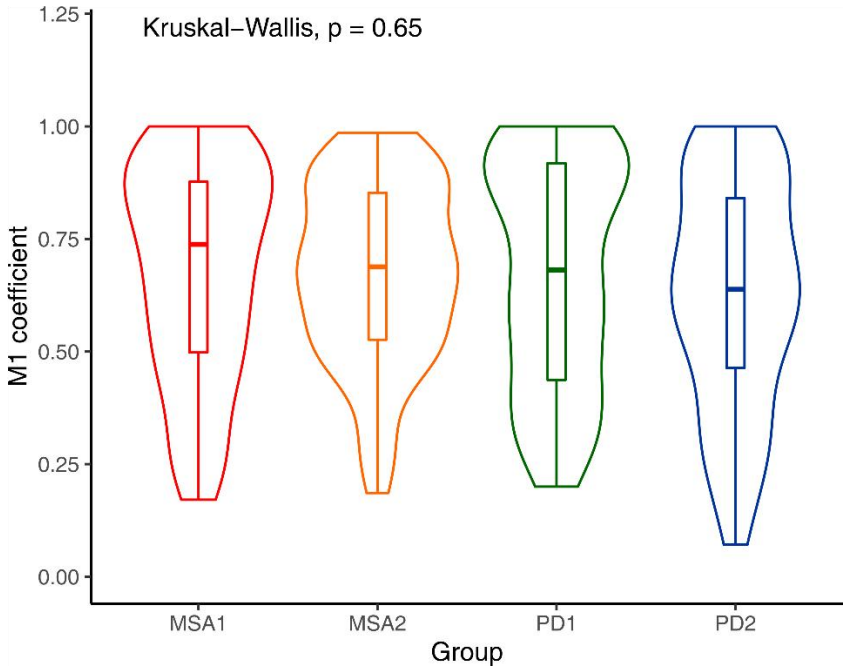

Figure 11: pS129-α-syn and CNPase positive signal. Exemplary image (A). (B) Equation for calculating the Manders' coefficient M1 (Adler and Parmryd, 2010). $R_{i,coloc}$ is the intensity of the red fluorophore in pixels where the green fluorophore is present. R_1 is the intensity of the red fluorophore in pixels. (C) Violin plot for the thresholded Manders' coefficient M1. M1 represents the fraction of pixels in the pS129-α-syn channel overlapping with those in the CNPase channel. Adapted from (Zhang et al., 2023).

3.5 No influence of α-syn-fibril injection on astrocytes

To analyze any influence of α-syn-fibril injection on astrocytes, five different brain regions (+ 1.18 mm, + 0.26 mm, - 0.34 mm, - 1.34 mm, -3.16 mm related to Bregma) were stained for GFAP. No significant differences were found in the GFAP-positive area per ROI for all five groups and for both hemispheres (ANOVA injected hemispheres p = 0.313; ANOVA non-injected hemispheres p = 0.132) (Figure 12).

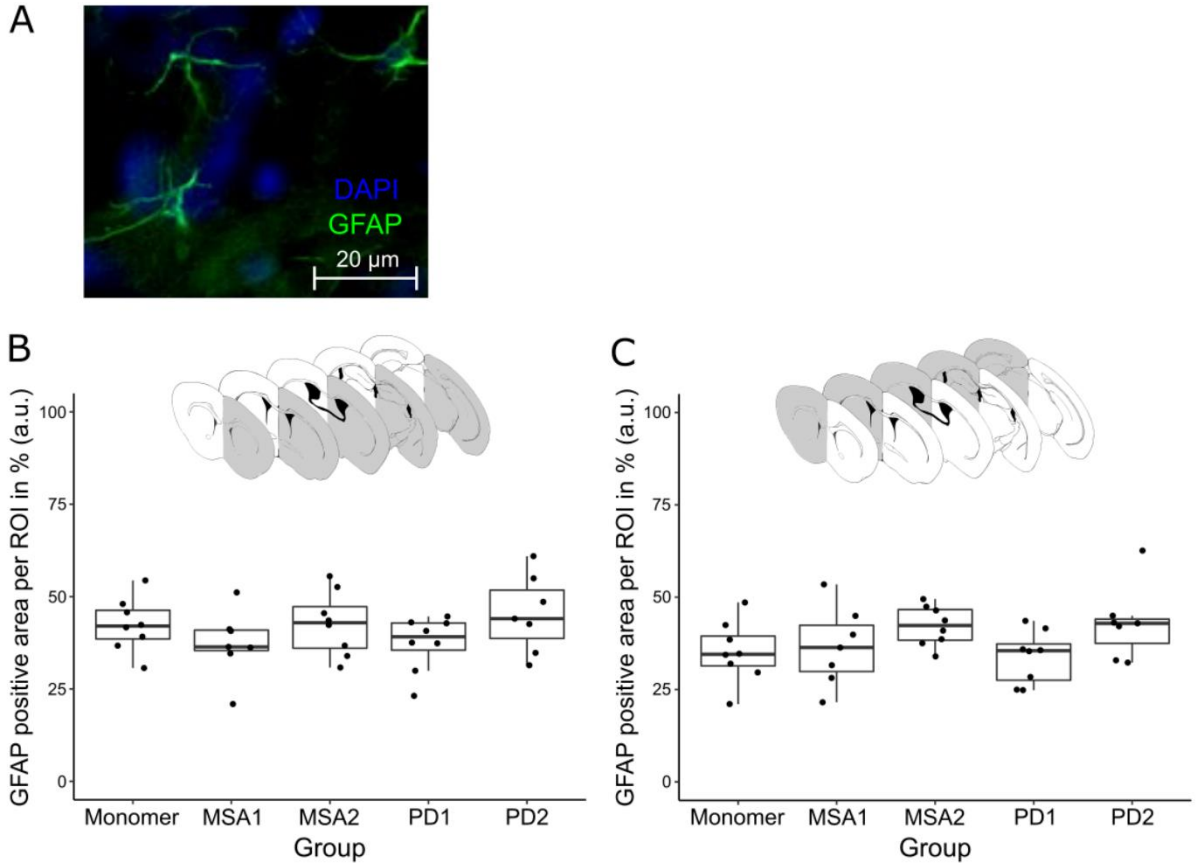

Figure 12: GFAP-positive signal per ROI. With exemplary image (A). Data shown for the injected (B) and the non-injected (C) hemisphere for regions + 1.18 mm, + 0.26 mm, - 0.34 mm, - 1.34 mm, and -3.16 mm related to Bregma. Quantification by area of GFAP-positive astrocytes divided by the total area of ROI. Adapted from (Zhang et al., 2023).

3.6 No significant loss of dopaminergic neurons after α-syn-fibril injection

Sections were labeled immunohistochemically for TH, and dopaminergic neurons in the SNpc were quantified to assess whether the injection of α-syn-fibril or α-syn-monomer had an impact on the survival of dopaminergic neurons in the SNpc (Figure 13). No significant differences were found in the number of TH-positive cells in the SNpc between the five groups in either hemisphere (ANOVA injected hemispheres p = 0.365; ANOVA non-injected hemispheres p = 0.681). When comparing both hemispheres in a paired t-test, no significant differences were found either (t = 1.4252, df = 33, p-value = 0.1635).

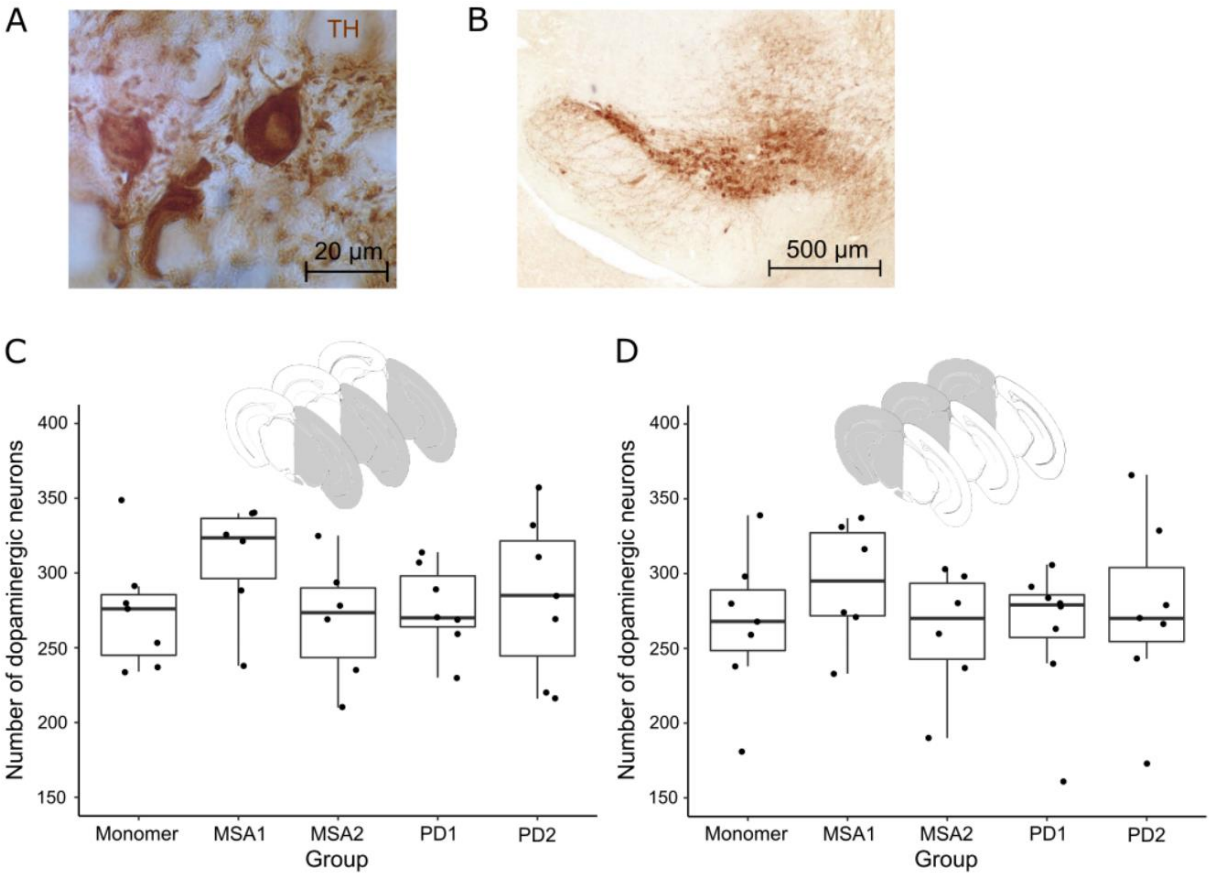

Figure 13: Number of dopaminergic neurons in the SNpc. Exemplary images in different magnifications (A, B). Data shown for the injected (C) and the non-injected (D) hemisphere for regions - 3.00 mm, - 3.15 mm, and - 3.30 mm related to Bregma.

4 Discussion

4.1 Structural differences of α-syn fibrils result in distinct levels of pS129-α-syn pathology

PD and MSA are both neurodegenerative movement disorders with the accumulation of pathological α-syn as the major histopathological hallmark. However, for both α-synucleinopathies, disease phenotypes often vary between patients, even within the same disease entity. Structural differences between patient-derived α-syn strains from PD and MSA patients may be responsible for different phenotypes, as cerebrospinal fluid (CSF) samples from PD and MSA patients were shown to contain different conformational strains of α-syn (Shahnawaz et al., 2020). Strain-dependent disease heterogeneity can be observed in our study and was also suggested by previous reports (Holec and Woerman, 2021).

In this study, α-syn fibrils amplified from two PD and two MSA patient brain extracts were injected into mouse brains to study α-syn seeding and spreading for individuals, next to comparing PD and MSA in general as demonstrated in previous studies. Employing multiple analysis methods, including nuclear magnetic resonance (NMR) spectroscopy, fluorescent probes, and electron paramagnetic resonance, Strohäker and colleagues have discovered that these patient-derived fibrils were structurally different from non-brain derived α-syn fibrils. Thus, injection of patient-derived fibrils may provide a more accurate model to study α-synucleinopathies. Additionally, fibrils did not have defined molecular structures for one type of disease but expressed great structural diversity, such as different protonation levels of specific residues (Strohäker et al., 2019). These structural differences are also reflected by the different levels of α-syn seeding and spreading in the mouse model of this doctoral thesis.

Here, the strongest α-syn pathology was found in mice injected with α-syn fibrils amplified from the brain homogenate of one of the two MSA patients (Figure 4). Patient MSA2 had a shorter disease duration (6 years) and died the youngest at age 71, compared to patient MSA1, who had a longer course of disease (7 years) and who died at an older age (82 years) (Table 2). The fibrils generated from the two PD patients, however, induced less spreading of α-syn pathology with different levels of spreading between PD1 and PD2. Brains injected with α-syn monomers as a control were the least abundant in pS129-positive α-syn pathology. Overall,

the rapidly progressive disease course and poor prognosis of MSA compared to PD are reflected by the histopathological differences between PD and MSA groups observed in this study. In alignment with this result, a similar study using α-syn PFFs has also reported that strains of MSA patients induced more α-syn-spreading pathology than those of PD patients (van der Perren et al., 2020). Injection of MSA-derived strains also resulted in more motor deficits, nigrostriatal degeneration, and inflammation than PD-derived strains (van der Perren et al., 2020). The here observed differences between the individual treatment groups, such as between MSA1 and MSA2 (Figure 4), may explain disease heterogeneity in α-synucleinopathies, even within the same disease entity.

4.1.1 Strain dependent α-syn spreading

pS129-α-syn-positive aggregates were detected throughout the whole brain, though the non-injected hemisphere was generally less affected except from the two regions Bregma - 0.34 mm and - 1.34 mm. Interestingly, the injection site at Bregma 0.38 mm did not show the strongest pS129-α-syn pathology (Figure 5), indicating that the α-syn aggregates have spread throughout the brain to regions connected to the injection site. Previous studies have also shown that α-syn pathology propagates through neuronal networks (Chung et al., 2019; Luk et al., 2012b; Masuda-Suzukake et al., 2014; Rey et al., 2018). Supporting these observations, LB-like inclusions are found in several areas innervating the striatum after striatal injection of recombinant α-syn-fibrils. These areas include the frontal and insular cortices, the amygdala, and the substantia nigra pars compacta (SNpc) (Masuda-Suzukake et al., 2014; Paumier et al., 2015). Lieu et al. have also described interhemispheric corticostriatal and nigrostriatal connections, which enable the spreading, as mentioned above, to the non-injected hemisphere (Lieu and Subramanian, 2012). Using positron emission tomography (PET) on α-syn-PFFs injected rats, α-syn pathology was found to propagate to the contralateral SN via the cross-hemispheric nigrostriatal pathway (Thomsen et al., 2021). Indeed, spreading to the contralateral hemisphere was also observed in this study (Figure 5).

However, injections of PFFs in the pedunculopontine nucleus demonstrated that the spreading of α-syn pathology is not only a matter of connectivity or synaptic contacts (Henrich et al., 2020). Different regular α-syn concentrations depending on the brain region, next to SNCA

gene expression and brain connectomics, make certain regions more susceptible to α-syn pathology than others when injected with PFFs (Rahayel et al., 2021). For instance, neurons without endogenous α-syn do not develop inclusions after being treated with PFFs (Volpicelli-Daley et al., 2011). This supports the hypothesis of prion-like spreading of pathologic α-syn where endogenous protein needs to be present to be converted to α-syn aggregates.

4.1.2 Strain variability and the SOC model

Distinct α-syn aggregates exhibit different morphological and structural traits and are suggested to cause variable disease phenotypes (Holec and Woerman, 2021; van der Perren et al., 2020). Recently, imaging and neuropathological data have suggested two disease onsets (body-first vs. brain-first) that may explain disease heterogeneity (Borghammer et al., 2021; Borghammer, 2021). As previously explained in the introduction, this model is the so-called α-synuclein origin and connectome (SOC) model (Borghammer, 2021). Scientists have considered disease initiation sites and structural confirmation of α-syn as determinants of the clinical and histopathological phenotype (Just et al., 2022). In brain-first PD, α-syn could aggregate in neurons in almost any brain region, influenced by other cell types such as microglia, astrocytes, and oligodendrocytes (George et al., 2019). As cellular environments impact α-syn strains, different disease initiation sites with distinct cellular milieus generate different strains, which then spread through the CNS and PNS (Peng et al., 2018). Strain development is then influenced by an interplay of neurons, glia, endocrine, immune, and epithelial cells in the gut, as well as the gut microbiome (Just et al., 2022). The SOC model could be a possible explanation for the structural differences found in the fibrils used in this study. Strohäker and colleagues discovered greater structural diversity in fibrils amplified from PD patients than from MSA patients (Strohäker et al., 2019). The different fibrils could originate from either brain-first or body-first PD patients with their distinct cellular environments. Thus, after intracerebral injection into the mouse brain, the two PD fibrils induced different levels of α-syn pathology (Figure 5).

4.1.3 Phenotypic variability

Recent cohort studies have confirmed the clinical experience of large phenotypic variability in PD patients (Bartl et al., 2022). Clinico-pathological studies have suggested different phenotypes, including early disease onset, tremor dominant, non-tremor dominant postural instability and gait dominated PD (PIGD subtype), and rapid disease progression without dementia (Selikhova et al., 2009; Wüllner et al., 2023). However, classifying patients into subtypes is often inconsistent, as shifts from one phenotype to another might make clinical prognosis more difficult to predict (Coelln et al., 2021; Lee et al., 2019). Therefore, PD subtypes need to be better defined, for example, by analyzing α-syn strains. These conformational strains are suggested to cause divergent clinical and neuropathological features, a concept that originated from prion diseases (Collinge and Clarke, 2007). Cryo-electron microscopy analysis confirmed structural differences of α-syn filaments between PD, DLB, and MSA brains (Schweighauser et al., 2020; Yang et al., 2022). In MSA patient brains, two types of α-syn filaments were found, whereas only one type of α-syn filament was found in aggregates from PD and DLB patients (Yang et al., 2022). Similar to our study, α-syn fibrils in DLB can vary between individuals. When analyzing α-syn in CSF from DLB patients, various fibrils were identified to display distinct potencies in amyloid dye binding, seeding new inclusions, and microglial pro-inflammatory responses (Sokratian et al., 2022).

To further analyze the properties of α-syn fibrils and use them for diagnostic purposes, α-syn seed amplification assays have been developed, which will be explained in the following chapter.

4.1.4 α-syn seed amplification assays

α-syn seed amplification assays (SAAs) like protein misfolding cyclic amplification (PMCA) and real-time quaking-induced conversion (RT-QuIC) are two methods to amplify α-syn aggregates from patient samples, such as brain tissue, CSF, saliva, and skin (Bellomo et al., 2022; Srivastava et al., 2022). These two techniques may have important future implications in the diagnosis of α-synucleinopathies and for characterizing strain-dependent differences following amplification (Siderowf et al., 2023).

Originally, SAAs were developed to detect and amplify prion aggregates in different biological fluids (Srivastava et al., 2022). PMCA is a cyclical process where the protein template grows and multiplies at the expense of a substrate – a concept similar to DNA amplification by polymerase chain reaction. By exponential amplification, the misfolded protein, i. e. the prion protein or the α-syn protein, can be detected and quantified (Shahnawaz et al., 2017). The α-syn-PMCA assay was shown to have a high sensitivity in discriminating between CSF samples from PD and MSA patients, confirming the existence of different conformational strains (Shahnawaz et al., 2020; Singer et al., 2020). Both α-syn-PMCA reaction and neurofilament light chain (NFL) reliably predicted which patients with pure autonomic failure (PAF) will eventually develop MSA (Singer et al., 2021). PMCA was also used in our study to amplify α-syn fibrils from PD and MSA patients. Strohäker et al. discovered that α-syn fibrils propagated from PD and MSA patients did not have disease-specific structural properties but rather expressed structural heterogeneity, especially for PD-derived fibrils (Strohäker et al., 2019). This is a possible reflection of PD's more significant phenotype variability compared to MSA.

For RT-QuIC assays, pathological α-syn seeds initiate recombinant α-syn to aggregate into amyloid fibrils. Then, these fibrils bind the fluorescence thioflavin T, and the generated fluorescence is monitored in real-time (Groveman et al., 2018). For detecting early α-syn aggregation in the brain and CSF, RT-QuIC assays have been developed for the clinical assessment of DLB and PD patients (Fairfoul et al., 2016). RT-QuIC assays have been optimized since then to be completed after 1-2 days with 93% diagnostic sensitivity and 100% specificity when beforehand, they took 5-13 days to be completed (Groveman et al., 2018). Differential seeding activity for PD, MSA-C, and MSA-P was also found when performing α-syn RT-QuIC analysis of olfactory mucosa (Bargar et al., 2021). Recently, researchers amplified α-syn from MSA patients using RT-QuIC and detected distinct α-syn seeding properties for different brains classifying them into high, intermediate, and low seeders (Martinez-Valbuena et al., 2022b). This heterogeneity in seeding capacity also exists for different brain regions when comparing α-syn derived from patients suffering from Lewy body disorders (LBDs). α-syn derived from the SN in patients with a motor-predominant phenotype had a higher seeding capacity than the α-syn from cognitive-predominant patients. However, hippocampal α-syn derived from cognitive-predominant patients seeded significantly more than α-syn from patients with a motor-predominant phenotype (Martinez-Valbuena et al., 2022a). α-syn from patients with a rapid disease course, i. e. less than 3 years to development of advanced disease, had the

highest seeding capacity of all the patients included (Martinez-Valbuena et al., 2022a). These findings are comparable to our study, as material from MSA2 (the patient with the shortest disease duration) was the most potent in seeding α-syn pathology. RT-QuIC analyses may also be of prognostic value, as α-syn positivity in the CSF of IRBD patients represents a prodromal marker for the later development of PD or DLB (Iranzo et al., 2021). In sum, SAAs are crucial for the amplification of α-syn to study its patient-specific properties and show promise as diagnostic biomarkers for α-synucleinopathies.

4.1.5 Factors influencing α-syn pathology in an animal model

Previous studies have shown that strain variability results in distinct toxicity levels, α-syn seeding, and propagation properties (Alam et al., 2019; Fares et al., 2016). Next to strain variability, the level of α-syn pathology induced in a mouse model depends on several other factors. First, the incubation time (days from inoculation to sacrifice) is crucial in allowing more or less time for the α-syn pathology to develop (Table 1). Experimental setups with a follow-up time of up to 23 months post-injection before sacrificing the animals were reported (Rey et al., 2018). According to Patterson et al., the levels of α-syn pathology may vary over time. In a rat model of α-syn PFF injection, around 5000 nigral neurons (40% of total nigral neurons) contained α-syn pathology at 2 months post-injection. In contrast, the number dropped to 600 neurons (5% of total nigral neurons) at 6 months post-injection, as nigral neurons with α-syn pathology degenerated over time (Patterson et al., 2019). Depending on the research focus of an animal model (α-syn pathology vs. nigral neurodegeneration), different time frames could be advantageous. In addition, the injection site is also essential as it determines how the α-syn aggregates will propagate through the brain. Development of α-syn pathology and neurodegeneration is also dependent on the dose of injected α-syn as doubling the dose of α-syn PFFs resulted in more pronounced α-syn pathology and more nigral neuronal death (Patterson et al., 2019).

Seeding ability and prion-like propagation of pathologic α-syn highly depend on the inoculum and the host. When injecting mice with human α-syn PFFs or human brain lysates from MSA patients, those treated with PFFs express the highest pathological burden (Lloyd et al., 2022). Mice expressing human α-syn with A53T mutation are also more susceptible to PFFs and MSA

brain lysate injection-induced paralysis than mice expressing WT human α-syn, suggesting that both host and inoculum influence the outcome of the animal model. In another study, mice expressing WT human α-syn showed an earlier onset of motor symptoms when injected with PFFs than with MSA brain homogenate (Holec et al., 2022). Thus, PFFs might not be the ideal inocula for replicating MSA pathology. The development of α-syn aggregates also depends on the type of mice used, i. e. transgenic or wild-type. Brain lysates from MSA patients induced α-syn pathology 5 months after injection in transgenic mice expressing human A53.aSyn but not in transgenic expressing wild-type human α-syn nor in non-transgenic mice (Dhillon et al., 2019). Previously, homozygous and/or hemizygous M83 neonates were inoculated intracerebrally or intraperitoneally with brain extract from other symptomatic M83 mice or with brain extract from an MSA patient passaged in M83 mice (Sargent et al., 2017). In homozygous M83 mice, higher levels of pathological phosphorylated α-syn were detected compared to hemizygous mice. Thus, the acceleration of α-synucleinopathy up to the clinical disease depends on the different inoculums and levels of α-syn expression (Sargent et al., 2017).

Another factor to consider is the species which the inoculation material is derived from. Human α-syn PFFs are less potent in inducing α-syn pathology and dopaminergic cell death in the SN compared to mice α-syn PFFs when injected into mouse brain (Luk et al., 2016; Rey et al., 2016). Sequence differences between human and mouse α-syn may limit the interaction between the pathogenic and endogenous α-syn, reducing the toxicity of human PFFs in rodent models (Luk et al., 2016). Additionally, mouse PFFs induce more α-syn pathology in rats than rat PFFs, suggesting that species homology is not the only determinant and that mouse α-syn may have more pronounced pathological properties (Howe et al., 2021).

Therefore, different animal models can represent various disease stages and disease courses. Our model mirrors an earlier disease stage without nigral neurodegeneration as the time frame with sacrificing mice at 90 dpi is relatively short compared to other models. We also used non-transgenic, wild-type mice with regular levels of endogenous α-syn. Moreover, cross-species seeding due to the use of human α-syn fibrils induced less seeding of α-syn pathology than if the fibrils were from mice.

At the same time, it is important to note that current immunohistochemical methods are optimized to detect macro-aggregates and may lack the sensitivity to detect smaller molecules

such as oligomers and proto-fibrils (Borghammer, 2018). Oligomers, however, were shown to spread more efficiently than fibrils which have higher molecular weight and might play an essential role in early disease stages (Peelaerts et al., 2015; Rey et al., 2013). A relatively new method, the so-called alpha-synuclein proximity ligation assay, can be applied to detect early-stage lesions such as pale bodies in a patient brain. It labels oligomeric α-syn, which differs from physiological, presynaptic α-syn, and aggregated α-syn within LBs (Roberts et al., 2015). Hence, this technique might be useful in earlier disease stages and could also be applied in animal models to heighten the sensitivity to detect α-syn aggregates.

4.2 α-syn pathology and immune response activation

4.2.1 Microglial activation by α-syn

A growing body of evidence has indicated an association between α-syn pathology and immune response activation in PD and MSA. Misfolded α-syn is suggested to trigger microglia activation, while activated microglia play a role in uptaking, processing, and eventually spreading α-syn (Caldi Gomes et al., 2022; Deyell et al., 2023; Di Vieira et al., 2015; Kannarkat et al., 2013; Schonhoff et al., 2020; Tansey and Romero-Ramos, 2019). Microglia are resident immune cells in the CNS. Under physiological conditions, they regulate homeostasis, regenerative functions, and neural proliferation and differentiation (Cserép et al., 2021; Prinz et al., 2019). When presented with danger signals, microglia produce pro-inflammatory cytokines and clear foreign antigens (Prinz et al., 2019).

To test the effects of α-syn fibril injection on the immune response, analyses of microglia activation were performed in the present study. After injection of brain-derived α-syn fibrils, different levels of microglia activation were found, with the MSA2-fibril injected group being the most abundant in Iba1-positive signal (Figure 8). Additionally, a positive correlation between α-syn-pathology and microglia abundance was detected in the injected hemisphere (Figure 10).

Upon exposure to α-syn fibrils, the microglial NLRP3 (nucleotide-binding oligomerization domain-like receptor pyrin domain-containing-3) inflammasome is activated, suggesting a link between α-syn aggregation and microglial activation (Pike et al., 2021; Trudler et al., 2021). This follows our results and supports the hypothesis that microglia activation is induced by α-syn aggregation. Other inflammatory mediators involved in microglial activation include IL-1β, TNF, and IL-6 (Lee et al., 2008; Sarkar et al., 2020). On the other hand, inhibition of the NLRP3 inflammasome has been found to prevent α-syn accumulation and dopaminergic neurodegeneration (Gordon et al., 2018). Thus, it is also possible that microglia activation is causing additional α-syn-pathology which explains the positive correlation detected in this study.

The role of microglia was also confirmed in patients with α-synucleinopathies. Reactive astrocytosis and microgliosis were detected in post-mortem MSA patients (Ishizawa et al.,

2004; Song et al., 2009). Widespread microglia activation was also found in patients with early-stage MSA-P (Kübler et al., 2019). Additionally, PET scans showed increased microglia activation in patients with α-synucleinopathies (Stokholm et al., 2017). For example, patients with IRBD had increased microglial response in the SN and reduced dopaminergic function in the putamen as imaged by 11C-PK11195-PET.

Both the central and peripheral immune systems are involved in PD and other α-synucleinopathies (Terkelsen et al., 2022). After intrastriatal injection of α-syn PFFs, inflammatory reactions with microglia and astrocyte activation and infiltration of peripheral immune cells were observed in animal models (Earls et al., 2019; Yun et al., 2018). Interestingly, alterations of leukocytes in the spleen and lymph nodes were also recorded, possibly due to the gut-brain axis (Earls et al., 2019). As previously explained in Chapter 4.1.2, body-first and brain-first PD could be caused by fibrils generated in different cellular environments. The involvement of the central and peripheral immune systems could contribute to distinct cellular milieus and might be an additional explanation for the heterogeneity observed in PD patients.

In sum, our findings support current theories of the involvement of neuroinflammation in PD and MSA patients. We also show that levels of microglia activation differ depending on the α-syn strain present in each patient.

4.2.2 Involvement of microglia in α-syn clearance and neurodegeneration

Microglia are suggested to be involved in the process of α-syn clearance, as an 80% reduction of microglia increased cell-to-cell transfer of α-syn in vivo (George et al., 2019). In the same study, mice were treated with lipopolysaccharide (LPS) to stimulate the microglia. These mice had significantly more α-syn transfer than non-LPS-exposed control mice implying that the immune profile of microglia also affects α-syn spreading (George et al., 2019). Synucleinophagy, the process of autophagy of α-syn, is stimulated by TLR4 (toll-like-receptor 4), which in turn activates the NF-κB cascade and transcription of p62, a receptor for forming α-syn-ubiquitin complexes for subsequent autophagy in microglia (Choi et al., 2020).

Scheiblich et al. demonstrated that α-syn is transferred between microglia through tunneling nanotubes and that healthy microglia donate mitochondria to those overloaded with α-syn

(Scheiblich et al., 2021). The transfer of α-syn does not necessarily lead to disease progression as passing α-syn to unburdened microglia attenuates the inflammatory microglia profile and facilitates the breakdown of α-syn (Scheiblich et al., 2021). Thus, microglia are suggested to have neuroprotective functions in early disease stages (Deyell et al., 2023).

Over the disease course, α-syn induces excessive microglial activation and inflammatory activity, contributing to the progression of neurodegenerative diseases (Scheiblich et al., 2021). Early disease sites may be more vulnerable to neuroinflammation and microglia activation, which might initiate the spreading of α-syn pathology along connectivity pathways (Freeze et al., 2019). Duffy et al. showed that microglia activation might contribute to neuronal degeneration in the SNpc, as reactive microgliosis and increased levels of major histocompatibility complex class II (MHC-II) expression preceded dopaminergic cell death. A correlation between pS129-α-syn-pathology and microglia expressing MHC-II was also observed in cortical regions and the SN but not in the striatum (Duffy et al., 2018b).

Interestingly, mice with selective α-syn accumulation in microglia developed neurodegeneration of dopaminergic neurons without endogenous α-syn aggregates. Microglia reached a state of phagocytic exhaustion, excessive production of proinflammatory mediators, and recruitment of peripheral immune cells, suggesting that this toxic environment led to dopaminergic neuronal death (Bido et al., 2021).

Other studies, however, observed microglial clearing of α-syn released from neurons and thus propose a neuroprotective function of microglia in early disease stages which switches to a more neurodegenerative function with disease progression (Deyell et al., 2023). The exact reasons for this shift remain unclear, but the build-up of aggregated α-syn may overwhelm the microglia and limit their homeostatic abilities (Deyell et al., 2023). As our model does not show any signs of dopaminergic neurodegeneration with relatively low levels of α-syn pathology, it may represent an earlier disease stage where activated microglia process pathological α-syn and are still neuroprotective.

4.2.3 Microglial interaction with different α-syn structures

Recent findings have shown that α-syn can impact the immune response and vice versa, that the immune system can influence α-syn levels and structure. When inflammatory responses are dysregulated due to genetic predisposition and aging, α-syn monomers will form oligomers. These are taken up by nerve endings and transported to the CNS, where they aggregate into fibrils. This process is suggested to cause neurodegenerative disease (Kasen et al., 2022).

In this thesis, structural differences in the injected fibrils resulted in different levels of neuroinflammation. Previous studies have indicated that conformational variations of α-syn influence the inflammatory response by microglia. An in-vitro study from Hoffmann et al. using BV2 cells, an immortalized murine microglia cell line, demonstrated that fibrillar α-syn induced highly inflammatory responses from BV2 cells. In contrast, oligomeric α-syn did not activate the BV2 cells (Hoffmann et al., 2016). Monomeric α-syn induced immunoreactive responses but to a lower degree than fibrils. Only fibrillar α-syn was taken up by BV2 cells. In a similar study, primary mouse microglia responded the strongest to α-syn PFFs, followed by α-syn monomers, with α-syn oligomers hardly generating any response (Feng et al., 2019). Our results confirm that α-syn fibrils induced stronger microglia activation than monomeric α-syn (Figure 8).

Overall, the link between activated microglia and α-syn aggregates is not fully understood, and it is yet unsolved how exactly microglia activation contributes to the formation of these aggregates. It is uncertain whether inflammation is the driver of protein accumulation, a response to neurodegeneration, or an aggravator of the process (Leńska-Mieciek et al., 2023). Thus, a better understanding of the interplay between α-syn and microglia could provide valuable insights into the pathogenesis of α-synucleinopathies and possibly provide another therapeutic approach for these disorders.

4.3 α-syn pathology and astrocytes

Next to microglia, astrocytes play an equally important role in PD and MSA. Astrocytes are the most common subtypes of glial cells in the CNS and are involved in the blood-brain barrier permeability, cell signaling, neuron support, metabolite homeostasis, and synapse plasticity (Ricci et al., 2009). Similar to microglia, astrocytes respond to α-syn in the extracellular space, internalize aggregated α-syn to clear toxic forms of the protein, and potentially participate in antigen presentation of α-syn peptides (Kasen et al., 2022). These processes might be responsible for the chronic inflammation in α-synucleinopathies (Kasen et al., 2022).

In this study, no reactive astrogliosis was found in all four treatment groups (Figure 12). However, regional astrogliosis in smaller, defined areas cannot be excluded and morphological analyses would have been necessary to exactly quantify astrocyte activation. As the main focus was to get an overview of GFAP-positivity throughout several brain regions, sections were imaged with MosaiX in a 10x magnification and morphological analyses would have required a larger magnification. Additionally, GFAP is a marker for reactive astrocytes and not for all resting astrocytes (Sofroniew and Vinters, 2010). Thus, astrocyte proliferation not detected by the anti-GFAP staining could also be present. In post-mortem MSA patient brain analyses, widespread microgliosis was found, especially in the white matter (Nykjaer et al., 2017). Just as in this thesis, no reactive astrogliosis was reported in those brains. Others have found astrogliosis in cells close to oligodendrocytes containing GCIs (Radford et al., 2015; Stefanova et al., 2005). Here, colocalization between CNPase and pS129-α-syn did not differ between the MSA- and PD-fibril-treated groups (Figure 11). Thus, the paucity of GCIs might explain the lack of astrocytosis in MSA-fibril-injected brains. For PD, reactive astrogliosis is known to occur in the SN (Lastres-Becker et al., 2012; Renkawek et al., 1999; Thannickal et al., 2007). In this study, these results were not reproduced, presumably because the employed mouse model represents an earlier disease stage.

In vitro, treatment of primary astrocytes with α-syn resulted in astrogliotic changes (Radford et al., 2015). Neurotoxic reactive astrocytes were shown to be induced by activated microglia, and blocking the conversion of astrocytes into the reactive A1 phenotype was protective in PD models (Liddelow et al., 2017; Yun et al., 2018). In contrast, prolonged astrocyte dysfunction and microglial activation accelerate the degeneration of dopaminergic nigral neurons (Kuter

et al., 2018). A recent review from Brandebura et al. reports on the role of astrocytes in neurodegeneration. Astrocytes may contribute to neurodegeneration through their dysfunction, altering cerebral homeostasis, and their reactivity, producing toxic factors (Brandebura et al., 2023).

Generally, neuroinflammation may act as a cause and a driver of α-syn pathology, driving it in a vicious circle. Neuronal dysfunction promotes α-syn aggregation, which activates astrocytes and microglia. In turn, these glial cells release pro-inflammatory markers, which cause stress on neurons to release more α-syn aggregates (Di Vieira et al., 2015). A deeper understanding of all cell types' neuroinflammation is crucial as inflammatory proteins may act as a biomarker to diagnose and monitor α-synucleinopathies (Leńska-Mieciek et al., 2023). Beta nerve growth factor (β-NGF) and Delta and Notch-like epidermal growth factor-related receptor (DNER), two inflammatory proteins in CSF, were suggested as potential biomarkers to differentiate between MSA and PD as both proteins were down-regulated in MSA compared to PD (Santaella et al., 2020). Higher levels of inflammatory biomarkers correlated with more severe motor function and cognitive impairment in PD patients (Hall et al., 2018). Thus, advancing research in the field of neuroinflammation and α-synucleinopathies may have significant diagnostic and therapeutic implications.

4.4 α-syn pathology and oligodendrocytes

GCIs are universally present in post-mortem MSA brain analyses (Papp and Lantos, 1994; Spillantini et al., 1998). Here, the M1 coefficient for the anti-pS129-α-syn and anti-CNPase double staining did not differ between the treatment groups, indicating a paucity of GCIs in the MSA-fibril-injected brains (Figure 11). It is reported that neuronal α-syn pathology develops weeks after injection with α-syn PFFs, while oligodendroglial α-syn pathology takes several months to emerge. Furthermore, the formation of GCIs is associated with the post-injection interval rather than aging (Uemura et al., 2019). We, therefore, hypothesize that at only 90 dpi, mice in this study did not have sufficient time to develop GCIs.

In vitro, MSA-derived GCI fractions were demonstrated to be toxic. Two years after intrastriatal injection of these GCI fractions, baboon monkeys exhibited nigral and striatal neurodegeneration (Teil et al., 2022). Additionally, oligodendrocytic cell loss led to demyelination and inflammation (Teil et al., 2022). In MSA, studies have shown a link between neuroinflammation and oligodendrocytes with α-syn inclusions that induced an immune response only in white matter regions (Hoffmann et al., 2019). Williams and al. demonstrated in a mouse model of MSA that α-syn aggregation in oligodendrocytes resulted in the upregulation of MCH-II on microglia and the infiltration of CD4-positive T-cells and monocytes from the blood. Vice versa, the dysfunction of oligodendrocytes was also driven by pro-inflammatory cells (Williams et al., 2020).

4.5 Influence of α-syn pathology on dopaminergic neurons

The loss of dopaminergic neurons in the SNpc is a pathological hallmark of PD. Mori et al. demonstrated a close relationship between α-syn aggregation, TH immunoreactivity, and neuronal loss (Mori et al., 2006). In several animal models with α-syn PFF injection, as listed in Table 1, cell loss of TH-positive neurons in the SNpc was replicated (Duffy et al., 2018a; Luk et al., 2012a; Milanese et al., 2018; Sorrentino et al., 2017). In contrast, no dopaminergic neuronal death in the SNpc was detected in our study (Figure 13). This is likely due to an incubation period of only 90 days compared to other animal models with more extended incubation periods. According to Braak's hypothesis, nigral neurodegeneration appears once α-syn pathology has reached the SN (Braak et al., 2003). In our model, α-syn spreading from the injection site has appeared but the α-syn pathology is relatively sparse in brain regions containing the SN (Bregma - 3.08 mm, - 3.16 mm, - 3.28 mm) compared to the striatal regions where the injection site is located (Bregma 1.18 mm, 0.38 mm, 0.26 mm) (Figure 5). Additionally, the injection of mouse fibrils into the mouse brain induces more pathology than cross-species seeding with fibrils from humans, which is the case in our study as explained in Chapter 4.1.5 (Earls et al., 2019; Luk et al., 2016).

5 Outlook

In sum, strain variability as the source of disease heterogeneity with different levels of α-syn aggregation and neuroinflammation must be considered in future animal and patient studies. Early intervention may be possible, as LBDs have a long prodromal phase. However, clinical phenotypes of α-synucleinopathies are highly heterogeneous and often overlap in early disease stages (Berg et al., 2021). To improve diagnostic accuracy, especially in early disease phases, reliable biomarkers are in dire need. In several meta-analyses, CSF total α-syn was lowered in PD patients compared to controls. However, the sensitivity of CSF α-syn in the diagnosis of PD ranged only between 78% to 88%, and specificity between 40% and 57 % (Eusebi et al., 2017; Gao et al., 2015; Parnetti et al., 2019). No significant differences in CSF total α-syn were found in one meta-analysis between PD, DLB, and MSA patients (Gao et al., 2015). In contrast, others have found increased CSF α-syn levels in PD patients compared to MSA patients (Zhou et al., 2015). NFLs also differ between patients suffering from PD and APS and may be a valuable biomarker to detect early APS (Marques et al., 2019). In recent studies, increased total plasma/serum α-syn levels were found in PD and are primarily observed in early disease stages (Zubelzu et al., 2022). Alternative protein biomarkers with less invasive approaches than CSF sampling are also suggested, being retrieved from blood, saliva, or urine (Cocco et al., 2023). Additionally, scientists have detected increased α-syn levels in tear fluid of PD patients compared to controls (Maass et al., 2020) which could be further analyzed in α-syn SAAs as prion protein seeding activity was found in tear fluids (Schmitz et al., 2023). Using α-syn SAA in combination with the more sensitive luminescent conjugated oligothiophenes (LCO) assays, pathology in fluids and biopsies can be better explored and stratified to allow personalized treatment at early disease stages (Just et al., 2022).

Currently, several studies aim to reduce the level of α-syn and its seeding by sequestering, degrading, or silencing α-syn expression using passive or active immunization, vectorized antibodies, antisense oligonucleotides, or inhibitory RNA (Menon et al., 2022). In pre-clinical and clinical trials, these therapies were shown to reduce the accumulation of α-syn (Rodger et al., 2023). α-syn post-translational modifications (PTMs) such as phosphorylation, nitration, and acetylation can influence the conformation of α-syn and may be another potential therapeutic target for α-synucleinopathies (Brembati et al., 2023). Epigenetic alterations as a

driving factor of PD pathogenesis, such as dysregulation of miRNAs, should also be further investigated as treatment options (Paccosi and Proietti-De-Santis, 2023).

A novel approach to treating PD and neurodegenerative diseases is using small extracellular vesicles that deliver drugs across the blood-brain barrier to targeted sites in the brain (Pan et al., 2023). Targeting neuroinflammation in diagnostics and therapeutic approaches may be another way to tackle α-synucleinopathies, as multiple studies have demonstrated the importance of neuroinflammation in the disease process (Harms et al., 2021). As shown in this thesis, different α-syn strains induce distinct levels of neuroinflammation that could be another target for potential treatments.

Lastly, PD and MSA subtypes must be better defined while recognizing that distinct α-syn strains may influence the clinical presentation and prognosis. Thus, specific strain-dependent disease mechanisms could be targeted in personalized treatments (Tolosa et al., 2021). For monogenetic PD, subtype-specific therapies are already being tested in clinical trials (Poewe et al., 2020). Using the aforementioned diagnostic approaches to detect individual α-syn strains, patients suffering from α-synucleinopathies could be better stratified into different populations for future clinical trials and treatments (So and Watts, 2023).

6 Summary

α-synucleinopathies, including PD and MSA, are neurodegenerative disorders with aggregation of pathological α-syn. Heterogeneities in clinical phenotypes and neuropathology are suggested to be caused by different strains of α-syn. To study disease-specific and interindividual differences in α-syn pathology and spreading, α-syn amplified from brain homogenates of two MSA patients and two PD patients were injected into C57Bl6/J mouse brains. 90 days post-injection, mice were sacrificed, and immunohistochemical stainings were performed. Anti-pS129-α-syn staining revealed different levels of α-syn spreading caused by the four different patient-derived fibrils. α-syn fibrils of one of the two MSA patients triggered the strongest α-syn pathology, followed by comparable levels of pS129-α-syn induced by the second MSA and one PD patient material. The formation of pS129-α-syn is further associated with increased microglial activation as detected by anti-Iba1 staining. However, no differences in astrogliotic changes, co-localization of α-syn in oligodendrocytes, or dopaminergic neuron numbers in the SNpc were detected between the different groups. In sum, the current study demonstrates differential spreading of α-syn pathology in PD and MSA caused by inoculation of patient material. Seeding and spreading heterogeneity between different groups may indicate the presence of patient immanent factors responsible for individual disease phenotypes. This study underlines the importance of future investigations with human-like models and larger patient numbers to better understand strain variability in α-synucleinopathies and their implications for diagnostic and therapeutic approaches.

7 References

Abdo, W.F., Borm, G.F., Munneke, M., Verbeek, M.M., Esselink, R.A.J., Bloem, B.R., 2006. Ten steps to identify atypical parkinsonism. Journal of neurology, neurosurgery, and psychiatry 77, 1367–1369. https://doi.org/10.1136/jnnp.2006.091322.

Adler, J., Parmryd, I., 2010. Quantifying colocalization by correlation: the Pearson correlation coefficient is superior to the Mander's overlap coefficient. Cytometry. Part A : the journal of the International Society for Analytical Cytology 77, 733–742. https://doi.org/10.1002/cyto.a.20896.

Alam, P., Bousset, L., Melki, R., Otzen, D.E., 2019. α-synuclein oligomers and fibrils: a spectrum of species, a spectrum of toxicities. Journal of neurochemistry 150, 522–534. https://doi.org/10.1111/jnc.14808.

Armstrong, M.J., Okun, M.S., 2020. Diagnosis and Treatment of Parkinson Disease: A Review. JAMA 323, 548–560. https://doi.org/10.1001/jama.2019.22360.

Arotcarena, M.-L., Dovero, S., Prigent, A., Bourdenx, M., Camus, S., Porras, G., Thiolat, M.-L., Tasselli, M., Aubert, P., Kruse, N., Mollenhauer, B., Trigo Damas, I., Estrada, C., Garcia-Carrillo, N., Vaikath, N.N., El-Agnaf, O.M.A., Herrero, M.T., Vila, M., Obeso, J.A., Derkinderen, P., Dehay, B., Bezard, E., 2020. Bidirectional gut-to-brain and brain-to-gut propagation of synucleinopathy in non-human primates. Brain 143, 1462–1475. https://doi.org/10.1093/brain/awaa096.

Ascherio, A., Schwarzschild, M.A., 2016. The epidemiology of Parkinson's disease: risk factors and prevention. The Lancet. Neurology 15, 1257–1272. https://doi.org/10.1016/S1474-4422(16)30230-7.

Balestrino, R., Schapira, A.H.V., 2020. Parkinson disease. European journal of neurology 27, 27–42. https://doi.org/10.1111/ene.14108.

Bargar, C., Luca, C.M.G. de, Devigili, G., Elia, A.E., Cilia, R., Portaleone, S.M., Wang, W., Tramacere, I., Bistaffa, E., Cazzaniga, F.A., Felisati, G., Legname, G., Di Fonzo, A., Xu, R., Gunzler, S.A., Giaccone, G., Eleopra, R., Chen, S.G., Moda, F., 2021. Discrimination of MSA-P and MSA-C by RT-QuIC analysis of olfactory mucosa: the first assessment of assay reproducibility between two specialized laboratories. Molecular Neurodegeneration 16, 82. https://doi.org/10.1186/s13024-021-00491-y.

Barone, P., Erro, R., Picillo, M., 2017. Quality of Life and Nonmotor Symptoms in Parkinson's Disease. International review of neurobiology 133, 499–516. https://doi.org/10.1016/bs.irn.2017.05.023.

Bartl, M., Dakna, M., Schade, S., Wicke, T., Lang, E., Ebentheuer, J., Weber, S., Trenkwalder, C., Mollenhauer, B., 2022. Longitudinal Change and Progression Indicators Using the Movement Disorder Society-Unified Parkinson's Disease Rating Scale in Two Independent Cohorts with Early Parkinson's Disease. Journal of Parkinson's Disease 12, 437–452. https://doi.org/10.3233/JPD-212860.

Beach, T.G., Adler, C.H., Lue, L., Sue, L.I., Bachalakuri, J., Henry-Watson, J., Sasse, J., Boyer, S., Shirohi, S., Brooks, R., Eschbacher, J., White, C.L., Akiyama, H., Caviness, J., Shill, H.A., Connor, D.J., Sabbagh, M.N., Walker, D.G., 2009. Unified staging system for Lewy body disorders: correlation with nigrostriatal degeneration, cognitive impairment and motor dysfunction. Acta Neuropathol 117, 613–634. https://doi.org/10.1007/s00401-009-0538-8.

Bellomo, G., Luca, C.M.G. de, Paoletti, F.P., Gaetani, L., Moda, F., Parnetti, L., 2022. α-Synuclein Seed Amplification Assays for Diagnosing Synucleinopathies: The Way Forward. Neurology 99, 195–205. https://doi.org/10.1212/WNL.0000000000200878.

Bendor, J.T., Logan, T.P., Edwards, R.H., 2013. The function of α-synuclein. Neuron 79, 1044–1066. https://doi.org/10.1016/j.neuron.2013.09.004.

Berg, D., Borghammer, P., Fereshtehnejad, S.-M., Heinzel, S., Horsager, J., Schaeffer, E., Postuma, R.B., 2021. Prodromal Parkinson disease subtypes - key to understanding heterogeneity. Nature reviews. Neurology 17, 349–361. https://doi.org/10.1038/s41582-021-00486-9.

Berg, S., Kutra, D., Kroeger, T., Straehle, C.N., Kausler, B.X., Haubold, C., Schiegg, M., Ales, J., Beier, T., Rudy, M., Eren, K., Cervantes, J.I., Xu, B., Beuttenmueller, F., Wolny, A., Zhang, C., Koethe, U., Hamprecht, F.A., Kreshuk, A., 2019. ilastik: interactive machine learning for (bio)image analysis. Nature methods 16, 1226–1232. https://doi.org/10.1038/s41592-019-0582-9.

Beyer, K., Ariza, A., 2013. α-Synuclein posttranslational modification and alternative splicing as a trigger for neurodegeneration. Molecular Neurobiology 47, 509–524. https://doi.org/10.1007/s12035-012-8330-5.

Bido, S., Muggeo, S., Massimino, L., Marzi, M.J., Giannelli, S.G., Melacini, E., Nannoni, M., Gambarè, D., Bellini, E., Ordazzo, G., Rossi, G., Maffezzini, C., Iannelli, A., Luoni, M., Bacigaluppi, M., Gregori, S., Nicassio, F., Broccoli, V., 2021. Microglia-specific overexpression of α-synuclein leads to severe dopaminergic neurodegeneration by phagocytic exhaustion and oxidative toxicity. Nat Commun 12, 6237. https://doi.org/10.1038/s41467-021-26519-x.

Bjorklund, G., Stejskal, V., Urbina, M.A., Dadar, M., Chirumbolo, S., Mutter, J., 2018. Metals and Parkinson's Disease: Mechanisms and Biochemical Processes. Current medicinal chemistry 25, 2198–2214. https://doi.org/10.2174/0929867325666171129124616.

Bloem, B.R., Okun, M.S., Klein, C., 2021. Parkinson's disease. Lancet (London, England) 397, 2284–2303. https://doi.org/10.1016/S0140-6736(21)00218-X.

Bolte, S., Cordelières, F.P., 2006. A guided tour into subcellular colocalization analysis in light microscopy. Journal of microscopy 224, 213–232. https://doi.org/10.1111/j.1365-2818.2006.01706.x.

Borghammer, P., 2018. How does parkinson's disease begin? Perspectives on neuroanatomical pathways, prions, and histology. Movement disorders : official journal of the Movement Disorder Society 33, 48–57. https://doi.org/10.1002/mds.27138.

Borghammer, P., 2021. The α-Synuclein Origin and Connectome Model (SOC Model) of Parkinson's Disease: Explaining Motor Asymmetry, Non-Motor Phenotypes, and Cognitive Decline. Journal of Parkinson's Disease 11, 455–474. https://doi.org/10.3233/JPD-202481.

Borghammer, P., Horsager, J., Andersen, K., van den Berge, N., Raunio, A., Murayama, S., Parkkinen, L., Myllykangas, L., 2021. Neuropathological evidence of body-first vs. brain-first Lewy body disease. Neurobiology of Disease 161, 105557. https://doi.org/10.1016/j.nbd.2021.105557.

Bousset, L., Pieri, L., Ruiz-Arlandis, G., Gath, J., Jensen, P.H., Habenstein, B., Madiona, K., Olieric, V., Böckmann, A., Meier, B.H., Melki, R., 2013. Structural and functional characterization of two alpha-synuclein strains. Nat Commun 4. https://doi.org/10.1038/ncomms3575.

Braak, H., Rüb, U., Del Tredici, K., 2006. Cognitive decline correlates with neuropathological stage in Parkinson's disease. Journal of the neurological sciences 248, 255–258. https://doi.org/10.1016/j.jns.2006.05.011.

Braak, H., Tredici, K.D., Rüb, U., Vos, R.A. de, Jansen Steur, E.N., Braak, E., 2003. Staging of brain pathology related to sporadic Parkinson’s disease. Neurobiology of Aging 24, 197–211. https://doi.org/10.1016/S0197-4580(02)00065-9.

Brandebura, A.N., Paumier, A., Onur, T.S., Allen, N.J., 2023. Astrocyte contribution to dysfunction, risk and progression in neurodegenerative disorders. Nature reviews. Neuroscience 24, 23–39. https://doi.org/10.1038/s41583-022-00641-1.

Breckenridge, C.B., Berry, C., Chang, E.T., Sielken, R.L., Mandel, J.S., 2016. Association between Parkinson's Disease and Cigarette Smoking, Rural Living, Well-Water Consumption, Farming and Pesticide Use: Systematic Review and Meta-Analysis. PloS one 11, e0151841. https://doi.org/10.1371/journal.pone.0151841.

Breen, D.P., Halliday, G.M., Lang, A.E., 2019. Gut-brain axis and the spread of α-synuclein pathology: Vagal highway or dead end? Movement disorders : official journal of the Movement Disorder Society 34, 307–316. https://doi.org/10.1002/mds.27556.

Brembati, V., Faustini, G., Longhena, F., Bellucci, A., 2023. Alpha synuclein post translational modifications: potential targets for Parkinson's disease therapy? Frontiers in molecular neuroscience 16, 1197853. https://doi.org/10.3389/fnmol.2023.1197853.

Brundin, P., Kordower, J.H., 2012. Neuropathology in transplants in Parkinson's disease: implications for disease pathogenesis and the future of cell therapy. Progress in brain research 200, 221–241. https://doi.org/10.1016/B978-0-444-59575-1.00010-7.

Brundin, P., Melki, R., 2017. Prying into the Prion Hypothesis for Parkinson's Disease. The Journal of neuroscience : the official journal of the Society for Neuroscience 37, 9808–9818. https://doi.org/10.1523/JNEUROSCI.1788-16.2017.

Caldi Gomes, L., Galhoz, A., Jain, G., Roser, A.-E., Maass, F., Carboni, E., Barski, E., Lenz, C., Lohmann, K., Klein, C., Bähr, M., Fischer, A., Menden, M.P., Lingor, P., 2022. Multi-omic landscaping of human midbrains identifies disease-relevant molecular targets and pathways in advanced-stage Parkinson's disease. Clinical and translational medicine 12, e692. https://doi.org/10.1002/ctm2.692.

Chen, S.W., Drakulic, S., Deas, E., Ouberai, M., Aprile, F.A., Arranz, R., Ness, S., Roodveldt, C., Guilliams, T., De-Genst, E.J., Klenerman, D., Wood, N.W., Knowles, T.P.J., Alfonso, C., Rivas, G., Abramov, A.Y., Valpuesta, J.M., Dobson, C.M., Cremades, N., 2015. Structural characterization of toxic oligomers that are kinetically trapped during α-synuclein fibril formation. Proceedings of the National Academy of Sciences of the United States of America 112, E1994-2003. https://doi.org/10.1073/pnas.1421204112.

Choi, I., Zhang, Y., Seegobin, S.P., Pruvost, M., Wang, Q., Purtell, K., Zhang, B., Yue, Z., 2020. Microglia clear neuron-released α-synuclein via selective autophagy and prevent neurodegeneration. Nat Commun 11, 1386. https://doi.org/10.1038/s41467-020-15119-w.

Chung, H.K., Ho, H.-A., Pérez-Acuña, D., Lee, S.-J., 2019. Modeling α-Synuclein Propagation with Preformed Fibril Injections. Journal of movement disorders 12, 139–151. https://doi.org/10.14802/jmd.19046.

Cocco, C., Manai, A.L., Manca, E., Noli, B., 2023. Brain-Biomarker Changes in Body Fluids of Patients with Parkinson's Disease. International journal of molecular sciences 24. https://doi.org/10.3390/ijms241310932.

Coelln, R. von, Gruber-Baldini, A.L., Reich, S.G., Armstrong, M.J., Savitt, J.M., Shulman, L.M., 2021. The inconsistency and instability of Parkinson's disease motor subtypes. Parkinsonism & related disorders 88, 13–18. https://doi.org/10.1016/j.parkreldis.2021.05.016.

Collinge, J., Clarke, A.R., 2007. A general model of prion strains and their pathogenicity. Science (New York, N.Y.) 318, 930–936. https://doi.org/10.1126/science.1138718.

Colosimo, C., Hughes, A.J., Kilford, L., Lees, A.J., 2003. Lewy body cortical involvement may not always predict dementia in Parkinson's disease. Journal of neurology, neurosurgery, and psychiatry 74, 852–856. https://doi.org/10.1136/jnnp.74.7.852.

Conway, K.A., Lee, S.J., Rochet, J.C., Ding, T.T., Williamson, R.E., Lansbury, P.T., 2000. Acceleration of oligomerization, not fibrillization, is a shared property of both alpha-synuclein mutations linked to early-onset Parkinson's disease: implications for pathogenesis and therapy. Proceedings of the National Academy of Sciences of the United States of America 97, 571–576. https://doi.org/10.1073/pnas.97.2.571.

Cserép, C., Pósfai, B., Dénes, Á., 2021. Shaping Neuronal Fate: Functional Heterogeneity of Direct Microglia-Neuron Interactions. Neuron 109, 222–240. https://doi.org/10.1016/j.neuron.2020.11.007.

Cykowski, M.D., Coon, E.A., Powell, S.Z., Jenkins, S.M., Benarroch, E.E., Low, P.A., Schmeichel, A.M., Parisi, J.E., 2015. Expanding the spectrum of neuronal pathology in multiple system atrophy. Brain 138, 2293–2309. https://doi.org/10.1093/brain/awv114.

Dauer Née Joppe, K., Tatenhorst, L., Caldi Gomes, L., Zhang, S., Parvaz, M., Carboni, E., Roser, A.-E., El DeBakey, H., Bähr, M., Vogel-Mikuš, K., Wang Ip, C., Becker, S., Zweckstetter, M., Lingor, P., 2021. Brain iron enrichment attenuates α-synuclein spreading after injection of preformed fibrils. Journal of neurochemistry 159, 554–573. https://doi.org/10.1111/jnc.15461.

Desplats, P., Lee, H.-J., Bae, E.-J., Patrick, C., Rockenstein, E., Crews, L., Spencer, B., Masliah, E., Lee, S.-J., 2009. Inclusion formation and neuronal cell death through neuron-to-neuron transmission of alpha-synuclein. Proceedings of the National Academy of Sciences of the United States of America 106, 13010–13015. https://doi.org/10.1073/pnas.0903691106.

Dettmer, U., Newman, A.J., Saucken, V.E. von, Bartels, T., Selkoe, D., 2015. KTKEGV repeat motifs are key mediators of normal α-synuclein tetramerization: Their mutation causes excess monomers and neurotoxicity. Proceedings of the National Academy of Sciences of the United States of America 112, 9596–9601. https://doi.org/10.1073/pnas.1505953112.

Dexter, D.T., Jenner, P., 2013. Parkinson disease: from pathology to molecular disease mechanisms. Free radical biology & medicine 62, 132–144. https://doi.org/10.1016/j.freeradbiomed.2013.01.018.

Deyell, J.S., Sriparna, M., Ying, M., Mao, X., 2023. The Interplay between α-Synuclein and Microglia in α-Synucleinopathies. International journal of molecular sciences 24. https://doi.org/10.3390/ijms24032477.

Dhillon, J.-K.S., Trejo-Lopez, J.A., Riffe, C., Levites, Y., Sacino, A.N., Borchelt, D.R., Yachnis, A.Y., Giasson, B.I., 2019. Comparative analyses of the in vivo induction and transmission of α-synuclein pathology in transgenic mice by MSA brain lysate and recombinant α-synuclein fibrils. Acta Neuropathologica Communications 7, 80. https://doi.org/10.1186/s40478-019-0733-3.

Di Vieira, B.M., Radford, R.A., Chung, R.S., Guillemin, G.J., Pountney, D.L., 2015. Neuroinflammation in Multiple System Atrophy: Response to and Cause of α-Synuclein Aggregation. Frontiers in Cellular Neuroscience 9, 437. https://doi.org/10.3389/fncel.2015.00437.

Donadio, V., Incensi, A., Piccinini, C., Cortelli, P., Giannoccaro, M.P., Baruzzi, A., Liguori, R., 2016. Skin nerve misfolded α-synuclein in pure autonomic failure and Parkinson disease. Annals of neurology 79, 306–316. https://doi.org/10.1002/ana.24567.

Dorsey, E.R., Sherer, T., Okun, M.S., Bloem, B.R., 2018. The Emerging Evidence of the Parkinson Pandemic. Journal of Parkinson's Disease 8, S3-S8. https://doi.org/10.3233/JPD-181474.

Duffy, M.F., Collier, T.J., Patterson, J.R., Kemp, C.J., Fischer, D.L., Stoll, A.C., Sortwell, C.E., 2018a. Quality Over Quantity: Advantages of Using Alpha-Synuclein Preformed Fibril Triggered Synucleinopathy to Model Idiopathic Parkinson's Disease. Frontiers in neuroscience 12, 621. https://doi.org/10.3389/fnins.2018.00621.

Duffy, M.F., Collier, T.J., Patterson, J.R., Kemp, C.J., Luk, K.C., Tansey, M.G., Paumier, K.L., Kanaan, N.M., Fischer, D.L., Polinski, N.K., Barth, O.L., Howe, J.W., Vaikath, N.N., Majbour, N.K., El-Agnaf, O.M.A., Sortwell, C.E., 2018b. Lewy body-like alpha-synuclein inclusions trigger reactive microgliosis prior to nigral degeneration. Journal of Neuroinflammation 15, 129. https://doi.org/10.1186/s12974-018-1171-z.

Earls, R.H., Menees, K.B., Chung, J., Barber, J., Gutekunst, C.-A., Hazim, M.G., Lee, J.-K., 2019. Intrastriatal injection of preformed alpha-synuclein fibrils alters central and peripheral immune cell profiles in non-transgenic mice. Journal of Neuroinflammation 16, 250. https://doi.org/10.1186/s12974-019-1636-8.

Earls, R.H., Menees, K.B., Chung, J., Gutekunst, C.-A., Lee, H.J., Hazim, M.G., Rada, B., Wood, L.B., Lee, J.-K., 2020. NK cells clear α-synuclein and the depletion of NK cells exacerbates synuclein

pathology in a mouse model of α-synucleinopathy. Proceedings of the National Academy of Sciences of the United States of America 117, 1762–1771. https://doi.org/10.1073/pnas.1909110117.

Eusebi, P., Giannandrea, D., Biscetti, L., Abraha, I., Chiasserini, D., Orso, M., Calabresi, P., Parnetti, L., 2017. Diagnostic utility of cerebrospinal fluid α-synuclein in Parkinson's disease: A systematic review and meta-analysis. Movement disorders : official journal of the Movement Disorder Society 32, 1389–1400. https://doi.org/10.1002/mds.27110.

Fairfoul, G., McGuire, L.I., Pal, S., Ironside, J.W., Neumann, J., Christie, S., Joachim, C., Esiri, M., Evetts, S.G., Rolinski, M., Baig, F., Ruffmann, C., Wade-Martins, R., Hu, M.T.M., Parkkinen, L., Green, A.J.E., 2016. Alpha-synuclein RT-QuIC in the CSF of patients with alpha-synucleinopathies. Annals of clinical and translational neurology 3, 812–818. https://doi.org/10.1002/acn3.338.

Fares, M.-B., Maco, B., Oueslati, A., Rockenstein, E., Ninkina, N., Buchman, V.L., Masliah, E., Lashuel, H.A., 2016. Induction of de novo α-synuclein fibrillization in a neuronal model for Parkinson's disease. Proceedings of the National Academy of Sciences of the United States of America 113, E912-21. https://doi.org/10.1073/pnas.1512876113.

Feng, Y., Zheng, C., Zhang, Y., Xing, C., Cai, W., Li, R., Chen, J., Duan, Y., 2019. Triptolide Inhibits Preformed Fibril-Induced Microglial Activation by Targeting the MicroRNA155-5p/SHIP1 Pathway. Oxidative medicine and cellular longevity 2019, 6527638. https://doi.org/10.1155/2019/6527638.

Freeze, B., Pandya, S., Zeighami, Y., Raj, A., 2019. Regional transcriptional architecture of Parkinson's disease pathogenesis and network spread. Brain 142, 3072–3085. https://doi.org/10.1093/brain/awz223.

Frigerio, R., Fujishiro, H., Ahn, T.-B., Josephs, K.A., Maraganore, D.M., DelleDonne, A., Parisi, J.E., Klos, K.J., Boeve, B.F., Dickson, D.W., Ahlskog, J.E., 2011. Incidental Lewy body disease: do some cases represent a preclinical stage of dementia with Lewy bodies? Neurobiology of Aging 32, 857–863. https://doi.org/10.1016/j.neurobiolaging.2009.05.019.

Fujiwara, H., Hasegawa, M., Dohmae, N., Kawashima, A., Masliah, E., Goldberg, M.S., Shen, J., Takio, K., Iwatsubo, T., 2002. alpha-Synuclein is phosphorylated in synucleinopathy lesions. Nature cell biology 4, 160–164. https://doi.org/10.1038/ncb748.

Gao, L., Tang, H., Nie, K., Wang, L., Zhao, J., Gan, R., Huang, J., Zhu, R., Feng, S., Duan, Z., Zhang, Y., Wang, L., 2015. Cerebrospinal fluid alpha-synuclein as a biomarker for Parkinson's disease diagnosis: a systematic review and meta-analysis. The International journal of neuroscience 125, 645–654. https://doi.org/10.3109/00207454.2014.961454.

García Ruiz, P.J., 2004. Prehistoria de la enfermedad de Parkinson [Prehistory of Parkinson's disease]. Neurologia (Barcelona, Spain) 19, 735–737.

Gasser, T., 1998. Genetics of Parkinson's disease. Annals of neurology 44, S53-7. https://doi.org/10.1002/ana.410440708.

Gelpi, E., Navarro-Otano, J., Tolosa, E., Gaig, C., Compta, Y., Rey, M.J., Martí, M.J., Hernández, I., Valldeoriola, F., Reñé, R., Ribalta, T., 2014. Multiple organ involvement by alpha-synuclein pathology in Lewy body disorders. Movement disorders : official journal of the Movement Disorder Society 29, 1010–1018. https://doi.org/10.1002/mds.25776.

George, S., Rey, N.L., Tyson, T., Esquibel, C., Meyerdirk, L., Schulz, E., Pierce, S., Burmeister, A.R., Madaj, Z., Steiner, J.A., Escobar Galvis, M.L., Brundin, L., Brundin, P., 2019. Microglia affect α-synuclein cell-to-cell transfer in a mouse model of Parkinson's disease. Molecular Neurodegeneration 14, 34. https://doi.org/10.1186/s13024-019-0335-3.

Gilman, S., Wenning, G.K., Low, P.A., Brooks, D.J., Mathias, C.J., Trojanowski, J.Q., Wood, N.W., Colosimo, C., Dürr, A., Fowler, C.J., Kaufmann, H., Klockgether, T., Lees, A., Poewe, W., Quinn, N., Revesz, T., Robertson, D., Sandroni, P., Seppi, K., Vidailhet, M., 2008. Second consensus statement

on the diagnosis of multiple system atrophy. Neurology 71, 670–676. https://doi.org/10.1212/01.wnl.0000324625.00404.15.
2018. Global, regional, and national burden of Parkinson's disease, 1990-2016: a systematic analysis for the Global Burden of Disease Study 2016. The Lancet. Neurology 17, 939–953. https://doi.org/10.1016/S1474-4422(18)30295-3.
Goedert, M., Masuda-Suzukake, M., Falcon, B., 2017. Like prions: the propagation of aggregated tau and α-synuclein in neurodegeneration. Brain 140, 266–278. https://doi.org/10.1093/brain/aww230.
Goldman, J.G., Postuma, R., 2014. Premotor and nonmotor features of Parkinson's disease. Current opinion in neurology 27, 434–441. https://doi.org/10.1097/WCO.0000000000000112.
Gordon, R., Albornoz, E.A., Christie, D.C., Langley, M.R., Kumar, V., Mantovani, S., Robertson, A.A.B., Butler, M.S., Rowe, D.B., O'Neill, L.A., Kanthasamy, A.G., Schroder, K., Cooper, M.A., Woodruff, T.M., 2018. Inflammasome inhibition prevents α-synuclein pathology and dopaminergic neurodegeneration in mice. Science translational medicine 10. https://doi.org/10.1126/scitranslmed.aah4066.
Groveman, B.R., Orrù, C.D., Hughson, A.G., Raymond, L.D., Zanusso, G., Ghetti, B., Campbell, K.J., Safar, J., Galasko, D., Caughey, B., 2018. Rapid and ultra-sensitive quantitation of disease-associated α-synuclein seeds in brain and cerebrospinal fluid by αSyn RT-QuIC. Acta Neuropathologica Communications 6, 7. https://doi.org/10.1186/s40478-018-0508-2.
Guo, J.L., Covell, D.J., Daniels, J.P., Iba, M., Stieber, A., Zhang, B., Riddle, D.M., Kwong, L.K., Xu, Y., Trojanowski, J.Q., Lee, V.M.Y., 2013. Distinct α-synuclein strains differentially promote tau inclusions in neurons. Cell 154, 103–117. https://doi.org/10.1016/j.cell.2013.05.057.
Hall, S., Janelidze, S., Surova, Y., Widner, H., Zetterberg, H., Hansson, O., 2018. Cerebrospinal fluid concentrations of inflammatory markers in Parkinson's disease and atypical parkinsonian disorders. Scientific Reports 8, 13276. https://doi.org/10.1038/s41598-018-31517-z.
Hansen, C., Angot, E., Bergström, A.-L., Steiner, J.A., Pieri, L., Paul, G., Outeiro, T.F., Melki, R., Kallunki, P., Fog, K., Li, J.-Y., Brundin, P., 2011. α-Synuclein propagates from mouse brain to grafted dopaminergic neurons and seeds aggregation in cultured human cells. The Journal of clinical investigation 121, 715–725. https://doi.org/10.1172/JCI43366.
Harms, A.S., Kordower, J.H., Sette, A., Lindestam Arlehamn, C.S., Sulzer, D., Mach, R.H., 2021. Inflammation in Experimental Models of α-Synucleinopathies. Movement disorders : official journal of the Movement Disorder Society 36, 37–49. https://doi.org/10.1002/mds.28264.
Henrich, M.T., Geibl, F.F., Lakshminarasimhan, H., Stegmann, A., Giasson, B.I., Mao, X., Dawson, V.L., Dawson, T.M., Oertel, W.H., Surmeier, D.J., 2020. Determinants of seeding and spreading of α-synuclein pathology in the brain. Science advances 6. https://doi.org/10.1126/sciadv.abc2487.
Hoffmann, A., Ettle, B., Battis, K., Reiprich, S., Schlachetzki, J.C.M., Masliah, E., Wegner, M., Kuhlmann, T., Riemenschneider, M.J., Winkler, J., 2019. Oligodendroglial α-synucleinopathy-driven neuroinflammation in multiple system atrophy. Brain pathology (Zurich, Switzerland) 29, 380–396. https://doi.org/10.1111/bpa.12678.
Hoffmann, A., Ettle, B., Bruno, A., Kulinich, A., Hoffmann, A.-C., Wittgenstein, J. von, Winkler, J., Xiang, W., Schlachetzki, J.C.M., 2016. Alpha-synuclein activates BV2 microglia dependent on its aggregation state. Biochemical and biophysical research communications 479, 881–886. https://doi.org/10.1016/j.bbrc.2016.09.109.
Holec, S.A.M., Lee, J., Oehler, A., Ooi, F.K., Mordes, D.A., Olson, S.H., Prusiner, S.B., Woerman, A.L., 2022. Multiple system atrophy prions transmit neurological disease to mice expressing wild-type human α-synuclein. Acta Neuropathol 144, 677–690. https://doi.org/10.1007/s00401-022-02476-7.

Holec, S.A.M., Woerman, A.L., 2021. Evidence of distinct α-synuclein strains underlying disease heterogeneity. Acta Neuropathol 142, 73–86. https://doi.org/10.1007/s00401-020-02163-5.

Horsager, J., Andersen, K.B., Knudsen, K., Skjærbæk, C., Fedorova, T.D., Okkels, N., Schaeffer, E., Bonkat, S.K., Geday, J., Otto, M., Sommerauer, M., Danielsen, E.H., Bech, E., Kraft, J., Munk, O.L., Hansen, S.D., Pavese, N., Göder, R., Brooks, D.J., Berg, D., Borghammer, P., 2020. Brain-first versus body-first Parkinson's disease: a multimodal imaging case-control study. Brain 143, 3077–3088. https://doi.org/10.1093/brain/awaa238.

Howe, J.W., Sortwell, C.E., Duffy, M.F., Kemp, C.J., Russell, C.P., Kubik, M., Patel, P., Luk, K.C., El-Agnaf, O.M.A., Patterson, J.R., 2021. Preformed fibrils generated from mouse alpha-synuclein produce more inclusion pathology in rats than fibrils generated from rat alpha-synuclein. Parkinsonism & related disorders 89, 41–47. https://doi.org/10.1016/j.parkreldis.2021.06.010.

Hoyer, W., Antony, T., Cherny, D., Heim, G., Jovin, T.M., Subramaniam, V., 2002. Dependence of α-Synuclein Aggregate Morphology on Solution Conditions. Journal of Molecular Biology 322, 383–393. https://doi.org/10.1016/S0022-2836(02)00775-1.

Iljina, M., Garcia, G.A., Horrocks, M.H., Tosatto, L., Choi, M.L., Ganzinger, K.A., Abramov, A.Y., Gandhi, S., Wood, N.W., Cremades, N., Dobson, C.M., Knowles, T.P.J., Klenerman, D., 2016. Kinetic model of the aggregation of alpha-synuclein provides insights into prion-like spreading. Proceedings of the National Academy of Sciences of the United States of America 113, E1206-15. https://doi.org/10.1073/pnas.1524128113.

Iranzo, A., Fairfoul, G., Ayudhaya, A.C.N., Serradell, M., Gelpi, E., Vilaseca, I., Sanchez-Valle, R., Gaig, C., Santamaria, J., Tolosa, E., Riha, R.L., Green, A.J.E., 2021. Detection of α-synuclein in CSF by RT-QuIC in patients with isolated rapid-eye-movement sleep behaviour disorder: a longitudinal observational study. The Lancet. Neurology 20, 203–212. https://doi.org/10.1016/S1474-4422(20)30449-X.

Irwin, D.J., Grossman, M., Weintraub, D., Hurtig, H.I., Duda, J.E., Xie, S.X., Lee, E.B., van Deerlin, V.M., Lopez, O.L., Kofler, J.K., Nelson, P.T., Jicha, G.A., Woltjer, R., Quinn, J.F., Kaye, J., Leverenz, J.B., Tsuang, D., Longfellow, K., Yearout, D., Kukull, W., Keene, C.D., Montine, T.J., Zabetian, C.P., Trojanowski, J.Q., 2017. Neuropathological and genetic correlates of survival and dementia onset in synucleinopathies: a retrospective analysis. The Lancet. Neurology 16, 55–65. https://doi.org/10.1016/S1474-4422(16)30291-5.

Ishizawa, K., Komori, T., Sasaki, S., Arai, N., Mizutani, T., Hirose, T., 2004. Microglial activation parallels system degeneration in multiple system atrophy. Journal of neuropathology and experimental neurology 63, 43–52. https://doi.org/10.1093/jnen/63.1.43.

Jellinger, K.A., 2009. A critical evaluation of current staging of alpha-synuclein pathology in Lewy body disorders. Biochimica et biophysica acta 1792, 730–740. https://doi.org/10.1016/j.bbadis.2008.07.006.

Johnson, M., Coulton, A.T., Geeves, M.A., Mulvihill, D.P., 2010. Targeted amino-terminal acetylation of recombinant proteins in E. coli. PloS one 5, e15801. https://doi.org/10.1371/journal.pone.0015801.

Johnson, M.E., Stecher, B., Labrie, V., Brundin, L., Brundin, P., 2019. Triggers, Facilitators, and Aggravators: Redefining Parkinson's Disease Pathogenesis. Trends in neurosciences 42, 4–13. https://doi.org/10.1016/j.tins.2018.09.007.

Just, M.K., Gram, H., Theologidis, V., Jensen, P.H., Nilsson, K.P.R., Lindgren, M., Knudsen, K., Borghammer, P., van den Berge, N., 2022. Alpha-Synuclein Strain Variability in Body-First and Brain-First Synucleinopathies. Frontiers in aging neuroscience 14, 907293. https://doi.org/10.3389/fnagi.2022.907293.

Kalaitzakis, M.E., Graeber, M.B., Gentleman, S.M., Pearce, R.K.B., 2008. The dorsal motor nucleus of the vagus is not an obligatory trigger site of Parkinson's disease: a critical analysis of alpha-

synuclein staging. Neuropathology and applied neurobiology 34, 284–295. https://doi.org/10.1111/j.1365-2990.2007.00923.x.

Kalia, L.V., Lang, A.E., 2015. Parkinson's disease. Lancet (London, England) 386, 896–912. https://doi.org/10.1016/S0140-6736(14)61393-3.

Kannarkat, G.T., Boss, J.M., Tansey, M.G., 2013. The role of innate and adaptive immunity in Parkinson's disease. Journal of Parkinson's Disease 3, 493–514. https://doi.org/10.3233/JPD-130250.

Kasen, A., Houck, C., Burmeister, A.R., Sha, Q., Brundin, L., Brundin, P., 2022. Upregulation of α-synuclein following immune activation: Possible trigger of Parkinson's disease. Neurobiology of Disease 166, 105654. https://doi.org/10.1016/j.nbd.2022.105654.

Kim, S., Kwon, S.-H., Kam, T.-I., Panicker, N., Karuppagounder, S.S., Lee, S., Lee, J.H., Kim, W.R., Kook, M., Foss, C.A., Shen, C., Lee, H., Kulkarni, S., Pasricha, P.J., Lee, G., Pomper, M.G., Dawson, V.L., Dawson, T.M., Ko, H.S., 2019. Transneuronal Propagation of Pathologic α-Synuclein from the Gut to the Brain Models Parkinson's Disease. Neuron 103, 627-641.e7. https://doi.org/10.1016/j.neuron.2019.05.035.

Kishimoto, Y., Zhu, W., Hosoda, W., Sen, J.M., Mattson, M.P., 2019. Chronic Mild Gut Inflammation Accelerates Brain Neuropathology and Motor Dysfunction in α-Synuclein Mutant Mice. Neuromolecular medicine 21, 239–249. https://doi.org/10.1007/s12017-019-08539-5.

Knudsen, K., Fedorova, T.D., Horsager, J., Andersen, K.B., Skjærbæk, C., Berg, D., Schaeffer, E., Brooks, D.J., Pavese, N., van den Berge, N., Borghammer, P., 2021. Asymmetric Dopaminergic Dysfunction in Brain-First versus Body-First Parkinson's Disease Subtypes. Journal of Parkinson's Disease 11, 1677–1687. https://doi.org/10.3233/JPD-212761.

Koga, S., Sekiya, H., Kondru, N., Ross, O.A., Dickson, D.W., 2021. Neuropathology and molecular diagnosis of Synucleinopathies. Molecular Neurodegeneration 16, 83. https://doi.org/10.1186/s13024-021-00501-z.

Kordower, J.H., Chu, Y., Hauser, R.A., Freeman, T.B., Olanow, C.W., 2008. Lewy body-like pathology in long-term embryonic nigral transplants in Parkinson's disease. Nature medicine 14, 504–506. https://doi.org/10.1038/nm1747.

Kordower, J.H., Freeman, T.B., Snow, B.J., Vingerhoets, F.J., Mufson, E.J., Sanberg, P.R., Hauser, R.A., Smith, D.A., Nauert, G.M., Perl, D.P., 1995. Neuropathological evidence of graft survival and striatal reinnervation after the transplantation of fetal mesencephalic tissue in a patient with Parkinson's disease. The New England journal of medicine 332, 1118–1124. https://doi.org/10.1056/NEJM199504273321702.

Krüger, R., Kuhn, W., Müller, T., Woitalla, D., Graeber, M., Kösel, S., Przuntek, H., Epplen, J.T., Schöls, L., Riess, O., 1998. Ala30Pro mutation in the gene encoding alpha-synuclein in Parkinson's disease. Nature genetics 18, 106–108. https://doi.org/10.1038/ng0298-106.

Kübler, D., Wächter, T., Cabanel, N., Su, Z., Turkheimer, F.E., Dodel, R., Brooks, D.J., Oertel, W.H., Gerhard, A., 2019. Widespread microglial activation in multiple system atrophy. Movement disorders : official journal of the Movement Disorder Society 34, 564–568. https://doi.org/10.1002/mds.27620.

Kubo, S., Nemani, V.M., Chalkley, R.J., Anthony, M.D., Hattori, N., Mizuno, Y., Edwards, R.H., Fortin, D.L., 2005. A combinatorial code for the interaction of alpha-synuclein with membranes. The Journal of biological chemistry 280, 31664–31672. https://doi.org/10.1074/jbc.M504894200.

Kuter, K., Olech, Ł., Głowacka, U., 2018. Prolonged Dysfunction of Astrocytes and Activation of Microglia Accelerate Degeneration of Dopaminergic Neurons in the Rat Substantia Nigra and Block Compensation of Early Motor Dysfunction Induced by 6-OHDA. Molecular Neurobiology 55, 3049–3066. https://doi.org/10.1007/s12035-017-0529-z.

Kuzuhara, S., Mori, H., Izumiyama, N., Yoshimura, M., Ihara, Y., 1988. Lewy bodies are ubiquitinated. A light and electron microscopic immunocytochemical study. Acta Neuropathol 75, 345–353. https://doi.org/10.1007/BF00687787.

Lashuel, H.A., Overk, C.R., Oueslati, A., Masliah, E., 2013. The many faces of α-synuclein: from structure and toxicity to therapeutic target. Nature reviews. Neuroscience 14, 38–48. https://doi.org/10.1038/nrn3406.

Lastres-Becker, I., Ulusoy, A., Innamorato, N.G., Sahin, G., Rábano, A., Kirik, D., Cuadrado, A., 2012. α-Synuclein expression and Nrf2 deficiency cooperate to aggravate protein aggregation, neuronal death and inflammation in early-stage Parkinson's disease. Human molecular genetics 21, 3173–3192. https://doi.org/10.1093/hmg/dds143.

Lau, A., So, R.W.L., Lau, H.H.C., Sang, J.C., Ruiz-Riquelme, A., Fleck, S.C., Stuart, E., Menon, S., Visanji, N.P., Meisl, G., Faidi, R., Marano, M.M., Schmitt-Ulms, C., Wang, Z., Fraser, P.E., Tandon, A., Hyman, B.T., Wille, H., Ingelsson, M., Klenerman, D., Watts, J.C., 2020. α-Synuclein strains target distinct brain regions and cell types. Nature neuroscience 23, 21–31. https://doi.org/10.1038/s41593-019-0541-x.

Lee, A., Gilbert, R.M., 2016. Epidemiology of Parkinson Disease. Neurologic clinics 34, 955–965. https://doi.org/10.1016/j.ncl.2016.06.012.

Lee, H.-J., Suk, J.-E., Bae, E.-J., Lee, S.-J., 2008. Clearance and deposition of extracellular alpha-synuclein aggregates in microglia. Biochemical and biophysical research communications 372, 423–428. https://doi.org/10.1016/j.bbrc.2008.05.045.

Lee, J.W., Song, Y.S., Kim, H., Ku, B.D., Lee, W.W., 2019. Alteration of Tremor Dominant and Postural Instability Gait Difficulty Subtypes During the Progression of Parkinson's Disease: Analysis of the PPMI Cohort. Frontiers in neurology 10, 471. https://doi.org/10.3389/fneur.2019.00471.

Leńska-Mieciek, M., Madetko-Alster, N., Alster, P., Królicki, L., Fiszer, U., Koziorowski, D., 2023. Inflammation in multiple system atrophy. Frontiers in Immunology 14, 1214677. https://doi.org/10.3389/fimmu.2023.1214677.

Levin, J., Kurz, A., Arzberger, T., Giese, A., Höglinger, G.U., 2016. The Differential Diagnosis and Treatment of Atypical Parkinsonism. Deutsches Arzteblatt international 113, 61–69. https://doi.org/10.3238/arztebl.2016.0061.

Li, J.-Y., Englund, E., Holton, J.L., Soulet, D., Hagell, P., Lees, A.J., Lashley, T., Quinn, N.P., Rehncrona, S., Björklund, A., Widner, H., Revesz, T., Lindvall, O., Brundin, P., 2008. Lewy bodies in grafted neurons in subjects with Parkinson's disease suggest host-to-graft disease propagation. Nature medicine 14, 501–503. https://doi.org/10.1038/nm1746.

Li, W., Englund, E., Widner, H., Mattsson, B., van Westen, D., Lätt, J., Rehncrona, S., Brundin, P., Björklund, A., Lindvall, O., Li, J.-Y., 2016. Extensive graft-derived dopaminergic innervation is maintained 24 years after transplantation in the degenerating parkinsonian brain. Proceedings of the National Academy of Sciences of the United States of America 113, 6544–6549. https://doi.org/10.1073/pnas.1605245113.

Liddelow, S.A., Guttenplan, K.A., Clarke, L.E., Bennett, F.C., Bohlen, C.J., Schirmer, L., Bennett, M.L., Münch, A.E., Chung, W.-S., Peterson, T.C., Wilton, D.K., Frouin, A., Napier, B.A., Panicker, N., Kumar, M., Buckwalter, M.S., Rowitch, D.H., Dawson, V.L., Dawson, T.M., Stevens, B., Barres, B.A., 2017. Neurotoxic reactive astrocytes are induced by activated microglia. Nature 541, 481–487. https://doi.org/10.1038/nature21029.

Lieu, C.A., Subramanian, T., 2012. The interhemispheric connections of the striatum: Implications for Parkinson's disease and drug-induced dyskinesias. Brain research bulletin 87, 1–9. https://doi.org/10.1016/j.brainresbull.2011.09.013.

Liu, B., Fang, F., Pedersen, N.L., Tillander, A., Ludvigsson, J.F., Ekbom, A., Svenningsson, P., Chen, H., Wirdefeldt, K., 2017. Vagotomy and Parkinson disease: A Swedish register-based matched-cohort study. Neurology 88, 1996–2002. https://doi.org/10.1212/WNL.0000000000003961.

Lloyd, G.M., Sorrentino, Z.A., Quintin, S., Gorion, K.-M.M., Bell, B.M., Paterno, G., Long, B., Prokop, S., Giasson, B.I., 2022. Unique seeding profiles and prion-like propagation of synucleinopathies are highly dependent on the host in human α-synuclein transgenic mice. Acta Neuropathol 143, 663–685. https://doi.org/10.1007/s00401-022-02425-4.

Lowe, J., Blanchard, A., Morrell, K., Lennox, G., Reynolds, L., Billett, M., Landon, M., Mayer, R.J., 1988. Ubiquitin is a common factor in intermediate filament inclusion bodies of diverse type in man, including those of Parkinson's disease, Pick's disease, and Alzheimer's disease, as well as Rosenthal fibres in cerebellar astrocytomas, cytoplasmic bodies in muscle, and mallory bodies in alcoholic liver disease. The Journal of pathology 155, 9–15. https://doi.org/10.1002/path.1711550105.

Lu, L., Neff, F., Alvarez-Fischer, D., Henze, C., Xie, Y., Oertel, W.H., Schlegel, J., Hartmann, A., 2005. Gene expression profiling of Lewy body-bearing neurons in Parkinson's disease. Experimental neurology 195, 27–39. https://doi.org/10.1016/j.expneurol.2005.04.011.

Luk, K.C., Covell, D.J., Kehm, V.M., Zhang, B., Song, I.Y., Byrne, M.D., Pitkin, R.M., Decker, S.C., Trojanowski, J.Q., Lee, V.M.-Y., 2016. Molecular and Biological Compatibility with Host Alpha-Synuclein Influences Fibril Pathogenicity. Cell reports 16, 3373–3387. https://doi.org/10.1016/j.celrep.2016.08.053.

Luk, K.C., Kehm, V., Carroll, J., Zhang, B., O'Brien, P., Trojanowski, J.Q., Lee, V.M.-Y., 2012a. Pathological α-synuclein transmission initiates Parkinson-like neurodegeneration in nontransgenic mice. Science (New York, N.Y.) 338, 949–953. https://doi.org/10.1126/science.1227157.

Luk, K.C., Kehm, V.M., Zhang, B., O'Brien, P., Trojanowski, J.Q., Lee, V.M.Y., 2012b. Intracerebral inoculation of pathological α-synuclein initiates a rapidly progressive neurodegenerative α-synucleinopathy in mice. The Journal of Experimental Medicine 209, 975–986. https://doi.org/10.1084/jem.20112457.

Maass, F., Rikker, S., Dambeck, V., Warth, C., Tatenhorst, L., Csoti, I., Schmitz, M., Zerr, I., Leha, A., Bähr, M., Lingor, P., 2020. Increased alpha-synuclein tear fluid levels in patients with Parkinson's disease. Scientific Reports 10, 8507. https://doi.org/10.1038/s41598-020-65503-1.

Mahul-Mellier, A.-L., Burtscher, J., Maharjan, N., Weerens, L., Croisier, M., Kuttler, F., Leleu, M., Knott, G.W., Lashuel, H.A., 2020. The process of Lewy body formation, rather than simply α-synuclein fibrillization, is one of the major drivers of neurodegeneration. Proceedings of the National Academy of Sciences of the United States of America 117, 4971–4982. https://doi.org/10.1073/pnas.1913904117.

Marques, T.M., van Rumund, A., Oeckl, P., Kuiperij, H.B., Esselink, R.A.J., Bloem, B.R., Otto, M., Verbeek, M.M., 2019. Serum NFL discriminates Parkinson disease from atypical parkinsonisms. Neurology 92, e1479-e1486. https://doi.org/10.1212/WNL.0000000000007179.

Martinez-Valbuena, I., Swinkin, E., Santamaria, E., Fernandez-Irigoyen, J., Sackmann, V., Kim, A., Li, J., Gonzalez-Latapi, P., Kuhlman, G., Bhowmick, S.S., Visanji, N.P., Lang, A.E., Kovacs, G.G., 2022a. α-Synuclein molecular behavior and nigral proteomic profiling distinguish subtypes of Lewy body disorders. Acta Neuropathol 144, 167–185. https://doi.org/10.1007/s00401-022-02453-0.

Martinez-Valbuena, I., Visanji, N.P., Kim, A., Lau, H.H.C., So, R.W.L., Alshimemeri, S., Gao, A., Seidman, M.A., Luquin, M.R., Watts, J.C., Lang, A.E., Kovacs, G.G., 2022b. Alpha-synuclein seeding shows a wide heterogeneity in multiple system atrophy. Translational Neurodegeneration 11, 7. https://doi.org/10.1186/s40035-022-00283-4.

Masuda-Suzukake, M., Nonaka, T., Hosokawa, M., Kubo, M., Shimozawa, A., Akiyama, H., Hasegawa, M., 2014. Pathological alpha-synuclein propagates through neural networks. Acta Neuropathologica Communications 2, 88. https://doi.org/10.1186/s40478-014-0088-8.

Mavroeidi, P., Arvanitaki, F., Karakitsou, A.-K., Vetsi, M., Kloukina, I., Zweckstetter, M., Giller, K., Becker, S., Sorrentino, Z.A., Giasson, B.I., Jensen, P.H., Stefanis, L., Xilouri, M., 2019. Endogenous oligodendroglial alpha-synuclein and TPPP/p25α orchestrate alpha-synuclein pathology in experimental multiple system atrophy models. Acta neuropathologica 138, 415–441. https://doi.org/10.1007/s00401-019-02014-y.

Mehra, S., Sahay, S., Maji, S.K., 2019. α-Synuclein misfolding and aggregation: Implications in Parkinson's disease pathogenesis. Biochimica et biophysica acta. Proteins and proteomics 1867, 890–908. https://doi.org/10.1016/j.bbapap.2019.03.001.

Mendez, I., Sanchez-Pernaute, R., Cooper, O., Viñuela, A., Ferrari, D., Björklund, L., Dagher, A., Isacson, O., 2005. Cell type analysis of functional fetal dopamine cell suspension transplants in the striatum and substantia nigra of patients with Parkinson's disease. Brain 128, 1498–1510. https://doi.org/10.1093/brain/awh510.

Menon, S., Armstrong, S., Hamzeh, A., Visanji, N.P., Sardi, S.P., Tandon, A., 2022. Alpha-Synuclein Targeting Therapeutics for Parkinson's Disease and Related Synucleinopathies. Frontiers in neurology 13, 852003. https://doi.org/10.3389/fneur.2022.852003.

Milanese, C., Cerri, S., Ulusoy, A., Gornati, S.V., Plat, A., Gabriels, S., Blandini, F., Di Monte, D.A., Hoeijmakers, J.H., Mastroberardino, P.G., 2018. Activation of the DNA damage response in vivo in synucleinopathy models of Parkinson's disease. Cell death & disease 9, 818. https://doi.org/10.1038/s41419-018-0848-7.

Mori, F., Nishie, M., Kakita, A., Yoshimoto, M., Takahashi, H., Wakabayashi, K., 2006. Relationship among alpha-synuclein accumulation, dopamine synthesis, and neurodegeneration in Parkinson disease substantia nigra. Journal of neuropathology and experimental neurology 65, 808–815. https://doi.org/10.1097/01.jnen.0000230520.47768.1a.

Nalls, M.A., Pankratz, N., Lill, C.M., Do, C.B., Hernandez, D.G., Saad, M., DeStefano, A.L., Kara, E., Bras, J., Sharma, M., Schulte, C., Keller, M.F., Arepalli, S., Letson, C., Edsall, C., Stefansson, H., Liu, X., Pliner, H., Lee, J.H., Cheng, R., Ikram, M.A., Ioannidis, J.P.A., Hadjigeorgiou, G.M., Bis, J.C., Martinez, M., Perlmutter, J.S., Goate, A., Marder, K., Fiske, B., Sutherland, M., Xiromerisiou, G., Myers, R.H., Clark, L.N., Stefansson, K., Hardy, J.A., Heutink, P., Chen, H., Wood, N.W., Houlden, H., Payami, H., Brice, A., Scott, W.K., Gasser, T., Bertram, L., Eriksson, N., Foroud, T., Singleton, A.B., 2014. Large-scale meta-analysis of genome-wide association data identifies six new risk loci for Parkinson's disease. Nature genetics 46, 989–993. https://doi.org/10.1038/ng.3043.

Nykjaer, C.H., Brudek, T., Salvesen, L., Pakkenberg, B., 2017. Changes in the cell population in brain white matter in multiple system atrophy. Movement disorders : official journal of the Movement Disorder Society 32, 1074–1082. https://doi.org/10.1002/mds.26979.

Olanow, C.W., Goetz, C.G., Kordower, J.H., Stoessl, A.J., Sossi, V., Brin, M.F., Shannon, K.M., Nauert, G.M., Perl, D.P., Godbold, J., Freeman, T.B., 2003. A double-blind controlled trial of bilateral fetal nigral transplantation in Parkinson's disease. Annals of neurology 54, 403–414. https://doi.org/10.1002/ana.10720.

Olanow, C.W., Perl, D.P., DeMartino, G.N., McNaught, K.S.P., 2004. Lewy-body formation is an aggresome-related process: a hypothesis. The Lancet Neurology 3, 496–503. https://doi.org/10.1016/S1474-4422(04)00827-0.

Orimo, S., Uchihara, T., Nakamura, A., Mori, F., Kakita, A., Wakabayashi, K., Takahashi, H., 2008. Axonal alpha-synuclein aggregates herald centripetal degeneration of cardiac sympathetic nerve in Parkinson's disease. Brain 131, 642–650. https://doi.org/10.1093/brain/awm302.

Ozawa, T., Paviour, D., Quinn, N.P., Josephs, K.A., Sangha, H., Kilford, L., Healy, D.G., Wood, N.W., Lees, A.J., Holton, J.L., Revesz, T., 2004. The spectrum of pathological involvement of the striatonigral and olivopontocerebellar systems in multiple system atrophy: clinicopathological correlations. Brain 127, 2657–2671. https://doi.org/10.1093/brain/awh303.

Paccosi, E., Proietti-De-Santis, L., 2023. Parkinson's Disease: From Genetics and Epigenetics to Treatment, a miRNA-Based Strategy. International journal of molecular sciences 24. https://doi.org/10.3390/ijms24119547.

Pan, R., Chen, D., Hou, L., Hu, R., Jiao, Z., 2023. Small extracellular vesicles: a novel drug delivery system for neurodegenerative disorders. Frontiers in aging neuroscience 15, 1184435. https://doi.org/10.3389/fnagi.2023.1184435.

Pan-Montojo, F., Reichmann, H., 2014. Considerations on the role of environmental toxins in idiopathic Parkinson's disease pathophysiology. Translational Neurodegeneration 3, 10. https://doi.org/10.1186/2047-9158-3-10.

Pan-Montojo, F., Schwarz, M., Winkler, C., Arnhold, M., O'Sullivan, G.A., Pal, A., Said, J., Marsico, G., Verbavatz, J.-M., Rodrigo-Angulo, M., Gille, G., Funk, R.H.W., Reichmann, H., 2012. Environmental toxins trigger PD-like progression via increased alpha-synuclein release from enteric neurons in mice. Scientific Reports 2, 898. https://doi.org/10.1038/srep00898.

Papp, M.I., Lantos, P.L., 1994. The distribution of oligodendroglial inclusions in multiple system atrophy and its relevance to clinical symptomatology. Brain 117 (Pt 2), 235–243. https://doi.org/10.1093/brain/117.2.235.

Parkinson, J., 2002. An essay on the shaking palsy. 1817. The Journal of neuropsychiatry and clinical neurosciences 14, 223-36; discussion 222. https://doi.org/10.1176/jnp.14.2.223.

Parkkinen, L., Pirttilä, T., Alafuzoff, I., 2008. Applicability of current staging/categorization of alpha-synuclein pathology and their clinical relevance. Acta Neuropathol 115, 399–407. https://doi.org/10.1007/s00401-008-0346-6.

Parnetti, L., Gaetani, L., Eusebi, P., Paciotti, S., Hansson, O., El-Agnaf, O., Mollenhauer, B., Blennow, K., Calabresi, P., 2019. CSF and blood biomarkers for Parkinson's disease. The Lancet. Neurology 18, 573–586. https://doi.org/10.1016/S1474-4422(19)30024-9.

Patterson, J.R., Duffy, M.F., Kemp, C.J., Howe, J.W., Collier, T.J., Stoll, A.C., Miller, K.M., Patel, P., Levine, N., Moore, D.J., Luk, K.C., Fleming, S.M., Kanaan, N.M., Paumier, K.L., El-Agnaf, O.M., Sortwell, C.E., 2019. Time course and magnitude of alpha-synuclein inclusion formation and nigrostriatal degeneration in the rat model of synucleinopathy triggered by intrastriatal α-synuclein preformed fibrils. Neurobiology of Disease 130, 104525. https://doi.org/10.1016/j.nbd.2019.104525.

Paumier, K.L., Luk, K.C., Manfredsson, F.P., Kanaan, N.M., Lipton, J.W., Collier, T.J., Steece-Collier, K., Kemp, C.J., Celano, S., Schulz, E., Sandoval, I.M., Fleming, S., Dirr, E., Polinski, N.K., Trojanowski, J.Q., Lee, V.M., Sortwell, C.E., 2015. Intrastriatal injection of pre-formed mouse α-synuclein fibrils into rats triggers α-synuclein pathology and bilateral nigrostriatal degeneration. Neurobiology of Disease 82, 185–199. https://doi.org/10.1016/j.nbd.2015.06.003.

Paxinos, G., Franklin, K., 2019. Paxinos and Franklin’s the Mouse Brain in Stereotaxic Coordinates. Elsevier Science.

Peelaerts, W., Bousset, L., van der Perren, A., Moskalyuk, A., Pulizzi, R., Giugliano, M., van den Haute, C., Melki, R., Baekelandt, V., 2015. α-Synuclein strains cause distinct synucleinopathies after local and systemic administration. Nature 522, 340–344. https://doi.org/10.1038/nature14547.

Peng, C., Gathagan, R.J., Covell, D.J., Medellin, C., Stieber, A., Robinson, J.L., Zhang, B., Pitkin, R.M., Olufemi, M.F., Luk, K.C., Trojanowski, J.Q., Lee, V.M.-Y., 2018. Cellular milieu imparts distinct pathological α-synuclein strains in α-synucleinopathies. Nature 557, 558–563. https://doi.org/10.1038/s41586-018-0104-4.

Peter, I., Dubinsky, M., Bressman, S., Park, A., Lu, C., Chen, N., Wang, A., 2018. Anti-Tumor Necrosis Factor Therapy and Incidence of Parkinson Disease Among Patients With Inflammatory Bowel Disease. JAMA neurology 75, 939–946. https://doi.org/10.1001/jamaneurol.2018.0605.

Pieri, L., Madiona, K., Bousset, L., Melki, R., 2012. Fibrillar α-synuclein and huntingtin exon 1 assemblies are toxic to the cells. Biophysical journal 102, 2894–2905. https://doi.org/10.1016/j.bpj.2012.04.050.

Pike, A.F., Varanita, T., Herrebout, M.A.C., Plug, B.C., Kole, J., Musters, R.J.P., Teunissen, C.E., Hoozemans, J.J.M., Bubacco, L., Veerhuis, R., 2021. α-Synuclein evokes NLRP3 inflammasome-mediated IL-1β secretion from primary human microglia. Glia 69, 1413–1428. https://doi.org/10.1002/glia.23970.

Poewe, W., Seppi, K., Marini, K., Mahlknecht, P., 2020. New hopes for disease modification in Parkinson's Disease. Neuropharmacology 171, 108085. https://doi.org/10.1016/j.neuropharm.2020.108085.

Poewe, W., Stankovic, I., Halliday, G., Meissner, W.G., Wenning, G.K., Pellecchia, M.T., Seppi, K., Palma, J.-A., Kaufmann, H., 2022. Multiple system atrophy. Nature reviews. Disease primers 8, 56. https://doi.org/10.1038/s41572-022-00382-6.

Polinski, N.K., 2021. A Summary of Phenotypes Observed in the In Vivo Rodent Alpha-Synuclein Preformed Fibril Model. Journal of Parkinson's Disease 11, 1555–1567. https://doi.org/10.3233/JPD-212847.

Postuma, R.B., Berg, D., Stern, M., Poewe, W., Olanow, C.W., Oertel, W., Obeso, J., Marek, K., Litvan, I., Lang, A.E., Halliday, G., Goetz, C.G., Gasser, T., Dubois, B., Chan, P., Bloem, B.R., Adler, C.H., Deuschl, G., 2015. MDS clinical diagnostic criteria for Parkinson's disease. Movement disorders : official journal of the Movement Disorder Society 30, 1591–1601. https://doi.org/10.1002/mds.26424.

Prinz, M., Jung, S., Priller, J., 2019. Microglia Biology: One Century of Evolving Concepts. Cell 179, 292–311. https://doi.org/10.1016/j.cell.2019.08.053.

Prusiner, S.B., Woerman, A.L., Mordes, D.A., Watts, J.C., Rampersaud, R., Berry, D.B., Patel, S., Oehler, A., Lowe, J.K., Kravitz, S.N., Geschwind, D.H., Glidden, D.V., Halliday, G.M., Middleton, L.T., Gentleman, S.M., Grinberg, L.T., Giles, K., 2015. Evidence for α-synuclein prions causing multiple system atrophy in humans with parkinsonism. Proceedings of the National Academy of Sciences of the United States of America 112, E5308-17. https://doi.org/10.1073/pnas.1514475112.

Radford, R., Rcom-H'cheo-Gauthier, A., Wong, M.B., Eaton, E.D., Quilty, M., Blizzard, C., Norazit, A., Meedeniya, A., Vickers, J.C., Gai, W.P., Guillemin, G.J., West, A.K., Dickson, T.C., Chung, R., Pountney, D.L., 2015. The degree of astrocyte activation in multiple system atrophy is inversely proportional to the distance to α-synuclein inclusions. Molecular and cellular neurosciences 65, 68–81. https://doi.org/10.1016/j.mcn.2015.02.015.

Rahayel, S., Mišić, B., Zheng, Y.-Q., Liu, Z.-Q., Abdelgawad, A., Abbasi, N., Caputo, A., Zhang, B., Lo, A., Kehm, V., Kozak, M., Soo Yoo, H., Dagher, A., Luk, K.C., 2021. Differentially targeted seeding reveals unique pathological alpha-synuclein propagation patterns. Brain. https://doi.org/10.1093/brain/awab440.

Recasens, A., Dehay, B., Bové, J., Carballo-Carbajal, I., Dovero, S., Pérez-Villalba, A., Fernagut, P.-O., Blesa, J., Parent, A., Perier, C., Fariñas, I., Obeso, J.A., Bezard, E., Vila, M., 2014. Lewy body extracts from Parkinson disease brains trigger α-synuclein pathology and neurodegeneration in mice and monkeys. Annals of neurology 75, 351–362. https://doi.org/10.1002/ana.24066.

Renkawek, K., Stege, G.J., Bosman, G.J., 1999. Dementia, gliosis and expression of the small heat shock proteins hsp27 and alpha B-crystallin in Parkinson's disease. Neuroreport 10, 2273–2276. https://doi.org/10.1097/00001756-199908020-00009.

Rey, N.L., George, S., Steiner, J.A., Madaj, Z., Luk, K.C., Trojanowski, J.Q., Lee, V.M.-Y., Brundin, P., 2018. Spread of aggregates after olfactory bulb injection of α-synuclein fibrils is associated with early neuronal loss and is reduced long term. Acta Neuropathol 135, 65–83. https://doi.org/10.1007/s00401-017-1792-9.

Rey, N.L., Petit, G.H., Bousset, L., Melki, R., Brundin, P., 2013. Transfer of human α-synuclein from the olfactory bulb to interconnected brain regions in mice. Acta Neuropathol 126, 555–573. https://doi.org/10.1007/s00401-013-1160-3.

Rey, N.L., Steiner, J.A., Maroof, N., Luk, K.C., Madaj, Z., Trojanowski, J.Q., Lee, V.M.-Y., Brundin, P., 2016. Widespread transneuronal propagation of α-synucleinopathy triggered in olfactory bulb mimics prodromal Parkinson's disease. The Journal of Experimental Medicine 213, 1759–1778. https://doi.org/10.1084/jem.20160368.

Ricci, G., Volpi, L., Pasquali, L., Petrozzi, L., Siciliano, G., 2009. Astrocyte-neuron interactions in neurological disorders. Journal of biological physics 35, 317–336. https://doi.org/10.1007/s10867-009-9157-9.

Roberts, R.F., Wade-Martins, R., Alegre-Abarrategui, J., 2015. Direct visualization of alpha-synuclein oligomers reveals previously undetected pathology in Parkinson's disease brain. Brain 138, 1642–1657. https://doi.org/10.1093/brain/awv040.

Rodger, A.T., ALNasser, M., Carter, W.G., 2023. Are Therapies That Target α-Synuclein Effective at Halting Parkinson's Disease Progression? A Systematic Review. International journal of molecular sciences 24. https://doi.org/10.3390/ijms241311022.

Santaella, A., Kuiperij, H.B., van Rumund, A., Esselink, R.A.J., van Gool, A.J., Bloem, B.R., Verbeek, M.M., 2020. Inflammation biomarker discovery in Parkinson's disease and atypical parkinsonisms. BMC neurology 20, 26. https://doi.org/10.1186/s12883-020-1608-8.

Sargent, D., Verchère, J., Lazizzera, C., Gaillard, D., Lakhdar, L., Streichenberger, N., Morignat, E., Bétemps, D., Baron, T., 2017. 'Prion-like' propagation of the synucleinopathy of M83 transgenic mice depends on the mouse genotype and type of inoculum. Journal of neurochemistry 143, 126–135. https://doi.org/10.1111/jnc.14139.

Sarkar, S., Dammer, E.B., Malovic, E., Olsen, A.L., Raza, S.A., Gao, T., Xiao, H., Oliver, D.L., Duong, D., Joers, V., Seyfried, N., Huang, M., Kukar, T., Tansey, M.G., Kanthasamy, A.G., Rangaraju, S., 2020. Molecular Signatures of Neuroinflammation Induced by αSynuclein Aggregates in Microglial Cells. Frontiers in Immunology 11, 33. https://doi.org/10.3389/fimmu.2020.00033.

Savica, R., Rocca, W.A., Ahlskog, J.E., 2010. When does Parkinson disease start? Archives of neurology 67, 798–801. https://doi.org/10.1001/archneurol.2010.135.

Scheiblich, H., Dansokho, C., Mercan, D., Schmidt, S.V., Bousset, L., Wischhof, L., Eikens, F., Odainic, A., Spitzer, J., Griep, A., Schwartz, S., Bano, D., Latz, E., Melki, R., Heneka, M.T., 2021. Microglia jointly degrade fibrillar alpha-synuclein cargo by distribution through tunneling nanotubes. Cell 184, 5089-5106.e21. https://doi.org/10.1016/j.cell.2021.09.007.

Schindelin, J., Arganda-Carreras, I., Frise, E., Kaynig, V., Longair, M., Pietzsch, T., Preibisch, S., Rueden, C., Saalfeld, S., Schmid, B., Tinevez, J.-Y., White, D.J., Hartenstein, V., Eliceiri, K., Tomancak, P., Cardona, A., 2012. Fiji: an open-source platform for biological-image analysis. Nature methods 9, 676–682. https://doi.org/10.1038/nmeth.2019.

Schmitz, M., Silva Correia, S., Hermann, P., Maass, F., Goebel, S., Bunck, T., Correia, A., Lingor, P., Fischer, A., Zerr, I., 2023. Detection of Prion Protein Seeding Activity in Tear Fluids. The New England journal of medicine 388, 1816–1817. https://doi.org/10.1056/NEJMc2214647.

Schonhoff, A.M., Williams, G.P., Wallen, Z.D., Standaert, D.G., Harms, A.S., 2020. Innate and adaptive immune responses in Parkinson's disease. Progress in brain research 252, 169–216. https://doi.org/10.1016/bs.pbr.2019.10.006.

Schweighauser, M., Shi, Y., Tarutani, A., Kametani, F., Murzin, A.G., Ghetti, B., Matsubara, T., Tomita, T., Ando, T., Hasegawa, K., Murayama, S., Yoshida, M., Hasegawa, M., Scheres, S.H.W., Goedert, M., 2020. Structures of α-synuclein filaments from multiple system atrophy. Nature 585, 464–469. https://doi.org/10.1038/s41586-020-2317-6.

Selikhova, M., Williams, D.R., Kempster, P.A., Holton, J.L., Revesz, T., Lees, A.J., 2009. A clinico-pathological study of subtypes in Parkinson's disease. Brain 132, 2947–2957. https://doi.org/10.1093/brain/awp234.

Shahnawaz, M., Mukherjee, A., Pritzkow, S., Mendez, N., Rabadia, P., Liu, X., Hu, B., Schmeichel, A., Singer, W., Wu, G., Tsai, A.-L., Shirani, H., Nilsson, K.P.R., Low, P.A., Soto, C., 2020. Discriminating α-synuclein strains in Parkinson's disease and multiple system atrophy. Nature 578, 273–277. https://doi.org/10.1038/s41586-020-1984-7.

Shahnawaz, M., Tokuda, T., Waragai, M., Mendez, N., Ishii, R., Trenkwalder, C., Mollenhauer, B., Soto, C., 2017. Development of a Biochemical Diagnosis of Parkinson Disease by Detection of α-Synuclein Misfolded Aggregates in Cerebrospinal Fluid. JAMA neurology 74, 163–172. https://doi.org/10.1001/jamaneurol.2016.4547.

Shimozawa, A., Ono, M., Takahara, D., Tarutani, A., Imura, S., Masuda-Suzukake, M., Higuchi, M., Yanai, K., Hisanaga, S., Hasegawa, M., 2017. Propagation of pathological α-synuclein in marmoset brain. Acta Neuropathologica Communications 5, 12. https://doi.org/10.1186/s40478-017-0413-0.

Siderowf, A., Concha-Marambio, L., Lafontant, D.-E., Farris, C.M., Ma, Y., Urenia, P.A., Nguyen, H., Alcalay, R.N., Chahine, L.M., Foroud, T., Galasko, D., Kieburtz, K., Merchant, K., Mollenhauer, B., Poston, K.L., Seibyl, J., Simuni, T., Tanner, C.M., Weintraub, D., Videnovic, A., Choi, S.H., Kurth, R., Caspell-Garcia, C., Coffey, C.S., Frasier, M., Oliveira, L.M.A., Hutten, S.J., Sherer, T., Marek, K., Soto, C., 2023. Assessment of heterogeneity among participants in the Parkinson's Progression Markers Initiative cohort using α-synuclein seed amplification: a cross-sectional study. The Lancet. Neurology 22, 407–417. https://doi.org/10.1016/S1474-4422(23)00109-6.

Singer, W., Schmeichel, A.M., Shahnawaz, M., Schmelzer, J.D., Boeve, B.F., Sletten, D.M., Gehrking, T.L., Gehrking, J.A., Olson, A.D., Savica, R., Suarez, M.D., Soto, C., Low, P.A., 2020. Alpha-Synuclein Oligomers and Neurofilament Light Chain in Spinal Fluid Differentiate Multiple System Atrophy from Lewy Body Synucleinopathies. Annals of neurology 88, 503–512. https://doi.org/10.1002/ana.25824.

Singer, W., Schmeichel, A.M., Shahnawaz, M., Schmelzer, J.D., Sletten, D.M., Gehrking, T.L., Gehrking, J.A., Olson, A.D., Suarez, M.D., Misra, P.P., Soto, C., Low, P.A., 2021. Alpha-Synuclein Oligomers and Neurofilament Light Chain Predict Phenoconversion of Pure Autonomic Failure. Annals of neurology 89, 1212–1220. https://doi.org/10.1002/ana.26089.

So, R.W.L., Watts, J.C., 2023. α-Synuclein Conformational Strains as Drivers of Phenotypic Heterogeneity in Neurodegenerative Diseases. Journal of Molecular Biology 435, 168011. https://doi.org/10.1016/j.jmb.2023.168011.

Sofroniew, M.V., Vinters, H.V., 2010. Astrocytes: biology and pathology. Acta Neuropathol 119, 7–35. https://doi.org/10.1007/s00401-009-0619-8.

Sokratian, A., Zhou, Y., Xu, E., Viverette, E., Dillard, L., Yuan, Y., Li, J.Y., Matarangas, A., Bouvette, J., Borgnia, M., Bartesaghi, A., West, A., 2022. Structural and functional landscape of α-synuclein fibril conformations amplified from cerebrospinal fluid.

Song, Y.J.C., Halliday, G.M., Holton, J.L., Lashley, T., O'Sullivan, S.S., McCann, H., Lees, A.J., Ozawa, T., Williams, D.R., Lockhart, P.J., Revesz, T.R., 2009. Degeneration in different parkinsonian syndromes relates to astrocyte type and astrocyte protein expression. Journal of neuropathology and experimental neurology 68, 1073–1083. https://doi.org/10.1097/NEN.0b013e3181b66f1b.

Sorrentino, Z.A., Brooks, M.M.T., Hudson, V., Rutherford, N.J., Golde, T.E., Giasson, B.I., Chakrabarty, P., 2017. Intrastriatal injection of α-synuclein can lead to widespread synucleinopathy independent of neuroanatomic connectivity. Molecular Neurodegeneration 12, 40. https://doi.org/10.1186/s13024-017-0182-z.

Spillantini, M.G., Crowther, R.A., Jakes, R., Cairns, N.J., Lantos, P.L., Goedert, M., 1998. Filamentous alpha-synuclein inclusions link multiple system atrophy with Parkinson's disease and dementia with Lewy bodies. Neuroscience letters 251, 205–208. https://doi.org/10.1016/s0304-3940(98)00504-7.

Spillantini, M.G., Schmidt, M.L., Lee, V.M., Trojanowski, J.Q., Jakes, R., Goedert, M., 1997. Alpha-synuclein in Lewy bodies. Nature 388, 839–840. https://doi.org/10.1038/42166.

Srivastava, A., Alam, P., Caughey, B., 2022. RT-QuIC and Related Assays for Detecting and Quantifying Prion-like Pathological Seeds of α-Synuclein. Biomolecules 12. https://doi.org/10.3390/biom12040576.

Stefanova, N., Reindl, M., Neumann, M., Haass, C., Poewe, W., Kahle, P.J., Wenning, G.K., 2005. Oxidative Stress in Transgenic Mice with Oligodendroglial α-Synuclein Overexpression Replicates the Characteristic Neuropathology of Multiple System Atrophy. The American journal of pathology 166, 869–876. https://doi.org/10.1016/s0002-9440(10)62307-3.

Stokholm, M.G., Danielsen, E.H., Hamilton-Dutoit, S.J., Borghammer, P., 2016. Pathological α-synuclein in gastrointestinal tissues from prodromal Parkinson disease patients. Annals of neurology 79, 940–949. https://doi.org/10.1002/ana.24648.

Stokholm, M.G., Iranzo, A., Østergaard, K., Serradell, M., Otto, M., Svendsen, K.B., Garrido, A., Vilas, D., Borghammer, P., Santamaria, J., Møller, A., Gaig, C., Brooks, D.J., Tolosa, E., Pavese, N., 2017. Assessment of neuroinflammation in patients with idiopathic rapid-eye-movement sleep behaviour disorder: a case-control study. The Lancet Neurology 16, 789–796. https://doi.org/10.1016/S1474-4422(17)30173-4.

Strohäker, T., Jung, B.C., Liou, S.-H., Fernandez, C.O., Riedel, D., Becker, S., Halliday, G.M., Bennati, M., Kim, W.S., Lee, S.-J., Zweckstetter, M., 2019. Structural heterogeneity of α-synuclein fibrils amplified from patient brain extracts. Nature communications 10, 5535. https://doi.org/10.1038/s41467-019-13564-w.

Sulzer, D., Edwards, R.H., 2019. The physiological role of α-synuclein and its relationship to Parkinson's Disease. Journal of neurochemistry 150, 475–486. https://doi.org/10.1111/jnc.14810.

Surmeier, D.J., Obeso, J.A., Halliday, G.M., 2017. Selective neuronal vulnerability in Parkinson disease. Nature reviews. Neuroscience 18, 101–113. https://doi.org/10.1038/nrn.2016.178.

Svensson, E., Horváth-Puhó, E., Thomsen, R.W., Djurhuus, J.C., Pedersen, L., Borghammer, P., Sørensen, H.T., 2015. Vagotomy and subsequent risk of Parkinson's disease. Annals of neurology 78, 522–529. https://doi.org/10.1002/ana.24448.

Tansey, M.G., Romero-Ramos, M., 2019. Immune system responses in Parkinson's disease: Early and dynamic. The European journal of neuroscience 49, 364–383. https://doi.org/10.1111/ejn.14290.

Teil, M., Dovero, S., Bourdenx, M., Arotcarena, M.-L., Camus, S., Porras, G., Thiolat, M.-L., Trigo-Damas, I., Perier, C., Estrada, C., Garcia-Carrillo, N., Morari, M., Meissner, W.G., Herrero, M.T., Vila, M., Obeso, J.A., Bezard, E., Dehay, B., 2022. Brain injections of glial cytoplasmic inclusions induce a multiple system atrophy-like pathology. Brain 145, 1001–1017. https://doi.org/10.1093/brain/awab374.

Terkelsen, M.H., Klaestrup, I.H., Hvingelby, V., Lauritsen, J., Pavese, N., Romero-Ramos, M., 2022. Neuroinflammation and Immune Changes in Prodromal Parkinson's Disease and Other Synucleinopathies. Journal of Parkinson's Disease 12, S149-S163. https://doi.org/10.3233/JPD-223245.

Thannickal, T.C., Lai, Y.-Y., Siegel, J.M., 2007. Hypocretin (orexin) cell loss in Parkinson's disease. Brain : a journal of neurology 130, 1586–1595. https://doi.org/10.1093/brain/awm097.

Thomsen, M.B., Ferreira, S.A., Schacht, A.C., Jacobsen, J., Simonsen, M., Betzer, C., Jensen, P.H., Brooks, D.J., Landau, A.M., Romero-Ramos, M., 2021. PET imaging reveals early and progressive dopaminergic deficits after intra-striatal injection of preformed alpha-synuclein fibrils in rats. Neurobiology of Disease 149, 105229. https://doi.org/10.1016/j.nbd.2020.105229.

Tolosa, E., Garrido, A., Scholz, S.W., Poewe, W., 2021. Challenges in the diagnosis of Parkinson's disease. The Lancet. Neurology 20, 385–397. https://doi.org/10.1016/S1474-4422(21)00030-2.

Trojanowski, J.Q., Revesz, T., 2007. Proposed neuropathological criteria for the post mortem diagnosis of multiple system atrophy. Neuropathology and applied neurobiology 33, 615–620. https://doi.org/10.1111/j.1365-2990.2007.00907.x.

Trudler, D., Nazor, K.L., Eisele, Y.S., Grabauskas, T., Dolatabadi, N., Parker, J., Sultan, A., Zhong, Z., Goodwin, M.S., Levites, Y., Golde, T.E., Kelly, J.W., Sierks, M.R., Schork, N.J., Karin, M., Ambasudhan, R., Lipton, S.A., 2021. Soluble α-synuclein-antibody complexes activate the NLRP3 inflammasome in hiPSC-derived microglia. Proceedings of the National Academy of Sciences of the United States of America 118. https://doi.org/10.1073/pnas.2025847118.

Tysnes, O.-B., Kenborg, L., Herlofson, K., Steding-Jessen, M., Horn, A., Olsen, J.H., Reichmann, H., 2015. Does vagotomy reduce the risk of Parkinson's disease? Annals of neurology 78, 1011–1012. https://doi.org/10.1002/ana.24531.

Tysnes, O.-B., Storstein, A., 2017. Epidemiology of Parkinson's disease. Journal of neural transmission (Vienna, Austria : 1996) 124, 901–905. https://doi.org/10.1007/s00702-017-1686-y.

Uemura, N., Uemura, M.T., Lo, A., Bassil, F., Zhang, B., Luk, K.C., Lee, V.M.-Y., Takahashi, R., Trojanowski, J.Q., 2019. Slow Progressive Accumulation of Oligodendroglial Alpha-Synuclein (α-Syn) Pathology in Synthetic α-Syn Fibril-Induced Mouse Models of Synucleinopathy. Journal of neuropathology and experimental neurology 78, 877–890. https://doi.org/10.1093/jnen/nlz070.

Ulusoy, A., Phillips, R.J., Helwig, M., Klinkenberg, M., Powley, T.L., Di Monte, D.A., 2017. Brain-to-stomach transfer of α-synuclein via vagal preganglionic projections. Acta Neuropathol 133, 381–393. https://doi.org/10.1007/s00401-016-1661-y.

van den Berge, N., Ferreira, N., Gram, H., Mikkelsen, T.W., Alstrup, A.K.O., Casadei, N., Tsung-Pin, P., Riess, O., Nyengaard, J.R., Tamgüney, G., Jensen, P.H., Borghammer, P., 2019. Evidence for bidirectional and trans-synaptic parasympathetic and sympathetic propagation of alpha-synuclein in rats. Acta Neuropathol 138, 535–550. https://doi.org/10.1007/s00401-019-02040-w.

van den Berge, N., Ulusoy, A., 2022. Animal models of brain-first and body-first Parkinson's disease. Neurobiology of Disease 163, 105599. https://doi.org/10.1016/j.nbd.2021.105599.

van der Perren, A., Gelders, G., Fenyi, A., Bousset, L., Brito, F., Peelaerts, W., van den Haute, C., Gentleman, S., Melki, R., Baekelandt, V., 2020. The structural differences between patient-derived α-synuclein strains dictate characteristics of Parkinson's disease, multiple system atrophy and dementia with Lewy bodies. Acta neuropathologica 139, 977–1000. https://doi.org/10.1007/s00401-020-02157-3.

van Laar, T., Chaudhuri, K.R., Antonini, A., Henriksen, T., Trošt, M., 2023. Infusion Therapies in the Treatment of Parkinson's Disease. Journal of Parkinson's Disease. https://doi.org/10.3233/JPD-225112.

Varkey, J., Isas, J.M., Mizuno, N., Jensen, M.B., Bhatia, V.K., Jao, C.C., Petrlova, J., Voss, J.C., Stamou, D.G., Steven, A.C., Langen, R., 2010. Membrane curvature induction and tubulation are common features of synucleins and apolipoproteins. The Journal of biological chemistry 285, 32486–32493. https://doi.org/10.1074/jbc.M110.139576.

Videnovic, A., 2017. Management of sleep disorders in Parkinson's disease and multiple system atrophy. Movement disorders : official journal of the Movement Disorder Society 32, 659–668. https://doi.org/10.1002/mds.26918.

Villumsen, M., Aznar, S., Pakkenberg, B., Jess, T., Brudek, T., 2019. Inflammatory bowel disease increases the risk of Parkinson's disease: a Danish nationwide cohort study 1977-2014. Gut 68, 18–24. https://doi.org/10.1136/gutjnl-2017-315666.

Volpicelli-Daley, L., Brundin, P., 2018. Prion-like propagation of pathology in Parkinson disease. Handbook of clinical neurology 153, 321–335. https://doi.org/10.1016/B978-0-444-63945-5.00017-9.

Volpicelli-Daley, L.A., Luk, K.C., Patel, T.P., Tanik, S.A., Riddle, D.M., Stieber, A., Meaney, D.F., Trojanowski, J.Q., Lee, V.M.-Y., 2011. Exogenous α-synuclein fibrils induce Lewy body pathology leading to synaptic dysfunction and neuron death. Neuron 72, 57–71. https://doi.org/10.1016/j.neuron.2011.08.033.

Wakabayashi, K., Hayashi, S., Yoshimoto, M., Kudo, H., Takahashi, H., 2000. NACP/alpha-synuclein-positive filamentous inclusions in astrocytes and oligodendrocytes of Parkinson's disease brains. Acta Neuropathol 99, 14–20. https://doi.org/10.1007/pl00007400.

Wakabayashi, K., Tanji, K., Odagiri, S., Miki, Y., Mori, F., Takahashi, H., 2013. The Lewy body in Parkinson's disease and related neurodegenerative disorders. Molecular Neurobiology 47, 495–508. https://doi.org/10.1007/s12035-012-8280-y.

Williams, G.P., Marmion, D.J., Schonhoff, A.M., Jurkuvenaite, A., Won, W.-J., Standaert, D.G., Kordower, J.H., Harms, A.S., 2020. T cell infiltration in both human multiple system atrophy and a novel mouse model of the disease. Acta Neuropathol 139, 855–874. https://doi.org/10.1007/s00401-020-02126-w.

Winner, B., Jappelli, R., Maji, S.K., Desplats, P.A., Boyer, L., Aigner, S., Hetzer, C., Loher, T., Vilar, M., Campioni, S., Tzitzilonis, C., Soragni, A., Jessberger, S., Mira, H., Consiglio, A., Pham, E., Masliah, E., Gage, F.H., Riek, R., 2011. In vivo demonstration that alpha-synuclein oligomers are toxic. Proceedings of the National Academy of Sciences of the United States of America 108, 4194–4199. https://doi.org/10.1073/pnas.1100976108.

Woerman, A.L., Stöhr, J., Aoyagi, A., Rampersaud, R., Krejciova, Z., Watts, J.C., Ohyama, T., Patel, S., Widjaja, K., Oehler, A., Sanders, D.W., Diamond, M.I., Seeley, W.W., Middleton, L.T., Gentleman, S.M., Mordes, D.A., Südhof, T.C., Giles, K., Prusiner, S.B., 2015. Propagation of prions causing synucleinopathies in cultured cells. Proceedings of the National Academy of Sciences of the United States of America 112, E4949-58. https://doi.org/10.1073/pnas.1513426112.

Wong, Y.C., Krainc, D., 2017. α-synuclein toxicity in neurodegeneration: mechanism and therapeutic strategies. Nature medicine 23, 1–13. https://doi.org/10.1038/nm.4269.

Wright Willis, A., Evanoff, B.A., Lian, M., Criswell, S.R., Racette, B.A., 2010. Geographic and ethnic variation in Parkinson disease: a population-based study of US Medicare beneficiaries. Neuroepidemiology 34, 143–151. https://doi.org/10.1159/000275491.

Wüllner, U., Borghammer, P., Choe, C.-U., Csoti, I., Falkenburger, B., Gasser, T., Lingor, P., Riederer, P., 2023. The heterogeneity of Parkinson's disease. Journal of neural transmission (Vienna, Austria : 1996) 130, 827–838. https://doi.org/10.1007/s00702-023-02635-4.

Yang, Y., Shi, Y., Schweighauser, M., Zhang, X., Kotecha, A., Murzin, A.G., Garringer, H.J., Cullinane, P.W., Saito, Y., Foroud, T., Warner, T.T., Hasegawa, K., Vidal, R., Murayama, S., Revesz, T., Ghetti, B., Hasegawa, M., Lashley, T., Scheres, S.H.W., Goedert, M., 2022. Structures of α-synuclein filaments from human brains with Lewy pathology. Nature 610, 791–795. https://doi.org/10.1038/s41586-022-05319-3.

Yun, S.P., Kam, T.-I., Panicker, N., Kim, S., Oh, Y., Park, J.-S., Kwon, S.-H., Park, Y.J., Karuppagounder, S.S., Park, H., Kim, S., Oh, N., Kim, N.A., Lee, S., Brahmachari, S., Mao, X., Lee, J.H., Kumar, M., An, D.,

Kang, S.-U., Lee, Y., Lee, K.C., Na, D.H., Kim, D., Lee, S.H., Roschke, V.V., Liddelow, S.A., Mari, Z., Barres, B.A., Dawson, V.L., Lee, S., Dawson, T.M., Ko, H.S., 2018. Block of A1 astrocyte conversion by microglia is neuroprotective in models of Parkinson's disease. Nature medicine 24, 931–938. https://doi.org/10.1038/s41591-018-0051-5.

Zarranz, J.J., Alegre, J., Gómez-Esteban, J.C., Lezcano, E., Ros, R., Ampuero, I., Vidal, L., Hoenicka, J., Rodriguez, O., Atarés, B., Llorens, V., Gomez Tortosa, E., del Ser, T., Muñoz, D.G., Yebenes, J.G. de, 2004. The new mutation, E46K, of alpha-synuclein causes Parkinson and Lewy body dementia. Annals of neurology 55, 164–173. https://doi.org/10.1002/ana.10795.

Zhang, S., Dauer, K., Strohäker, T., Tatenhorst, L., Caldi Gomes, L., Mayer, S., Jung, B.C., Kim, W.S., Lee, S.-J., Becker, S., Liesche-Starnecker, F., Zweckstetter, M., Lingor, P., 2023. Alpha-synuclein fibrils amplified from multiple system atrophy and Parkinson's disease patient brain spread after intracerebral injection into mouse brain. Brain pathology (Zurich, Switzerland). https://doi.org/10.1111/bpa.13196.

Zhou, B., Wen, M., Yu, W.-F., Zhang, C.-L., Jiao, L., 2015. The Diagnostic and Differential Diagnosis Utility of Cerebrospinal Fluid α -Synuclein Levels in Parkinson's Disease: A Meta-Analysis. Parkinson's Disease 2015, 567386. https://doi.org/10.1155/2015/567386.

Zubelzu, M., Morera-Herreras, T., Irastorza, G., Gómez-Esteban, J.C., Murueta-Goyena, A., 2022. Plasma and serum alpha-synuclein as a biomarker in Parkinson's disease: A meta-analysis. Parkinsonism & related disorders 99, 107–115. https://doi.org/10.1016/j.parkreldis.2022.06.001.

8 Acknowledgments

First and foremost, I would like to thank Prof. Dr. Paul Lingor for his unwavering support and excellent guidance throughout the whole journey of this project. I have learned so much professionally, scientifically, and personally. I also thank Lucas Caldi Gomes for his expert supervision in the lab and constant availability. I am so amazed at how much you do for everyone around the lab. Special thanks to Mojan Parvaz for her support. You always have an open ear, no matter what. I am very grateful for Lucas and Mojan introducing me to the lab and making the first couple of months so much easier with their help and expertise. Thank you to Antonia Demleitner for the insightful discussions we had. Thank you to Simon Mayer for helping me with imaging during the manuscript revision. Thank you to my fellow MDs Lena-Sophie Scholl and Pia Gutsmiedl, for your uplifting spirits. A great “thank you” to everyone in the Lingor Lab for all your input and support.

Thank you to all my collaborators Karina Dauer, Timo Strohäker, Lars Tatenhorst, Simon Mayer, Byung Chul Jung, Woojin S. Kim, Seung-Jae Lee, Stefan Becker, and Markus Zweckstetter. Without your contributions and support, this work would not have been possible.

Thank you to my thesis mentor Friederike Liesche-Starnecker for her expertise in neuropathology. Additionally, I want to thank Sandra Baur for teaching me IHC and IF and our neighboring lab members, especially Goutam Kumar Tanti and Rajneesh Srivastava, for being so kind and available.

Finally, I would like to thank my friends and family for always being my biggest supporters and cheerleaders - I dedicate this thesis to all of you.